

Wild Wall Crossing and BPS Giants

Dmitry Galakhov,¹ Pietro Longhi,² Tom Mainiero,³ Gregory W. Moore,⁴ and Andrew Neitzke⁵

¹*Institute for Theoretical and Experimental Physics,
Moscow, Russia,*

^{1,2,4}*NHETC and Department of Physics and Astronomy, Rutgers University,
Piscataway, NJ 08855-0849, USA*

³*Department of Physics, University of Texas at Austin,
Austin, TX 78712, USA*

⁵*Department of Mathematics, University of Texas at Austin,
Austin, TX 78712, USA*

E-mail: galakhov@physics.rutgers.edu, longhi@physics.rutgers.edu,
mainiero@physics.utexas.edu, gmoore@physics.rutgers.edu,
neitzke@math.utexas.edu

ABSTRACT: We show that the BPS spectrum of pure $SU(3)$ four-dimensional super Yang-Mills with $\mathcal{N} = 2$ supersymmetry exhibits a surprising phenomenon: there are regions of the Coulomb branch where the growth of the BPS degeneracies with the charge is *exponential*. We show this using spectral networks and independently using wall-crossing formulae and quiver methods. The computations using spectral networks provide a very nontrivial example of how these networks determine the four-dimensional BPS spectrum. We comment on some physical implications of the wild spectrum: for example, exponentially many field-theoretic BPS states with large charge are gigantic. Finally, we exhibit some surprising, thus far unexplained, regularities of the BPS spectrum.

Contents

1	Introduction & Conclusion	2
2	Brief Review of Spectral Networks	5
2.1	The Setting	5
2.1.1	Spectral Cover Crash Course	6
2.1.2	BPS objects in $S[A_{K-1}, C, D]$	7
2.1.3	Adding a Little Twist	12
2.2	The \mathcal{W}_ϑ Networks	15
2.2.1	\mathcal{K} -walls and Degenerate Networks	16
2.2.2	Formal Variables	17
2.2.3	Computing $\Omega(n\gamma_c)$	20
3	Spectral network analysis of a wild point on the Coulomb branch	23
3.1	Horses and Herds	23
3.2	Connection with Kontsevich-Soibelman, Gross-Pandharipande	27
3.3	Herds of horses are wild (for $m \geq 3$)	30
3.4	Herds in the pure $SU(3)$ theory	32
4	Wild regions for pure $SU(3)$ theory from wall-crossing	32
4.1	Strong Coupling Regime of the Pure $SU(3)$ Theory	33
4.2	A path on the Coulomb branch	34
4.3	Cohorts in pure $SU(3)$	35
4.4	Wall-crossings with intersections $m > 3$	38
5	Some Numerical Checks on the $m = 3$ Wild Spectrum	40
5.1	The spectrum generator technique	40
5.2	Factorizing the spectrum generator	41
5.3	Exponential growth of the BPS degeneracies	43
6	Relation to quivers	44
6.1	Derivation of the Kronecker m -quivers from the strong coupling regime	45
6.2	A nontrivial symmetry of BPS degeneracies	47
6.3	Asymptotics of BPS degeneracies	49
6.4	Numerical check of Weist's conjecture	49
7	Physical estimates and expectations	51
7.1	An apparent paradox	51
7.2	Denef equations	52
7.3	Resolution and Revised Bound	53

7.4	Discussion of validity of the semiclassical picture	54
7.4.1	A toy example: the Hall halo	55
7.4.2	Estimating the contribution of the maximal partition	56
8	Spectral Moonshine	57
8.1	Scaling behavior of the spin degeneracies	57
8.2	Partitions and relation to modular functions	59
9	Open Problems	60
A	Protected spin characters of the 3-Kronecker quiver	62
A.1	Spin decompositions	62
A.2	The data	64
B	The Six-Way Junction	67
C	m-Herds in Detail	70
C.1	Notational Definitions	70
C.2	Duality	72
C.3	The Horse as a Machine	72
C.3.1	Outgoing Soliton Generating Functions	76
C.3.2	Outgoing Street Factors	77
C.3.3	Internal Street Factors	77
C.4	A Global Interlude	81
C.5	Identifications of Generating Functions	85
C.6	Proof of Proposition 3.1	85
C.6.1	Proof of Equations (3.3)	85
C.6.2	Proof of the Algebraic Equation (3.2)	89
C.7	Proof of the Decomposition of $\widehat{\gamma}_c$	90
C.7.1	Example: $\widehat{\gamma}_c$ for m -herds on the cylinder	90
C.7.2	General Proof	91
C.8	Proof of Proposition 3.2	94
C.9	Table of m -herd BPS indices $\Omega(n\gamma_c)$, for low values of n and m	99
D	Proof of Proposition 3.4	99
E	A sign rule	101
F	Spectral networks and algebraic equations	101

1 Introduction & Conclusion

One good reason to investigate the BPS spectra of four-dimensional $\mathcal{N} = 2$ field theories is that one might discover new phenomena in field theory. This paper demonstrates an example of such a new phenomenon.

In the past few years there has been much progress in understanding the BPS spectra of $\mathcal{N} = 2, d = 4$ theories. For recent reviews see [35–37]. These methods have been particularly powerful when applied to the theories of class $S[A_1]$. As one example, the spectrum generator technique of [19] gives an algorithm which can — in principle — give the BPS spectrum of any theory of class $S[A_1]$ anywhere on its Coulomb branch. Advances in quiver technology have also been very effective in investigating this class of theories [30, 39]. In contrast, theories associated to higher rank gauge groups, such as theories of class $S[A_{K-1}]$ for $K > 2$, have been less explored.

It has been noted by various authors that theories of class $S[A_{K-1}]$ for $K > 2$ could have higher spin BPS states, beyond the familiar hypermultiplets and vectormultiplets which occur in theories of class $S[A_1]$. One result of this paper is that this expectation is indeed correct: higher spin BPS multiplets do occur at some points of the Coulomb branch in one explicit theory of class $S[A_2]$, namely the pure $d = 4, \mathcal{N} = 2, SU(3)$ theory.

In addition, we find a much more surprising phenomenon: theories of class S can have *wild BPS spectra*, i.e. at some points of the Coulomb branch, the number of BPS states with mass $\leq M$ grows *exponentially* with M . The main result of this paper is two independent demonstrations, in Sections 3 and 4, that wild spectra appear in the pure $d = 4, \mathcal{N} = 2, SU(3)$ theory.

As explained in Section 7 below, this exponential growth is physically a bit surprising. Indeed, the existence of a conformal fixed point defining the 4d theory, plus dimensional analysis, implies that the degeneracy of BPS states at energy E in finite volume V cannot grow faster than $\exp[\text{const} \times V^{1/4} E^{3/4}]$. On the other hand, here we are finding that the spectrum of BPS 1-particle states grows like $\exp[\text{const} \times E]$. The resolution of this puzzle must lie in the difference between BPS 1-particle states and states in the finite volume Hilbert space; we propose that the size of the objects represented by the BPS 1-particle states grows with E , so that for any fixed V , most of the BPS 1-particle states simply do not fit into the finite-volume Hilbert space. Indeed, in Section 7, using Denef’s picture of BPS bound states, we demonstrate directly that their size does indeed grow with E . The invalid exchange of large E and large V limits when accounting for field theory entropy should perhaps serve as a cautionary tale.

Here is the fundamental idea which we use to find wild BPS degeneracies. Suppose we have an $\mathcal{N} = 2$ theory and a point of the Coulomb branch in which the spectrum contains two BPS hypermultiplets, of charges γ and γ' , and no bound states thereof — i.e. we have the BPS degeneracies $\Omega(\gamma) = 1, \Omega(\gamma') = 1, \Omega(a\gamma + b\gamma') = 0$ for all other $a, b \geq 0$. Then suppose we move on the Coulomb branch to a point where the central charges Z_γ and $Z_{\gamma'}$ have the same phase. Such a point lies on a wall of marginal stability. On the other side

of the wall, the spectrum includes bound states with charge $a\gamma + b\gamma'$ for various a, b . Their precise degeneracies can be determined by the Kontsevich-Soibelman wall-crossing formula, and indeed depend *only* on the integer $m = \langle \gamma, \gamma' \rangle$. For this reason we call the collection of BPS states thus generated an “ m -cohort.”

The cases $m = 1$ and $m = 2$ occur already in the theories of class $S[A_1]$. For $m = 1$ an m -cohort contains only a single bound state; for $m = 2$ an m -cohort contains an infinite set of hypermultiplets plus a single vector multiplet. In either case, at any rate, one does not get wild degeneracies. In contrast, for $m > 2$ the wall-crossing formula shows that an m -cohort does contain wild degeneracies. Indeed, even if one restricts attention to charges of the form $n(\gamma + \gamma')$, one already has exponential growth. This is explained and made precise in Proposition 3.4, Section 5.3, and Section 6.3 below. With this in mind, for any $m > 2$, we will say that a theory contains “ m -wild degeneracies” if its BPS spectrum contains an m -cohort.

The BPS degeneracies arising in m -cohorts have been studied at some length in the mathematics literature because they arise as Donaldson-Thomas invariants attached to the m -Kronecker quiver in one region of its stability parameter space. The latter have been intensively studied in [7, 8, 13, 17, 18, 31]. One interesting feature noted there is that for $m > 2$, the phases of the central charges of BPS states in an m -cohort are *dense* in some arc of the circle.

This discussion motivates two approaches to the problem of exhibiting wild degeneracies in a physical theory. Our first approach goes via the “spectral networks” of [33, 34]: rather than studying the wall-crossing directly, we make a guess about the kind of spectral networks which *could* arise from wall-crossing involving two hypermultiplets with arbitrary $m = \langle \gamma, \gamma' \rangle$. For $m = 1$ the network we draw looks like a saddle, which motivates an equine terminology: our networks are built from constituents we call “horses” (defined in Section 3.1, Figure 3, and detailed in Appendix C), glued together to form “ m -herds.” See Figure 4 for some examples. We show moreover that m -herds indeed occur in physical spectral networks at some particular points of the Coulomb branch of the $SU(3)$ theory: see Figure 5 for the evidence. The general rules of spectral networks, combined with Proposition 3.1 and Proposition 3.2 below, lead to the following formula for the BPS spectrum for charges of the form $n(\gamma + \gamma') := n\gamma_c$ in the wild region. We first form a generating function $P_m(z)$ related to the BPS spectrum by

$$P_m(z) = \prod_{n=1}^{\infty} (1 - (-1)^{mn} z^n)^{n\Omega(n\gamma_c)/m}. \quad (1.1)$$

Then, Proposition 3.1 states that $P_m(z)$ is a solution of the algebraic equation (3.2), which we reproduce here:

$$P_m = 1 + z (P_m)^{(m-1)^2}. \quad (1.2)$$

This equation had been identified previously by Kontsevich and Soibelman [16] and by Gross and Pandharipande [20], as the one governing the generating function of BPS degeneracies of an m -cohort, for charges of the form $n(\gamma + \gamma')$. It follows that if we have an m -herd

($m > 2$) somewhere in our theory, then our theory does contain at least the part of an m -cohort corresponding to charges of the form $n(\gamma + \gamma')$. In particular, if the theory contains an m -herd, then it does contain wild degeneracies. Since we have found m -herds at some points of the Coulomb branch in the pure $SU(3)$ theory, we conclude that we indeed have wild degeneracies in that theory.

The algebraic equation (1.2) is an instance of a more general phenomenon. It has been observed by Kontsevich that the generating functions of Donaldson-Thomas invariants are often solutions of algebraic equations. In fact, for the Kronecker quiver this has been proved [41]. Our analysis via spectral networks produces the algebraic equation (1.2) directly. Moreover, we expect that this will happen more generally, as we explain in Appendix F; thus spectral networks seem to be a natural framework for explaining Kontsevich’s observation.

Our second method of demonstrating the existence of wild spectra uses wall-crossing more directly. Namely, in Section 4.2 we exhibit a path on the Coulomb branch which begins in a strong coupling chamber with a finite set of BPS states, and leads to a wall-crossing between two hypermultiplet charges γ, γ' with $\langle \gamma, \gamma' \rangle = 3$. As we have discussed above, the existence of such a path directly implies the existence of wild spectra. In fact this gives more than we got from the spectral network: it shows that there is a whole 3-cohort in the spectrum. In Section 5.2 we perform some nontrivial checks of this statement by factorizing the spectrum generator derived from the known finite spectrum in a strong coupling chamber. In Section 5.3 we also check numerically the exponential growth of the BPS degeneracies for sequences of charges of the form $n(a\gamma + b\gamma')$, $n \rightarrow \infty$, for various values of a, b .

In Section 6 we discuss the behavior of the “BPS quivers” of the $SU(3)$ theory along the path found in Section 4.2. It turns out that the Kronecker 3-quiver is in fact a subquiver of the BPS quiver, after one has performed suitable mutations and made a suitable choice of half-plane to define simple roots. We similarly argue that for *all* $m \geq 3$ (not only $m = 3$) there are Kronecker m -subquivers and corresponding m -wild spectra on the Coulomb branch of the $SU(3)$ theory.

In the course of our investigations we also studied the protected spin characters (a.k.a. “refined BPS degeneracies”) for the m -Kronecker quiver in the wild region. Our main tool was the “motivic” Kontsevich-Soibelman formula [16, 21]. While investigating these spin degeneracies we discovered some beautiful but strange systematics. Some of these were previously discovered by Weist and Reineke in [31] and [8], respectively, but some are new. We collect them in Section 8. Perhaps the most notable new observation is that the spin degeneracies appear, (on the basis of numerical data), to obey a universal scaling law. See equations (8.2) and (8.3).

In Section 9 we discuss a few open problems and questions raised by the present work. Appendix A reviews definitions of protected spin characters and presents some data. The remaining appendices address more technical points of spectral networks.

Acknowledgements

We thank Ofer Aharony, Tom Banks, Frederik Denef, Emanuel Diaconescu, Maxim Kontsevich, Jan Manschot and Steve Shenker for useful discussions and correspondence. The work of DG, PL, and GM is supported by the DOE under grant DE-FG02-96ER40959. GM also gratefully acknowledges partial support from a Simons Fellowship and hospitality of the Aspen Center for Physics (NSF Grant 1066293) during part of this research. The work of AN is supported by the NSF under grant numbers DMS-1006046 and DMS-1151693. The work of GM and AN is jointly supported by an NSF Focused Research Group award DMS-1160461 and DMS-1160591. The work of DG was partly supported by Ministry of Education and Science of the Russian Federation under contract 8207, by NSh-3349.2012.2, by RFBR grants 13-02-00457, 12-02-31535-mol-a. The work of TM was partly supported by the NSF under an NSF Research Training Group award DMS-0636557.

2 Brief Review of Spectral Networks

In this section we give a brief review of the spectral network machinery and its use for computing BPS spectra in $\mathcal{N} = 2$, $d = 4$ theories of class S . For a more complete discussion we refer the reader to [33]. For a more informal (but incomplete) review see [35].

2.1 The Setting

Recall that the $\mathcal{N} = 2$, $d = 4$ theories of class S are specified by three pieces of data [19, 40]:

1. A Lie algebra \mathfrak{g} of ADE type (as in [33] the following discussion assumes $\mathfrak{g} = A_{K-1}$),
2. a compact Riemann surface C with punctures at points $\mathfrak{s}_1, \dots, \mathfrak{s}_n \in C$,
3. a collection of defect operators D located at the punctures.

To shed some light on this collection of data, we note that such theories can be constructed via a partial twist (preserving eight supercharges) of the $\mathcal{N} = (2, 0)$, $d = 6$ theory $S[\mathfrak{g}]$ defined on $\mathbb{R}^{3,1} \times C$. The defect operators D are codimension-2 defects located at $\mathbb{R}^{3,1} \times \{\mathfrak{s}_1\}, \dots, \mathbb{R}^{3,1} \times \{\mathfrak{s}_n\}$. A four-dimensional $\mathcal{N} = 2$ field theory is produced after integrating out the degrees of freedom along C and is labeled $S[\mathfrak{g}, C, D]$.

We now present some useful definitions.

Definitions

1. The *Coulomb branch* \mathcal{B} of $S[\mathfrak{g}, C, D]$ is the set of tuples (ϕ_2, \dots, ϕ_K) of holomorphic r -differentials ϕ_r with singularities at $\mathfrak{s}_1, \dots, \mathfrak{s}_n \in C$ prescribed by the defect operators D .

2. Let $u = (\phi_2, \dots, \phi_r) \in \mathcal{B}$ and denote the holomorphic cotangent bundle of C as \mathcal{T}^*C . Then the *spectral cover* is a K -sheeted branched cover $\pi_u : \Sigma_u \rightarrow C$, where Σ_u is the subvariety¹

$$\Sigma_u := \{\lambda \in \mathcal{T}^*C : \lambda^K + \sum_{r=2}^K \phi_r \lambda^{K-r} = 0\} \subset \mathcal{T}^*C, \quad (2.1)$$

and the projection π_u is the restriction of the standard projection $\mathcal{T}^*C \rightarrow C$.

3. As $\Sigma_u \subset \mathcal{T}^*C$ it carries a natural holomorphic 1-form which is just the restriction of the tautological (Liouville) 1-form. In the spirit of its tautological nature we abuse notation and denote this 1-form λ_u .

Often we will work over a fixed $u \in \mathcal{B}$; so eventually the index u will be dropped where there is no ambiguity.

2.1.1 Spectral Cover Crash Course

Let us make some observations about the spectral cover. First, the fibers are given by

$$\pi_u^{-1}(z) = \{\lambda(z) \in \mathcal{T}_z^*C : \lambda(z)^K + \sum_{r=2}^K \phi_r(z) \lambda^{K-r}(z) = 0\},$$

i.e. the roots of the defining polynomial of Σ_u at the point z . Generically, $\pi_u^{-1}(z)$ consists of K distinct roots, although at particular values of z (branch points) two or more roots may coincide. In fact, letting $C' = C - \{\text{branch points}\}$, $\pi_u|_{C'}$ is a K -fold (unramified) cover of C' .

If $\pi_u|_{C'}$ is a non-trivial cover, the roots do not fit together into global holomorphic 1-forms on C as they undergo monodromy around branch points. However, restricted to the complement of a choice of branch cuts on C , the cover is trivializable: a projection of K distinct sheets onto the complement. Each sheet is the graph traced out by a root of the defining polynomial; such roots are distinct holomorphic differential forms. A choice of trivialization of the restricted cover is a bijective map between the set of K sheets and the set $\{1, 2, \dots, K\}$, or equivalently, a labeling of the roots of the defining polynomial from 1 to K .

Definitions

1. Make a suitable choice of branch cuts for the branched cover $\pi_u : \Sigma_u \rightarrow C$. The complement of these branch cuts in C will be denoted by C^c .
2. A choice of trivialization of $\pi^{-1}(C^c) \rightarrow C^c$ will be denoted by a labeling of the roots of the defining polynomial for Σ , i.e. a labeling $\lambda_i \in H^0(C^c; K)$, $i = 1, \dots, K$, where each λ_i (a holomorphic 1-form on C^c) is a distinct root of the defining polynomial for Σ . Note that this gives us a labeling of sheets: the i th sheet is the graph of λ_i in \mathcal{T}^*C . If we wish, we can extend the $\lambda_i(z)$ to branch points z to speak of ‘‘collisions’’ of sheets.

¹ Σ_u is also called the Seiberg-Witten curve.

3. For later convenience, we define

$$\lambda_{ij} := \lambda_i - \lambda_j \in H^0(C^c; K).$$

As in [33] we will assume that all branch points are simple, i.e. at most two sheets of Σ collide at any z .

Definition A branch point of type ij ($i, j \in 1, \dots, K$) is a point $z \in C$ where the i th and j th sheets of Σ_u collide, i.e. $\lambda_i(z) = \lambda_j(z)$.

The data of the full spectral cover can be recovered after trivializing by specifying the monodromy around all branch points, and all closed cycles of C . In this paper, we assume *simple ramification*: in a neighborhood around each branch point, the spectral cover looks like the branched cover $z \mapsto z^2$ of the disk. Thus, for a simple closed curve surrounding a branch point of type ij , there is a $\mathbb{Z}/2\mathbb{Z}$ monodromy

$$\lambda_i \leftrightarrow \lambda_j.$$

Monodromy around an arbitrary closed cycle of C may permute the sheets in a more complicated fashion.

2.1.2 BPS objects in $S[A_{K-1}, C, D]$

Theories of class S admit a zoo rich in BPS species, each of which has a different classical description from the point of view of the six-dimensional geometry of $\mathbb{R}^{3,1} \times C$. Our ultimate interest in this paper is in the 4D (vanilla) BPS states, but the power behind the spectral network machine draws heavily on the symbiosis between these different species; so we take a moment to project each of them into the spotlight.

BPS Strings and “vanilla” 4D BPS states

4D BPS states in the four-dimensional $\mathcal{N} = 2$ theory arise from extended objects in the 6D description: BPS strings. In the effective IR description, at a point $u \in \mathcal{B}$, BPS strings wrap closed paths p on the branched cover $\Sigma_u \subset \mathcal{T}^*C \rightarrow C$. The resulting states are classified by their homology classes $\gamma = [p] \in H_1(\Sigma_u; \mathbb{Z})$ in the sense that there is a natural grading of the Hilbert space of BPS strings as

$$\mathcal{H}^{\text{BPS}}(u) = \bigoplus_{\gamma \in H_1(\Sigma_u; \mathbb{Z})} \mathcal{H}(\gamma; u),$$

commuting with the action of the super-Poincaré group.

Definition The *charge lattice* of 4D BPS states at a point $u \in \mathcal{B}$ is $\Gamma_u = H_1(\Sigma_u; \mathbb{Z})$. It is equipped with an antisymmetric pairing $\langle \cdot, \cdot \rangle : \Gamma_u \times \Gamma_u \rightarrow \mathbb{Z}$ given by the intersection form on $H_1(\Sigma_u; \mathbb{Z})$.

To count the number of BPS states of a particular charge γ we recall a major celebrity of this paper: the second helicity supertrace (a.k.a. the “BPS degeneracy” or “BPS index”)

$$\Omega(\gamma; u) = -\frac{1}{2} \text{Tr}_{\mathcal{H}(\gamma; u)} (2J_3)^2 (-1)^{2J_3},$$

where J_3 is any generator of the rotation subgroup of the massive little group. This index is piecewise constant on \mathcal{B} , jumping across real codimension-1 walls of marginal stability on \mathcal{B} where two BPS states with linearly independent charges $\gamma, \gamma' \in \Gamma_u$ have central charges of the same phase: $\arg(Z_\gamma) = \arg(Z_{\gamma'})$. To compute this index we will not rely on its definition as a supertrace, but instead utilize the geometric methods of the spectral network machine.

Remarks

1. On \mathcal{B} there may be (complex) codimension-1 loci where a cycle of Σ_u degenerates. Let $\mathcal{B}^* = \mathcal{B} - \{\text{degeneration loci}\}$. Then the collection $\widehat{\Gamma} = \{\Gamma_u\}_{u \in \mathcal{B}^*}$ forms a local system of lattices $\widehat{\Gamma} \rightarrow \mathcal{B}^*$. This local system is often equipped with a non-trivial monodromy action.
2. As mentioned previously, we will often drop the subscript $u \in \mathcal{B}$ as we will often be working over a single point on the Coulomb branch, or choosing a local trivialization of the local system of lattices on some open set.
3. Strictly speaking, the lattice of charges Γ_u is not quite $H_1(\Sigma_u; \mathbb{Z})$ [19]; in the theory we consider in this paper, though, Γ_u is just a sublattice of $H_1(\Sigma_u; \mathbb{Z})$, and for our considerations there is no harm in replacing Γ_u by $H_1(\Sigma_u; \mathbb{Z})$. (If we considered the theory with $\mathfrak{g} = \mathfrak{gl}(K)$ instead of $\mathfrak{g} = \mathfrak{sl}(K)$ then the charge lattice would be literally $H_1(\Sigma_u; \mathbb{Z})$.)
4. From the four-dimensional point of view, Γ_u is the lattice of electric/magnetic and flavor charges in the IR effective abelian gauge theory defined at u .

Fix $u \in \mathcal{B}$. The central charge and mass of a string $p : S^1 \rightarrow \Sigma$ are²

$$\begin{aligned} Z_p &= \frac{1}{\pi} \int_p \lambda, \\ M_p &= \frac{1}{\pi} \int_p |\lambda|. \end{aligned}$$

With this, the BPS condition $|Z_p| = M_p$ is given by

$$\int_p \lambda = e^{i\vartheta} \int_p |\lambda| \tag{2.2}$$

²The integral $\int_p \lambda$ is only a function of the class $[p] \in H_1(\Sigma; \mathbb{Z})$; hence, the central charge reduces to a function $\Gamma \rightarrow \mathbb{C}$.

for some $\vartheta = \arg(Z_p) \in \mathbb{R}/2\pi\mathbb{Z}$. The value of ϑ specifies which four-dimensional BPS subalgebra is preserved. We can rewrite this condition in more useful form; indeed, let v_p denote a vector field along the path p , then (2.2) is true iff

$$\mathrm{Im} \left[e^{-i\vartheta} \langle \lambda, v_p \rangle \right] = 0. \quad (2.3)$$

Solitons

The theory $S[\mathfrak{g}, C, D]$ is equipped with a special set of BPS surface defect operators $\{\mathbb{S}_z\}_{z \in C}$ parameterized (in the UV³) by points on C . In the IR, for fixed $u \in \mathcal{B}$, the operator \mathbb{S}_z possesses finitely many massive vacua labeled by the set $\pi^{-1}(z)$ (with $\pi = \pi_u$). Letting $z \in C'$, then *solitons* are BPS states⁴ bound to the defect \mathbb{S}_z , which interpolate between two different vacua. Classically, they are given by oriented paths $s : [0, 1] \rightarrow \Sigma$ with endpoints $s(0), s(1) \in \pi^{-1}(z)$; furthermore, each such path satisfies a BPS condition that we will now describe.

Consider a soliton path s such that, after choosing a trivialization, s only runs along sheets i and j and such that the projection $s_C := \pi \circ s$ is a connected open path on C . Let v_{s_C} be a vector field along the path s_C . Then, the BPS condition is the differential equation

$$\mathrm{Im} \left[e^{-i\vartheta} \langle \lambda_{ij}, v_{s_C} \rangle \right] = 0 \quad (2.4)$$

for some fixed angle ϑ . For more complicated solitons that travel along more than two sheets, we can break the soliton up into a concatenation of partial solitons running along various pairs of sheets; each partial soliton involved in the concatenation must satisfy (2.4) where ij is replaced by the relevant pair of sheets, and ϑ is the same for each partial soliton. Hence, the BPS condition for solitons leads to a system of $\binom{K}{2}$ differential equations on C' (one for each disjoint pair of sheets). For such a soliton s , broken into partial solitons $\{s^r\}_{r=1}^L$ as described above, its central charge and mass are

$$\begin{aligned} Z_s &= \sum_{r=1}^L \frac{1}{\pi} \int_{s_C^r} \lambda_{ij} \\ M_s &= \sum_{r=1}^L \frac{1}{\pi} \int_{s_C^r} |\lambda_{ij}|. \end{aligned} \quad (2.5)$$

We can now identify the angle as the phase of the central charge, $\vartheta = \arg(Z_s)$, and indeed the BPS condition is equivalent to $M_s = |Z_s|$.

As with 4D BPS states, solitons also carry a charge, but now given by a relative homology class as they are open paths.

Let $z \in C'$; choose a labeling of the K points in $\pi^{-1}(z) \in C'$.

³In the six-dimensional UV description, the operator \mathbb{S}_z attached to a point $z \in C$ is a surface defect which intersects C at a single point.

⁴After insertion of \mathbb{S}_z there are four remaining supercharges. A BPS soliton preserves two supercharges.

Definition

1. Let $z_l \in \pi^{-1}(z)$ denote the pre-image of $z \in C'$ on the l th sheet. Then a soliton is of type ij if it is given by a path that begins on z_i and ends on z_j . We also refer to such solitons as *ij-solitons*.
2. $\Gamma_{ij}(z, z)$ is the set of charges of ij -solitons, i.e.

$$\Gamma_{ij}(z, z) := \{[a] \in H_1(\Sigma, \{z_i\} \cup \{z_j\}; \mathbb{Z}) : a \text{ is a 1-chain with } \partial a = z_j - z_i\}.$$

3. The total set of soliton charges is

$$\Gamma(z, z) := \bigsqcup_{i,j=1}^K \Gamma_{ij}(z, z).$$

Remarks

1. A soliton s can be extended by “parallel transporting” its endpoints. Indeed, let s be a soliton of type ij with $s(0), s(1) \in \pi^{-1}(z)$. Now, given a path $q : [0, 1] \rightarrow C'$ from z to z' , let $q\{n\}$ denote the lift of q to the n th sheet of Σ defined by lifting the initial point $q(0)$ to sheet n ; then one can define the transported path,

$$\mathbb{P}_q s = q\{j\} \star s \star q^{-}\{i\} \tag{2.6}$$

where \star denotes concatenation of paths, and $q^{-}\{i\}$ is $q\{i\}$ with reversed orientation. The resulting path on Σ has endpoints in $\pi^{-1}(z')$. If s is an ij soliton, then the path $\mathbb{P}_q s$ is a soliton iff q satisfies (2.4) for the same pair of sheets ij .

2. $\bigcup_{z \in C'} \Gamma(z, z) \rightarrow C'$ is a local system over C' : for any path $q : [0, 1] \rightarrow C$ there is a parallel transport map $P_q : \Gamma(q(0), q(0)) \rightarrow \Gamma(q(1), q(1))$, induced by the map \mathbb{P}_q defined above, and only depending on the homotopy class of q relative to the endpoints. (Henceforth we abbreviate this as “rel endpoints.”)
3. If there is an extension of an ij -soliton through a branch cut emanating from an ij branch point, it becomes a ji -soliton. More generally, if a soliton passes through any branch cut, its type is permuted according to the permutation of sheets across the branch cut.

Just as with 4D vanilla BPS states, for each $a_z \in \Gamma(z, z)$, there is an index $\mu(a_z) \in \mathbb{Z}$ that counts BPS solitons of charge a_z . Again, this can be defined as a supertrace over an appropriate BPS subspace, however, we will compute it via geometric methods. Using the parallel transport map described in the remarks above, this BPS index is also stable along extensions of solitons at generic $z \in C'$; ⁵ it jumps only at points $z \in C'$ where solitons of different types exist and interact. This motivates the following (notation-simplifying) definitions.

⁵In the sense that if s is an ij soliton, and q is a sufficiently small path on Σ satisfying (2.4), then $\mu([s]) = \mu(P_q[s])$

Definitions

1. A soliton $s : [0, 1] \rightarrow \Sigma$ is said to be of *phase* θ if it satisfies the BPS condition⁶ (2.4) for $\vartheta = \theta$.
2. A point $z \in C$ is said to *support* a soliton of phase ϑ if there exists a soliton s with $[s] \in \Gamma(z, z)$ and $\mu([s]) \neq 0$. A path p on C supports a family of solitons of phase ϑ if each point on p supports a soliton fitting into a 1-parameter family of solitons of phase ϑ . When the phase ϑ is clear from context, occasionally we will just say that p supports a family of solitons.
3. Let $p \subset C$ be a path on C supporting a family of solitons of phase ϑ extending a soliton s_0 with charge $a_z = [s_0] \in \Gamma(z, z)$. With an abuse of notation, occasionally a will denote any one of the parallel transports of a_z along the path p .
4. Let $z \in p$ and $a_z \in \Gamma(z, z)$. If the index $\mu(a_z)$ is constant for any soliton in the family generated by parallel transports of $a_z \in \Gamma(z, z)$ along $p \subset C$, then we will denote the index by $\mu(a, p) \in \mathbb{Z}$.

Framed 2D-4D States

We consider one final BPS construction: the framed 2D-4D states. Given $\vartheta \in \mathbb{R}/(2\pi\mathbb{Z})$, $z_1, z_2 \in C$, and \wp a path on C from z_1 to z_2 , one can associate two surface defects \mathbb{S}_{z_1} and \mathbb{S}_{z_2} , along with a supersymmetric interface $L_{\wp, \vartheta}$ between these two surface defects.⁷ The interface is supersymmetric in the sense that it preserves two out of the four supercharges preserved by the surface defects; the parameter ϑ controls which two are preserved. Framed 2D-4D states are the vacua of the theory after insertion of this defect.

Geometrically, such a state is represented by a path $f : [0, 1] \rightarrow \Sigma$ such that there exists a finite subdivision of times

$$[0, 1] = [0, t_1] \cup [t_1, t_2] \cup \cdots \cup [t_{N-1}, 1]$$

and, with respect to this subdivision:

- $f|_{[0, t_1]}$ and $f|_{[t_N, 1]}$ have images in $\pi^{-1}(\wp)$ (in particular, the path begins on a lift of z_1 and ends on a lift of z_2).
- If $1 < i < N - 2$, then $f|_{[t_i, t_{i+1}]}$ is either a soliton of phase ϑ , or has image in $\pi^{-1}(\wp)$.

When f is projected to C the resulting path looks like \wp with finitely many diversions to solitons (and back) along the way. In [23], such a path f is referred to as a *millipede with body \wp and phase ϑ* .

⁶Thought of as a system of equations on each “partial soliton” as described above.

⁷From the four-dimensional perspective, $L_{\wp, \vartheta}$ is a line defect extended along $\mathbb{R}^{0,1}$ and living on the interface between \mathbb{S}_{z_1} and \mathbb{S}_{z_2} .

Similar to solitons, we can classify framed 2D-4D states by their values in a set of charges given by relative homology classes $[f]$, for f a millipede; as the geometric description above suggests, now the relative cycles can have boundaries on pre-images of two different points on C .

Definition Let $\wp : [0, 1] \rightarrow C$ with $\wp(0) = z$ and $\wp(1) = w$; with a choice of labeling of sheets above $\pi^{-1}(z)$ and $\pi^{-1}(w)$, let z_i (resp. w_i) be a point on the i th sheet in $\pi^{-1}(z)$ (resp. $\pi^{-1}(w)$). Then, the set of charges of framed 2D-4D states corresponding to \wp is

$$\Gamma(z, w) := \bigsqcup_{i,j=1}^K \{[a] \in H_1(\Sigma, \{z_i\} \cup \{z_j\}; \mathbb{Z}) : a \text{ is a 1-chain with } \partial a = w_j - z_i \}.$$

Furthermore, for each $a \in \Gamma(z, w)$ we define the counting index $\overline{\Omega}(L_{\wp, \vartheta}, a)$ that, once again, can be defined via a supertrace over an appropriate Hilbert space, but we will only utilize its interpretation from a geometric perspective.

Remark It is believed that the theory obtained after insertion of the defect $L_{\wp, \vartheta}$ only depends on the homotopy class (rel boundary) of \wp . This homotopy invariance is the key ingredient that ties the story of spectral networks together.

2.1.3 Adding a Little Twist

Before proceeding to the definition of the \mathcal{W}_ϑ networks, we make an important technical detour. As discussed in [33], the indices $\mu(a)$ and $\overline{\Omega}(L_{\wp, \vartheta}, a)$ are only well-defined up to a sign, due to potential integer shift ambiguities in the fermion number operators that enter their definitions. To correct these ambiguities globally over all regions of parameter space, it suffices to construct (geometrically motivated) $\mathbb{Z}/2\mathbb{Z}$ extensions of Γ and $\Gamma(z, w)$. First, a bit of notation that will be used throughout this section and part of Appendix C.

Definition Let S be a real surface, then $\xi^S : \tilde{S} \rightarrow S$ is the unit tangent bundle projection to S .

The map $\xi_*^S : H_1(\tilde{S}; \mathbb{Z}) \rightarrow H_1(S; \mathbb{Z})$ has a kernel generated by the homology class that has a representative winding once around some fiber.

Definition Let $H \in H_1(\tilde{\Sigma}; \mathbb{Z})$ denote the homology class represented by a 1-chain that winds once around a fiber of $\tilde{\Sigma} \rightarrow \Sigma$, then

$$\tilde{\Gamma} := H_1(\tilde{\Sigma}; \mathbb{Z}) / (2H).$$

We abuse notation and denote the image of H in $\tilde{\Gamma}$ by H again.

It follows that $\tilde{\Gamma}$ is a $\mathbb{Z}/2\mathbb{Z}$ extension of Γ , i.e there is an exact sequence of abelian groups,

$$0 \rightarrow \mathbb{Z}/2\mathbb{Z} \rightarrow \tilde{\Gamma} \rightarrow \Gamma \rightarrow 0.$$

Similarly, for framed states and solitons we define extended charge sets. First we pass through an intermediate construction.

Definition Let $\tilde{\pi} : \tilde{\Sigma} \rightarrow \tilde{C}$ be the restriction of $d\pi : T\Sigma \rightarrow TC$ to the unit tangent bundle. For fixed $\tilde{z}, \tilde{w} \in \tilde{C}$, choose a labeling of sheets above $\pi^{-1}(z)$ and $\pi^{-1}(w)$; let z_i (resp. w_i) be a point on the i th sheet in $\pi^{-1}(z)$ (resp. $\pi^{-1}(w)$), then define

$$\begin{aligned} G_{ij}(\tilde{z}, \tilde{w}) &:= \left\{ [a] \in H_1(\tilde{\Sigma}, \{\tilde{z}_i\} \cup \{\tilde{w}_j\}; \mathbb{Z}) : a \text{ is a 1-chain with } \partial a = \tilde{w}_j - \tilde{z}_i \right\}, \\ G(\tilde{z}, \tilde{w}) &:= \bigsqcup_{i,j=1}^K G_{ij}(\tilde{z}, \tilde{w}). \end{aligned} \tag{2.7}$$

Remark $G(\tilde{z}, \tilde{w})$ is equipped with an $H_1(\tilde{\Sigma}; \mathbb{Z})$ action given by the addition of a closed cycle (at the level of chains).

This allows us to make the following definition,

Definition

$$\tilde{\Gamma}(\tilde{z}, \tilde{w}) := G(\tilde{z}, \tilde{w}) / \langle 2H \rangle. \tag{2.8}$$

Sometimes it is useful to view $\tilde{\Gamma}(\tilde{z}, \tilde{w})$ as a disjoint union of quotients of G_{ij} :

Definition

$$\tilde{\Gamma}_{ij}(\tilde{z}, \tilde{w}) := G_{ij}(\tilde{z}, \tilde{w}) / \langle 2H \rangle.$$

So we may write,

$$\tilde{\Gamma}(\tilde{z}, \tilde{w}) := \bigsqcup_{i,j=1}^K \tilde{\Gamma}_{ij}(\tilde{z}, \tilde{w}).$$

Remark

$\tilde{\Gamma}(\tilde{z}, \tilde{w})$ is equipped with a $\tilde{\Gamma}$ action, descending from addition of a closed cycle with a relative cycle. For $\gamma \in \tilde{\Gamma}$ and $a \in \tilde{\Gamma}(\tilde{z}, \tilde{w})$ we will denote this action by $\gamma : a \mapsto a + \gamma = \gamma + a$. In fact, for any ordered pair ij , $\tilde{\Gamma}_{ij}(\tilde{z}, \tilde{w})$ is a torsor for $\tilde{\Gamma}$.

$\tilde{\Gamma}(\tilde{z}, \tilde{w})$ carries an extra $\mathbb{Z}/2\mathbb{Z}$'s worth of ‘‘winding’’ information in the sense that $\tilde{\Gamma}(\tilde{z}, \tilde{w}) \xrightarrow{\text{proj}} \Gamma(z, w)$ is a principal $\mathbb{Z}/2\mathbb{Z}$ bundle, with proj given by forgetting lifts⁸, and the $\mathbb{Z}/2\mathbb{Z}$ action given by adding H .

⁸More precisely, proj is the map descending from the induced map on relative homology $(\xi^\Sigma)_* : H_1(\tilde{\Sigma}, \pi^{-1}(\tilde{z}) \cup \pi^{-1}(\tilde{w}); \mathbb{Z}) \rightarrow H_1(\Sigma, \pi^{-1}(z) \cup \pi^{-1}(w); \mathbb{Z})$ where $z = (\pi \circ \xi^\Sigma)(\tilde{z})$ and $w = (\pi \circ \xi^\Sigma)(\tilde{w})$.

Now, a soliton is a smooth curve on Σ ; furthermore, the tangent vectors at the endpoints (which lie on disjoint sheets) of a soliton are oppositely oriented in the sense that their pushforwards to C are oppositely oriented.

Definition Let $\tilde{z} \in \tilde{C}$, then $-\tilde{z} \in \tilde{C}$ is the unit tangent vector pointing in the opposite direction to \tilde{z} .

Remark To every soliton (represented by a smooth path) there is a natural lifted charge in $\tilde{\Gamma}(\tilde{z}, -\tilde{z})$ that descends from the relative homology class of the soliton's tangent framing lift.

We introduce one final piece of technology. First, note that for each $\tilde{z} \in \tilde{C}'$ there is a disjoint union of K lattices inside of the set $\tilde{\Gamma}(\tilde{z}, \tilde{z})$:

$$\bigsqcup_{i=1}^K \tilde{\Gamma}_{ii}(\tilde{z}, \tilde{z}) \subset \tilde{\Gamma}(\tilde{z}, \tilde{z}).$$

Any representative of an element in $\tilde{\Gamma}_{ii}(\tilde{z}, \tilde{z})$ has zero boundary, hence, is actually a cycle. Indeed, there is a canonical “basepoint forgetting” isomorphism of lattices $\tilde{\Gamma}_{ii}(\tilde{z}, \tilde{z}) \cong \tilde{\Gamma}$ for each $i = 1, \dots, K$, descending from the identity map at the level of chain representatives. This allows us to define the *closure* map.

Definition

$$\text{cl} : \bigsqcup_{i=1}^K \tilde{\Gamma}_{ii}(\tilde{z}, \tilde{z}) \rightarrow \tilde{\Gamma}$$

is the map which acts on each component by the “basepoint-forgetting” map described above.

Now, due to the sign ambiguity in μ and $\bar{\Omega}$ then, naïvely, only their absolute values are well-defined: i.e. we have functions,

$$\begin{aligned} \mu_{\geq 0} &: \bigcup_{z \in C'} \Gamma(z, z) \rightarrow \mathbb{Z}_{\geq 0} \\ \bar{\Omega}_{\geq 0}(\varphi, \cdot) &: \bigcup_{(z, w) \in C' \times C'} \Gamma(z, w) \rightarrow \mathbb{Z}_{\geq 0}. \end{aligned}$$

However, with our “lifted charge” definitions, we can lift $\mu_{\geq 0}$ to a function $\mu : \bigcup_{\tilde{z} \in \tilde{C}'} \tilde{\Gamma}(\tilde{z}, -\tilde{z}) \rightarrow \mathbb{Z}$ such that $\forall a \in \bigcup_{\tilde{z} \in \tilde{C}'} \tilde{\Gamma}(\tilde{z}, -\tilde{z})$,

$$\begin{aligned} |\mu(a)| &= \mu_{\geq 0}(\xi_*^\Sigma a) \\ \mu(a + H) &= -\mu(a). \end{aligned} \tag{2.9}$$

Similarly, fixing a path φ on C , the framed BPS degeneracies lift to well-defined functions $\bar{\Omega}(L_{\varphi, \vartheta}, \cdot) : \bigcup_{(\tilde{z}, \tilde{w}) \in \tilde{C}' \times \tilde{C}'} \tilde{\Gamma}(\tilde{z}, \tilde{w}) \rightarrow \mathbb{Z}$ such that $\forall a \in \bigcup_{(\tilde{z}, \tilde{w}) \in \tilde{C}' \times \tilde{C}'} \tilde{\Gamma}(\tilde{z}, \tilde{w})$,

$$\begin{aligned} |\bar{\Omega}(L_{\varphi, \vartheta}, a)| &= \bar{\Omega}_{\geq 0}(L_{\varphi, \vartheta}, \xi_*^\Sigma a) \\ \bar{\Omega}(L_{\varphi, \vartheta}, a + H) &= -\bar{\Omega}(L_{\varphi, \vartheta}, a). \end{aligned} \tag{2.10}$$

2.2 The \mathcal{W}_ϑ Networks

Using (2.4), we can produce a concrete picture of (the projections to C of) ij -solitons on the curve C . This motivates the following definitions.

Definition Fix $\vartheta \in \mathbb{R}/2\pi\mathbb{Z}$, for each (ordered) pair of sheets ij we define a (real) oriented line field $l_{ij}(\vartheta)$ on C^c given at every $z \in C^c$ by

$$l_{ij,z}(\vartheta) := \left\{ v \in T_z C : \operatorname{Im} \left[e^{-i\vartheta} \langle \lambda_{ij}, v \rangle \right] = 0 \right\},$$

with v positively oriented if $\operatorname{Re} \left[e^{-i\vartheta} \langle \lambda_{ij}, v \rangle \right] > 0$.

Given an integral curve p of $l_{ij}(\vartheta)$, the orientation of $l_{ij}(\vartheta)$ tells us how to lift the curve back to a curve p_Σ on Σ .

Definition Any integral curve p (on C') of $l_{ij}(\vartheta)$ has a lift to a curve p_Σ on Σ defined as the union of $p\{i\}$ (the lift of p to the i th sheet), and $p^-\{j\}$ (the lift of p to the j th sheet, reversing orientation).

Remarks

- Fix $z_* \in C^c$ and take a neighborhood U of z_* that does not contain any branch cuts of type ij . Then for each ordered pair ij we can define local coordinates $w_{ij} : U \rightarrow \mathbb{C}$ by

$$w_{ij}(z) = \int_{z_*}^z (\lambda_i - \lambda_j). \quad (2.11)$$

In these coordinates, the integral curves of $l_{ij}(\vartheta)$ are precisely the straight lines of inclination ϑ .

- Note that the line field $l_{ji}(\vartheta)$ is just $l_{ij}(\vartheta)$ with reversed orientation.
- On a cycle surrounding a branch point of type ij , the monodromy action induces $\lambda_{ij} \mapsto \lambda_{ji} = -\lambda_{ij}$; hence, $l_{ij}(\vartheta) \mapsto l_{ji}(\vartheta)$ (i.e., the line field orientation reverses when passing through a branch cut extending from a branch point.)

We can finally define the (real) codimension-1 networks of interest.

Definition

$$\mathcal{W}_\vartheta = \bigcup_{\text{ordered pairs } ij} \{p : p \text{ is an integral curve of } l_{ij}(\vartheta) \text{ and } p \text{ supports a soliton of phase } \vartheta\} \subset C'.$$

The network \mathcal{W}_ϑ is composed of individual integral curve segments, which may interact and join each other at vertices on C' .

Definitions

1. An individual integral curve segment on \mathcal{W}_ϑ is called a *street*.⁹ A *street of type ij* is a street that is an integral curve of $l_{ij}(\vartheta)$.
2. A *joint* is a point on C' where two or more streets of different types meet.

The upshot of all these constructions is that now we have a solidified picture of solitons via a network on C' . Indeed, we can lift \mathcal{W}_ϑ to a graph on $\text{Lift}(\mathcal{W}_\vartheta) \subset \Sigma$ by taking the union of the lifts (as defined above) p_Σ of each street p . Then an ij soliton of phase ϑ traces out a path supported on $\text{Lift}(\mathcal{W}_\vartheta)$, and begins and ends on points z_i, z_j that are lifts to the i th and j th streets (respectively) of a point z on a street of type ij . In particular, an ij street of \mathcal{W}_ϑ represents the endpoints of a set of solitons of type ij .

From a constructive viewpoint, however, the reader may feel unsatisfied as we have not yet defined how to determine the condition that $p \subset \mathcal{W}_\vartheta$ actually *supports* a soliton of phase ϑ , i.e. $\mu(a, p) \neq 0$, for some a the charge of a soliton of phase ϑ . To fill this void we remark that there are exactly three integral curves of $l_{ij}(\vartheta) \cup l_{ji}(\vartheta)$ emerging from each ij -branch point. On each such integral curve p there is a family of solitons represented by “small” paths: for $z \subset p$ and $z_i, z_j \in \pi^{-1}(z)$ lifts of z to sheet i and sheet j (respectively), there is a soliton supported on p_Σ traveling from $z_i \in \Sigma$, through the ramification point on Σ , to $z_j \in \Sigma$. Such solitons become arbitrarily light as z approaches the branch point. Furthermore, as argued in [33], letting a be the (lifted) charge of any soliton in this family, we assign

$$\mu(a, p) = +1. \tag{2.12}$$

Terminology The “light” solitons described in the previous paragraph will be called *simpletons*.

We defer the problem of determining the soliton indices μ on all other streets until the appropriate definitions are developed in the next section; for now it will suffice to say that, with this condition, the soliton indices on all other streets can be determined via a set of algebraic equations.

2.2.1 \mathcal{K} -walls and Degenerate Networks

Of particular interest in this paper will be \mathcal{W}_ϑ networks of a very special type.

Definition A street $p \subset \mathcal{W}_\vartheta$ is *two-way* if it consists of a coincident ij -street and a ji -street. Equivalently, p supports ij -solitons and ji -solitons. A street that is not two-way is called *one-way*. A network that contains a two-way street is said to be *degenerate*.

We adopt the following convention in order to keep track of the individual directions of the constituent one-way streets of a two-way street.

⁹In [33] these were also referred to as S -walls.

Convention Let p be a two-way street consisting of coincident ij and ji -streets, then we will say p is of type ij and assign it the orientation of its constituent ij -street. (Or, equivalently, we will say p is of type ji and assign it the orientation of its constituent ji -street.)

As described in [33], sec. 6.2, for generic values of ϑ , the network \mathcal{W}_ϑ will only contain one-way streets due to a bifurcation behavior of integral curves near branch points. However, at critical values $\vartheta_c \in \mathbb{R}/\mathbb{Z}$, an ij street will collide with a ji street and the network $\mathcal{W}_{\vartheta_c}$ will contain two-way streets. Now we make an important claim:

\mathcal{W}_ϑ contains a two-way street $\Rightarrow \exists$ a homologically non-trivial closed loop on Σ satisfying (2.3) for some phase $\vartheta \in \mathbb{R}/2\mathbb{Z}$.

To see this, fix a point $z \in p \subset C$ on any two-way street p ; without loss of generality we will say p is of type ij . Then z supports a soliton of type ij and a soliton of type ji , both of the same phase ϑ ; the concatenation of these two paths yields a closed loop l satisfying (2.3) for the phase ϑ . Moreover, this loop is homologically non-trivial. Indeed, the period of l is just the sum of the periods of the two solitons forming it. However, both have periods (central charges) of the same phase; so the sum must be nonzero.

Thus, via the claim, a degenerate network automatically leads to a possible 4D BPS state of charge $[l] \in \Gamma$; in fact, there are possible BPS states of charges $n[l]$, $n \in \mathbb{Z}_{>0}$. All that remains is to determine the BPS indices $\Omega(n[l])$ which, as expressed more explicitly below, are computable from the soliton data supported on \mathcal{W}_ϑ .

In practice, degenerate networks can be found by looking for discontinuous changes in the topology of \mathcal{W}_ϑ as ϑ is varied. Indeed, if a region $R \subset \mathbb{R}/\mathbb{Z}$ does not contain any degenerate networks then, as ϑ is varied continuously in R , the network \mathcal{W}_ϑ also varies continuously (in the sense described in [33]). However, if the region R contains a single critical angle ϑ_c , the bifurcation of integral curves near a branch point induces a discontinuous change in the topology of \mathcal{W}_ϑ as ϑ is varied¹⁰ past ϑ_c . (If we consider the parameter space of ϑ and the Coulomb branch then the locus where degenerate networks appear defines \mathcal{K} -walls.)

2.2.2 Formal Variables

In order to construct the generating functions that keep track of various BPS degeneracy indices, it is helpful to construct spaces of formal variables with some algebraic structure.

¹⁰However, there may be an accumulation point of critical angles as in the picture of the vector multiplet when $K = 2$ (see [33]). Around such an accumulation point the topology of \mathcal{W}_ϑ rapidly changes, and there is no open region containing the accumulation point where the topology smoothly varies. Even “worse,” as we will see, the critical angles can densely fill an open interval.

Definition $\mathbb{Z}[\tilde{\Gamma}]$ is the commutative ring of formal series generated by formal variables X_γ , $\gamma \in \tilde{\Gamma}$ such that

$$\begin{aligned} X_0 &= 1, \\ X_H &= -1, \\ X_\gamma X_{\gamma'} &= X_{\gamma+\gamma'}. \end{aligned}$$

To define an algebraic structure for formal variables in 2D-4D/soliton charges, we note that there is a partially defined “addition” operation.

Definitions

1. Let $a \in \tilde{\Gamma}(\tilde{z}_1, \tilde{z}_2)$, then

$$\begin{aligned} \text{end}(a) &= \tilde{z}_2 \\ \text{start}(a) &= \tilde{z}_1. \end{aligned}$$

2. Let $a, b \in \bigcup_{\tilde{z}, \tilde{w} \in \tilde{C}} \tilde{\Gamma}(\tilde{z}, \tilde{w})$, then if $\text{end}(a) = \text{start}(b)$ there is a well-defined operation (concatenation of paths) $a + b \in \bigcup_{\tilde{z}, \tilde{w} \in \tilde{C}} \tilde{\Gamma}(\tilde{z}, \tilde{w})$ descending from the usual addition of relative homology cycles.

With this we can define the space of interest.

Definition The *homology path algebra* \mathcal{A} is the non-commutative $\mathbb{Z}[\tilde{\Gamma}]$ -algebra of formal series generated by formal variables X_a , for every $a \in \bigcup_{\tilde{z}, \tilde{w} \in \tilde{C}} \tilde{\Gamma}(\tilde{z}, \tilde{w})$; such that

1. For $\gamma \in \tilde{\Gamma}$,

$$X_\gamma X_a = X_{a+\gamma} = X_{\gamma+a},$$

2. for any $a, b \in \bigcup_{\tilde{z}, \tilde{w} \in \tilde{\Sigma}} \tilde{\Gamma}(\tilde{z}, \tilde{w})$

$$X_a X_b = \begin{cases} X_{a+b}, & \text{if } \text{end}(a) = \text{start}(b) \\ 0, & \text{otherwise} \end{cases}.$$

There are two important $\mathbb{Z}[\tilde{\Gamma}]$ -subalgebras of \mathcal{A} .

Definition

1. \mathcal{A}_S is the $\mathbb{Z}[\tilde{\Gamma}]$ -subalgebra generated by formal variables in soliton charges $a \in \bigcup_{\tilde{z} \in \tilde{C}} \tilde{\Gamma}(\tilde{z}, -\tilde{z})$.

2. \mathcal{A}_C is the (commutative) $\mathbb{Z}[\tilde{\Gamma}]$ -subalgebra generated by formal variables in $a \in \bigcup_{\tilde{z} \in \tilde{C}} \bigsqcup_{i=1}^K \tilde{\Gamma}_{ii}(\tilde{z}, \tilde{z})$.

The closure map can be easily extended to \mathcal{A}_C .

Definition

$$\text{cl} : \mathcal{A}_C \rightarrow \mathbb{Z}[\tilde{\Gamma}]$$

is the linear extension of the map

$$\text{cl}(X_a) = X_{\text{cl}(a)}.$$

We now define generating functions for BPS indices.

Definition For each path φ from $z \in C$ to $w \in C$ that represents an interface $L_{\varphi, \vartheta}$, we associate the framed generating function

$$F(\varphi, \vartheta) := \sum_{a_* \in \Gamma(z, w)} \bar{\Omega}(L_{\varphi, \vartheta}, a) X_a \in \mathcal{A},$$

where $a \in \tilde{\Gamma}(\tilde{z}, \tilde{w})$ is a lift of the charge $a_* \in \Gamma(z, w)$ such that \tilde{z} and \tilde{w} are the unit tangent vectors at the ends of φ .

For each street p of type ij , we associate two *soliton generating functions*: $\Upsilon(p)$, that encodes the indices of solitons of type ij , and $\Delta(p)$, that encodes the indices of solitons of type ji .

Definition Let $z \in p \subset C$, then we define

$$\Upsilon_z(p) := \sum_{a_* \in \Gamma_{ij}(z, z)} \mu(a) X_a \in \mathcal{A}_S \tag{2.13}$$

$$\Delta_z(p) := \sum_{b_* \in \Gamma_{ji}(z, z)} \mu(b) X_b \in \mathcal{A}_S, \tag{2.14}$$

where $a \in \tilde{\Gamma}_{ij}(\tilde{z}, -\tilde{z})$, $b \in \tilde{\Gamma}_{ji}(-\tilde{z}, \tilde{z})$ denote respective lifts of $a_* \in \Gamma_{ij}(z, z)$ and $b_* \in \Gamma_{ji}(z, z)$, for $\tilde{z} \in \tilde{C}$ the unit tangent vector agreeing with the orientation of p at the point $z \in C$.¹¹

Definition From the soliton generating functions on a street p , we can define the *street factor*,

$$\begin{aligned} Q(p) &:= \text{cl} [1 + \Upsilon_z(p) \Delta_z(p)] \\ &= 1 + \sum_{a_* \in \Gamma_{ij}(z, z), b_* \in \Gamma_{ji}(z, z)} \mu(a) \mu(b) X_{\text{cl}(a+b)} \in \mathbb{Z}[\tilde{\Gamma}]. \end{aligned}$$

where $z \in C$ is any point on p .

¹¹As $\tilde{\Gamma}(\tilde{z}, -\tilde{z})$ is a principal $\mathbb{Z}/2\mathbb{Z}$ bundle over $\Gamma(z, z)$, there are two possible lifts of a_* related by addition of H . Via $X_H = -1$ along with (2.9) and (2.10), the definition of $\Upsilon_z(p)$ is independent of the choice of lift. This argument also applies to $\Delta_z(p)$.

Remark As the notation suggests, $Q(p)$ is independent of the choice of point z . This follows as the index $\mu(a)$ is constant as any charge a is parallel transported along any path supported on $p \subset C$. By the same reasoning, for any $z, z' \in p$, $\Upsilon_z(p)$ and $\Upsilon_{z'}(p)$ are related by applying an appropriate parallel transport map¹² (similarly for $\Delta_z(p)$ and $\Delta_{z'}(p)$).

And now for the punchline.

2.2.3 Computing $\Omega(n\gamma_c)$

The power of the spectral network machine can be summarized with the following squiggly arrows:

$$\begin{array}{ccc} \text{Jumping of Framed 2D-4D} & \overset{(A)}{\rightsquigarrow} & \text{Soliton Spectrum} & \overset{(B)}{\rightsquigarrow} & \text{(Vanilla) 4D spectrum.} \\ \text{Spectrum + Homotopy In-} & & & & \\ \text{variance of } L_{\varphi, \vartheta} & & & & \end{array}$$

To understand (A): the framed generating function $F(\varphi, \vartheta)$ is piecewise constant in the sense that as the endpoints of φ are varied on $C - \mathcal{W}_\vartheta$, then $F(\varphi, \vartheta)$ does not vary in \mathcal{A} ; however, if an endpoint of φ is varied across a street of \mathcal{W}_ϑ , then $F(\varphi, \vartheta)$ will jump in a manner depending on the spectrum of solitons located on that street. Indeed, $F(\varphi, \vartheta)$ is the sum of the charges of “millipedes,” and as the “body” φ of each such millipede crosses the street p , then the millipede can gain an extra leg by detouring along a soliton supported along p ; hence, the spectrum of 2D-4D states (represented by millipedes) will jump. To reproduce the soliton spectrum we utilize the homotopy invariance of the operator $L_{\varphi, \vartheta}$ to equate the different jumps of $F(\varphi, \vartheta)$ across different, but homotopic (rel endpoints), paths φ . The resulting equations are equivalent to conditions on the soliton generating functions. These conditions, combined with the simpleton input data (2.12), allow us to completely determine the soliton generating functions, which encapsulate the soliton spectrum.

To describe (B), let $\Gamma_c \subset \Gamma$ be the lattice of charges γ with $e^{-i\vartheta_c} Z_\gamma \in \mathbb{R}_-$; then the degenerate network $\mathcal{W}_{\vartheta_c}$ captures all of the 4D BPS states carrying charges $\gamma \in \Gamma_c$. Their spectrum can be extracted from the generating functions $Q(p)$. But, first we have to deal with a technical point.

Definitions

1. For every curve q on a surface S , there is a canonical “lift” \widehat{q} to a curve on \widetilde{S} , given by the tangent framing.
2. For each $\gamma \in \Gamma$, we define another lift $\widetilde{\gamma} \in \widetilde{\Gamma}$ by the following rule. First, represent γ as a union of smooth closed curves β_m on Σ . Then $\widetilde{\gamma}$ is the sum of $\widehat{\beta}_m$, shifted by $\left(\sum_{m \leq n} \delta_{mn} + \#(\beta_m \cap \beta_n)\right) H$ (of course, because we work modulo $2H$, all that matters here is whether this sum is odd or even.)

¹²For this reason, the point z in soliton generating functions is often dropped as in the calculations of Appendix C.

One can check directly (see Appendix E) that $\tilde{\gamma}$ so defined is independent of the choice of how we represent γ as a union of β_m ; this requirement is what forced us to add the tricky-looking shift.

Then, for each street p , we factorize $Q(p)$ as a product:

Definition

$$Q(p) = \prod_{\gamma \in \Gamma_c} (1 - X_{\tilde{\gamma}})^{\alpha_{\gamma}(p)}. \quad (2.15)$$

This representation determines the coefficients $\alpha_{\gamma}(p)$.

Definition Let $p_{\Sigma} \in C_1(\Sigma; \mathbb{Z})$ be the one-chain corresponding to the lift p_{Σ} , then we define¹³

$$L(\gamma) := \sum_{\text{streets } p} \alpha_{\gamma}(p) p_{\Sigma} \in C_1(\Sigma; \mathbb{Z}). \quad (2.16)$$

Now, as shown in [33], the magic of this definition is that $L(\gamma)$ is actually a 1-cycle satisfying the BPS condition (2.2) for $\vartheta = \vartheta_c$.¹⁴ Let us make the further assumption that Γ_c is a rank-1 lattice, which holds automatically off of the walls of marginal stability on \mathcal{B} , then it follows that both γ and $[L(\gamma)]$ are multiples of a choice of generator $\gamma_c \in \Gamma_c$. With this in mind, the journey to the end of the squiggly arrow (B) follows by analyzing the jumping of $F(\wp, \vartheta)$, but now as ϑ is varied across the critical angle ϑ_c (fixing \wp). The resulting analysis (see [33], sec. 6) leads us to the desired result:

$$[L(\gamma)] = \Omega(\gamma)\gamma, \quad \gamma \in \Gamma_c, \quad (2.17)$$

from which all BPS indices of 4D BPS states with central charge phase ϑ_c can be computed.

Abstract Spectral Networks

It is possible to abstract the properties of the \mathcal{W}_{\wp} networks in order to draw networks on C that do not necessarily come from integral curves of (2.4). It is not necessary to give a precise list of the properties here, and we instead refer the interested reader to Section 9 of [33]. There, the abstracted networks are particularly useful for defining the “non-abelianization map” between moduli spaces of flat $GL(1)$ -bundles on Σ , and flat $GL(K)$ -bundles on C . In this paper, however, our interest in abstract spectral networks will be in constructions of *potential* \mathcal{W}_{\wp} networks. Indeed, the m -herds mentioned in the introduction, and introduced in Section 3.1, are examples of abstract networks on an arbitrary curve C . By searching the parameter space of the pure $SU(3)$ theory, where $C = S^1 \times \mathbb{R}$ and $K = 3$, it turns out that a large subset of m -herds actually arise as \mathcal{W}_{\wp} networks at various points on the Coulomb branch.

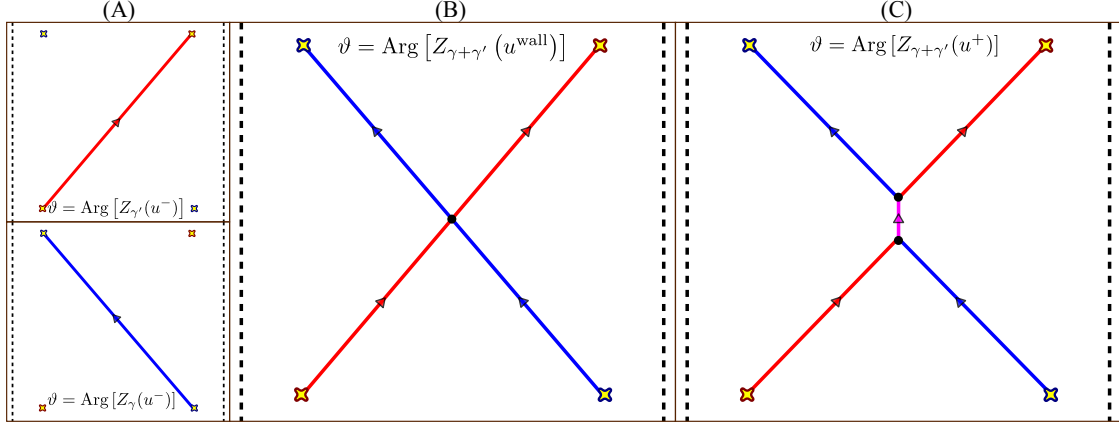


Figure 1. A hypothetical wall-crossing of two hypermultiplets with charges γ, γ' such that $\langle \gamma, \gamma' \rangle = 1$. Streets of type 12 are shown in red, 23 in blue, and 13 in fuchsia; only two-way streets are depicted. Arrows denote street orientations according to the convention described in Section 2.2.1. Yellow crosses denote branch points. Arrows denote the direction of solitons of type 12, 23, or 13 (according to the street). The black dotted lines are identified to form the cylinder. (A): The two hypermultiplet networks at a point u^- just “before” the wall of marginal stability. (B): The hypermultiplet networks at a point u^{wall} on the wall of marginal stability and at phase $\vartheta = \arg [Z_{\gamma}(u^{\text{wall}})] = \arg [Z_{\gamma'}(u^{\text{wall}})] = \arg [Z_{\gamma+\gamma'}(u^{\text{wall}})]$. (C): Slightly “after” the wall at a point u^+ , a BPS bound state of charge $\gamma + \gamma'$ is born and a two-way street of type 13 “grows” as one proceeds away from the wall.

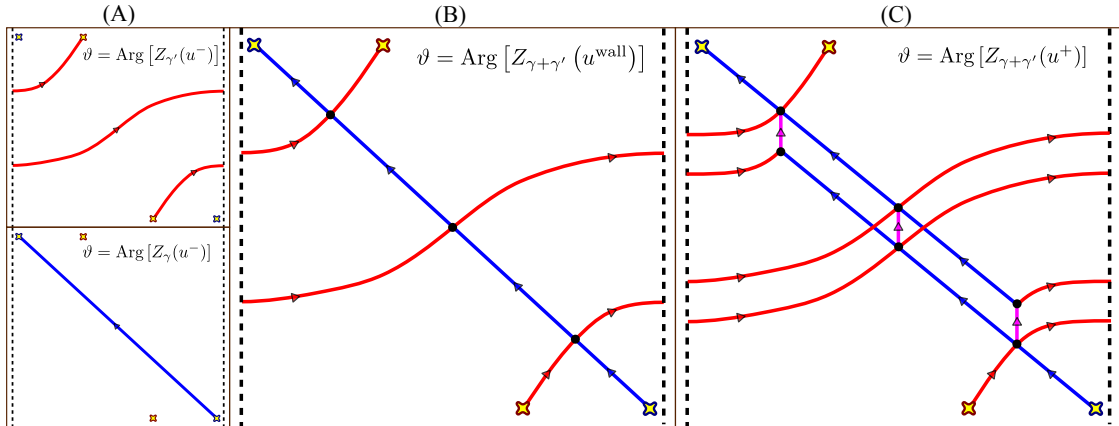


Figure 2. A hypothetical wall-crossing of two hypermultiplets with charges γ, γ' such that $\langle \gamma, \gamma' \rangle = 3$. The story is similar to that described in the caption of Fig. 1.

3 Spectral network analysis of a wild point on the Coulomb branch

3.1 Horses and Herds

We begin by describing a sequence of spectral networks that may arise in the hypothetical wall-crossing between two BPS hypermultiplets of charges $\gamma, \gamma' \in \Gamma$ such that $\langle \gamma, \gamma' \rangle = m$. Indeed, assume at some point on the Coulomb branch there are two BPS states (occurring at different phases) such that the degenerate network associated to each state has a single two-way street given by a simple curve passing through two branch points of the same type (frame (A) of Figs. 1-2); such spectral networks are associated to BPS hypermultiplets. Now, assume that there exists a marginal stability wall on the Coulomb branch associated to the (central charge phase) crossing of these two hypermultiplets (and no other BPS states). On the other side of the wall, a possible bound state of charge $\gamma + \gamma'$ may be formed (where γ, γ' are the charges of the original hypermultiplets). Figs. 1-2 depict three hypothetical snapshots along a path passing through the wall of marginal stability for the cases $m = 1, 3$; frame (C) depicts a guess at the appearance of the degenerate network associated to the bound state of charge $\gamma + \gamma'$. After drawing such pictures for progressively higher m , and given a sufficient dose of mildly-confused staring, one will begin to notice that the (two-way streets of) networks associated to the bound state of charge $\gamma + \gamma'$ can be decomposed into m -components that look like “extended” saddles; as they are the generalization of saddles we have no choice but to call each such component a “horse.”

Definitions

1. A *horse street* $p \in \{a_1, a_2, a_3, b_1, b_2, b_3, c, \bar{a}_1, \bar{a}_2, \bar{a}_3, \bar{b}_1, \bar{b}_2, \bar{b}_3\}$ is one of the streets of Fig. 3 (left frame).
2. Let N be a spectral network (subordinate to some branched cover $\Sigma \rightarrow C$) and $U \subset C'$ be an open disk region. Then $U \cap N$ is a *horse* if a subset of its streets can be identified with Fig. 3 in a way such that:
 - (a) every two-way street is a horse street,
 - (b) there is always a two-way street identified with the street labeled c .

We can reconstruct the two-way streets of the full spectral network by gluing m horses back together. This leads us to the following working definition (a more complete definition is provided in Appendix C), which we extend to any curve C .

Working Definition Given a collection of m horses, let $p^{(l)}$ denote a horse street on the l th horse ($l = 1, \dots, m$). A spectral network on a curve C is an m -herd if its two-way streets are

¹³Note that the sum over streets in (2.16) reduces to a sum over two-way streets; indeed, $Q(p) \neq 1$ iff p is two-way.

¹⁴This last comment follows from the fact that $\int_{p_\Sigma} \lambda = \int_p \lambda_{ij} \in e^{i\vartheta} \mathbb{R}_{<0}$ for any street p of type ij .

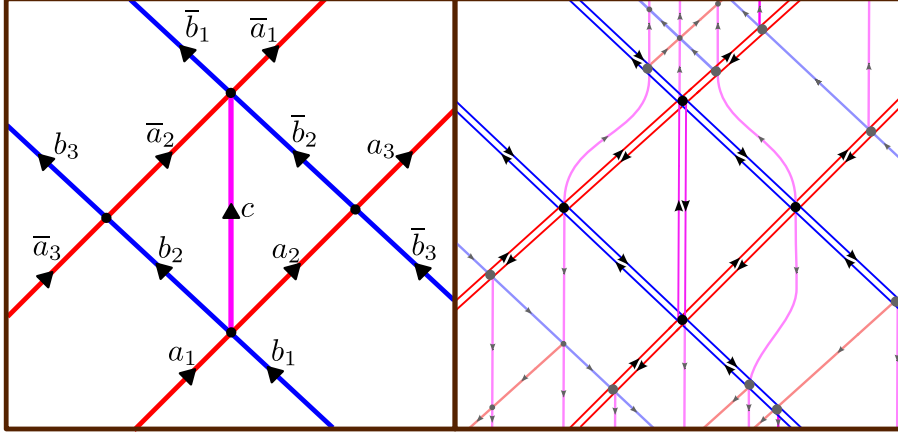


Figure 3. *Left Frame:* Two-way streets of a horse on some open disk U ; the solid streets depicted are capable of being two-way; one-way streets are not shown. The sheets of the cover $\Sigma \rightarrow C$ are (locally) labeled from 1 to $K \geq 3$. Red streets are of type 12, blue streets are of type 23, and fuchsia streets are of type 13. We choose an orientation for this diagram such that all streets “flow up.” *Right Frame:* A relatively simple example of a horse with one-way streets shown as partially transparent and two-way streets resolved (using the “British resolution”, cf. Appendix B or [33]). One can imagine horses with increasingly intricate “backgrounds” of one-way streets.

generated by gluing together m horses using the following relations:

$$\begin{aligned}
 a_1^{(l)} &= a_3^{(l-1)} \\
 b_1^{(l)} &= b_3^{(l-1)} \\
 \bar{a}_1^{(l)} &= \bar{a}_3^{(l+1)} \\
 \bar{b}_1^{(l)} &= \bar{b}_3^{(l+1)},
 \end{aligned}
 \tag{3.1}$$

and such that $a_1^{(1)}$, $b_1^{(1)}$, $\bar{a}_1^{(m)}$, and $\bar{b}_1^{(m)}$ are connected to four distinct branch points.

Remark It can be shown from our definition that a 1-herd (which consists of a single horse) is just a saddle. Indeed, a small computation will show that $Q(p)$ is nontrivial ($Q(p) \neq 1$) only for $p = a_1, \bar{a}_1, b_1, \bar{b}_1$, and c ; this leads us to the picture of a saddle extending from four branch points (pictured in the top left corner of Fig. 4).

An advantage of the decomposition into horses is computability: a horse should be thought of as a scattering machine which takes inflowing solitons, and regurgitates outgoing solitons as well as all spectral data “bound” to the horse.¹⁵ The combinatorial problem of computing the BPS degeneracies $\Omega(n\gamma_c)$, $n \geq 1$, using spectral network machinery, is then greatly simplified and explicit results can be obtained for all $m \geq 1$. In fact, we have the following.

¹⁵See Appendix C.3 for a the precise and explicit description of the horse as a scattering machine.

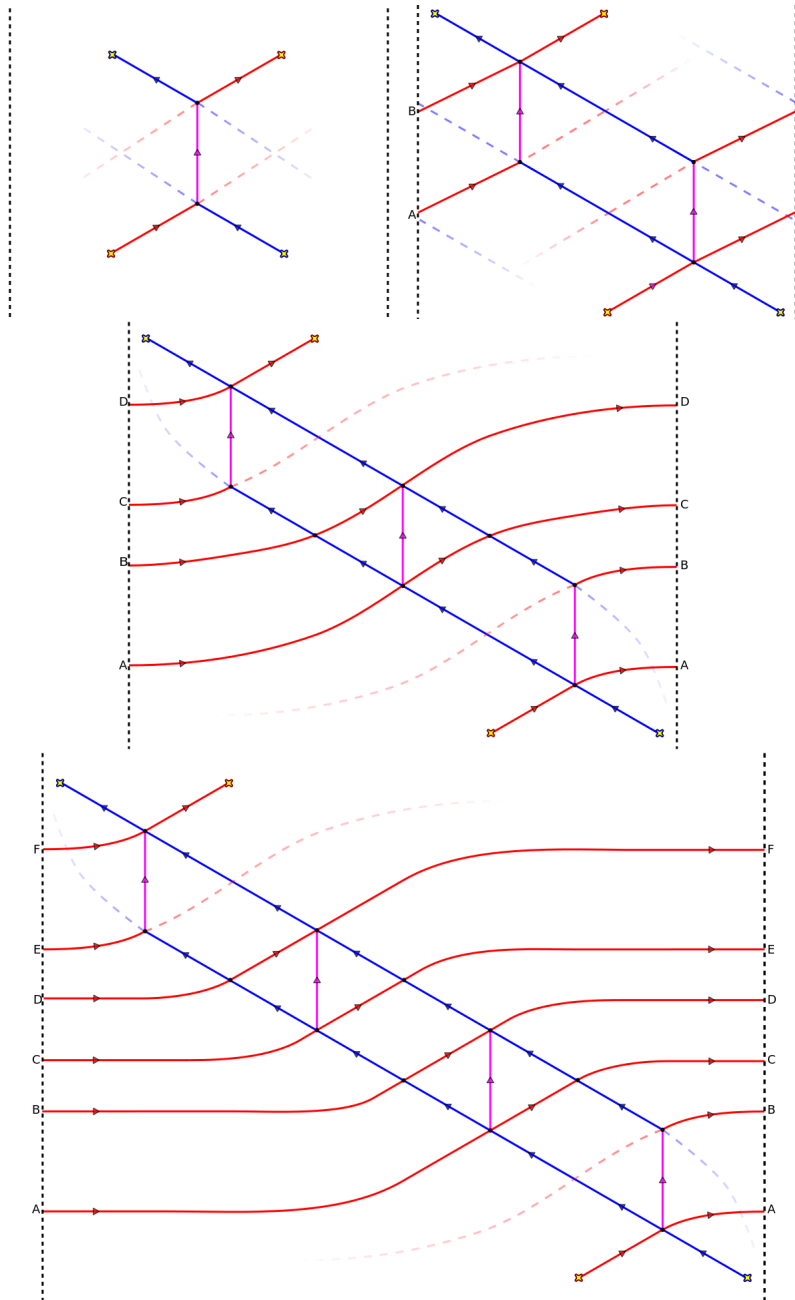


Figure 4. The first four herds on the cylinder. Solid streets are two-way; dotted, transparent streets are streets of Fig. 3 that happen to be only one-way as indicated by Prop. 3.1. The black dotted lines are identified to form the cylinder and capital Latin letters are placed on either side to aid in the identification of streets. Top row (from left to right): The 1-herd (saddle) and 2-herd. The middle row shows a 3-herd and the bottom row shows a 4-herd.

Proposition 3.1. *Let N be an m -herd, then $Q(p)$ for all two-way streets p on N are given in terms of powers of a single generating function P_m satisfying the algebraic equation*

$$P_m = 1 + z (P_m)^{(m-1)^2}, \quad (3.2)$$

where $z = (-1)^m X_{\tilde{\gamma} + \tilde{\gamma}'}$ for some $\gamma, \gamma' \in H_1(\Sigma; \mathbb{Z})$ such that $\langle \gamma, \gamma' \rangle = m$. In particular, adopting the notation $Q(p, l) := Q(p^{(l)})$,

$$\begin{aligned} P_m &= Q(c, l) \\ (P_m)^{m-l} &= Q(a_2, l) = Q(b_2, l) = Q(a_3, l) = Q(b_3, l) \\ (P_m)^{l-1} &= Q(\bar{a}_2, l) = Q(\bar{b}_2, l) = Q(\bar{a}_3, l) = Q(\bar{b}_3, l) \\ (P_m)^{m-l+1} &= Q(a_1, l) = Q(b_1, l) \\ (P_m)^l &= Q(\bar{a}_1, l) = Q(\bar{b}_1, l). \end{aligned} \quad (3.3)$$

for $l = 1, \dots, m$.

Proof. See Appendix C.6 for the full calculational proof. \square

The precise cycle $\gamma_c = \gamma + \gamma'$ that appears depends on the embedding of N in C as a graph. Further, as shown at the end of Appendix C.6, there are cycles representing γ and γ' that look like the charges of simple ‘‘saddle-connection’’ hypermultiplets. Indeed, the cycle representing either γ or γ' projects down to a path on C that runs between two distinct branch points of the same type. These are precisely the (hypothetical) hypermultiplets whose wall-crossing motivated the construction of m -herds.¹⁶

Remarks

- A street p is two-way iff $Q(p) \neq 1$. Thus, (3.3) states that on the first ($l = 1$) and last ($l = m$) horses, some streets depicted in Fig. 3 are only one-way.
- When $m = 1, 2$, (3.2) has easily derivable solutions:

$$P_1 = 1 + z, \quad (3.4)$$

$$P_2 = (1 - z)^{-1}. \quad (3.5)$$

For a saddle ($m = 1$), this result, combined with (3.3), states that there are five two-way streets; each such two-way street p is equipped with a generating function $Q(p) = 1 + z$, as originally derived in [33].

¹⁶The representative cycles discussed here, however, do not live entirely on $\text{Lift}(N) \subset \Sigma$. Roughly speaking representatives of γ, γ' are given by the lifts of paths running along the a_i, \bar{a}_i and b_i, \bar{b}_i respectively, but these do not define closed paths on Σ without running through at least one street of type 13.

3.2 Connection with Kontsevich-Soibelman, Gross-Pandharipande

The algebraic equation (3.2) and relevant solutions appear in a conjecture by Kontsevich and Soibelman (KS) [16], later proven by Reineke [17] and generalized by Gross-Pandharipande (GP) [20]. A series solution of (3.2) can be obtained using the Lagrange formula for reversion of series and the result for $m > 1$ is [16]:

$$\begin{aligned} P_m &= \sum_{n=0}^{\infty} \frac{1}{1 + (m^2 - 2m)n} \binom{(m-1)^2 n}{n} z^n, \\ &= \exp \left[\sum_{n=1}^{\infty} \frac{1}{(m-1)^2 n} \binom{(m-1)^2 n}{n} z^n \right]. \end{aligned} \tag{3.6}$$

To describe the connection between our result and that of KS and GP, we review the generalized conjecture of GP, briefly adopting their notation in [20].

The algebraic equation (3.2) appears in [20].¹⁷ There, the object of study is a group of (formal 1-parameter families of) automorphisms of the torus $\mathbb{C}^* \times \mathbb{C}^*$ generated by $\theta_{(a,b),f}$ that are defined by

$$\theta_{(a,b),f}(x) = f^{-b} \cdot x, \quad \theta_{(a,b),f}(y) = f^a \cdot y$$

where x and y are coordinate functions on the two factors of $\mathbb{C}^* \times \mathbb{C}^*$, $(a, b) \in \mathbb{Z}^2$, and f is a formal series of the form

$$f = 1 + x^a y^b \left[t f_1(x^a y^b) + t^2 f_2(x^a y^b) + \cdots \right], \quad f_i(z) \in \mathbb{C}[z].$$

Alternatively we may say $f \in \mathbb{C}[x, x^{-1}, y, y^{-1}][[t]]$ (i.e. f is a formal power series in t with coefficients Laurent polynomials in x and y). Such automorphisms preserve the holomorphic symplectic form

$$\omega = (xy)^{-1} dx \wedge dy.$$

Now, letting

$$S_q = \theta_{(1,0),(1+tx)^q}, \quad T_r = \theta_{(0,1),(1+ty)^r},$$

we consider the commutator

$$T_r^{-1} \circ S_q \circ T_r \circ S_q^{-1} = \overrightarrow{\prod} \theta_{(a,b),f_{(a,b)}} \tag{3.7}$$

where the product on the right hand side is over primitive vectors $(a, b) \in \mathbb{Z}^2$ (i.e. $\gcd(a, b) = 1$) such that $a, b > 0$, and the order of the product is taken with increasing slope a/b from left to right. The conjecture of Gross-Pandharipande involves the slope 1 term of (3.7).

Conjecture (Gross-Pandharipande)

For arbitrary (q, r) , the slope 1 term $\theta_{(1,1),f_{(1,1)}}$ in (3.7) is specified by

$$f_{1,1} = \left(\sum_{n=0}^{\infty} \frac{1}{(qr - q - r)n + 1} \binom{(q-1)(r-1)n}{n} t^{2n} x^n y^n \right)^{qr}.$$

¹⁷A different, but related, algebraic equation on the quantity $(P_m)^m$ was originally stated by Kontsevich and Soibelman in [16].

The case $q = r$ was first conjectured by KS, and later proven by Reineke. Now, letting

$$\mathcal{P}_{q,r} = \sum_{n=0}^{\infty} \frac{1}{(qr - q - r)n + 1} \binom{(q-1)(r-1)n}{n} t^{2n} x^n y^n, \quad (3.8)$$

For general q, r , Gross and Pandharipande noted that $\mathcal{P}_{q,r}$ satisfies the equation

$$t^2 xy (\mathcal{P}_{q,r})^{(q-1)(r-1)} - \mathcal{P}_{q,r} + 1 = 0; \quad (3.9)$$

so that $f_{1,1}$ is an algebraic function (over $\mathbb{Q}(t, x, y)$).

In the case $q = r = m$, the equation (3.9) and solution (3.8) bear striking similarity to (3.2) and (3.6), which motivates identifying $t^2 xy = z$ in hopes of identifying $\mathcal{P}_{m,m}$ with P_m .

To motivate the identification $t^2 xy = z$, we turn our attention back to the original motivation for our definition of m -herds: they are expected to arise after two hypermultiplets of charges γ, γ' , with $\langle \gamma, \gamma' \rangle = m$, cross a wall of marginal stability. If m -herds do arise in this manner, then in the resulting wall-crossing formula we should expect the P_m to be related to the generating function for the KS transformations attached to the charges $n(\gamma + \gamma')$, $n > 0$. We now go about unpacking the identification of such a wall crossing formula with (3.7).

Assume on one side of the wall $\arg(Z_\gamma) < \arg(Z_{\gamma'})$, then the wall crossing formula reads (see Section 5.1)

$$\mathcal{K}_\gamma \mathcal{K}_{\gamma'} = \mathcal{K}_{\gamma'} \left[\prod_{(a,b) \in \mathbb{Z}^2} (\mathcal{K}_{a\gamma + b\gamma'})^{\Omega(a\gamma + b\gamma')} \right] \mathcal{K}_\gamma \quad (3.10)$$

where all products are taken in order of increasing central charge phase (when read from left to right) and the \mathcal{K}_α are transformations on a twisted Poisson algebra of functions on the torus $T = \Gamma \otimes_{\mathbb{Z}} \mathbb{C}^\times$, i.e. the space of functions generated by polynomials in formal variables $Y_\alpha, \alpha \in \Gamma$ equipped with twisted product given by

$$Y_\alpha Y_\beta = (-1)^{\langle \alpha, \beta \rangle} Y_{\alpha + \beta}. \quad (3.11)$$

T is equipped with a holomorphic symplectic form induced by the symplectic pairing on Γ ; it is equivalently given by the holomorphic Poisson bracket

$$\{Y_\alpha, Y_\beta\} = \langle \alpha, \beta \rangle Y_\alpha Y_\beta. \quad (3.12)$$

Now, the \mathcal{K}_α are symplectomorphisms that act as

$$\mathcal{K}_\alpha : Y_\beta \mapsto (1 - Y_\alpha)^{\langle \alpha, \beta \rangle} Y_\beta. \quad (3.13)$$

For $\langle \gamma, \gamma' \rangle = m$, it follows that

$$\begin{aligned} \mathcal{K}_\gamma : Y_\gamma &\mapsto Y_\gamma, & \mathcal{K}_{\gamma'} : Y_\gamma &\mapsto (1 - Y_{\gamma'})^{-m} Y_\gamma, \\ \mathcal{K}_\gamma : Y_{\gamma'} &\mapsto (1 - Y_\gamma)^m Y_{\gamma'}, & \mathcal{K}_{\gamma'} : Y_{\gamma'} &\mapsto Y_{\gamma'}. \end{aligned} \quad (3.14)$$

We identify the torus $\mathbb{C}^\times \times \mathbb{C}^\times$ of Gross-Pandharipande by the subtorus of T generated by

$$\begin{aligned} x &:= Y_\gamma \\ y &:= Y_{\gamma'}; \end{aligned}$$

then by (3.14) we have¹⁸

$$\begin{aligned} \mathcal{K}_\gamma &= \theta_{(1,0),(1-x)^m} = S_m \\ \mathcal{K}_{\gamma'} &= \theta_{(0,1),(1-y)^m} = T_m. \end{aligned}$$

Furthermore, noting that

$$x^a y^b = (-1)^{(a\gamma, b\gamma')} Y_{a\gamma+b\gamma'} = (-1)^{mab} Y_{a\gamma+b\gamma'}, \quad (3.15)$$

then

$$\begin{aligned} \mathcal{K}_{a\gamma+b\gamma'} : x = Y_\gamma &\mapsto (1 - Y_{a\gamma+b\gamma'})^{-mb} Y_\gamma = (1 - (-1)^{mab} x^a y^b)^{mb} x \\ &: y = Y_{\gamma'} \mapsto (1 - Y_{a\gamma+b\gamma'})^{-ma} Y_{\gamma'}^{ma} = (1 - (-1)^{mab} x^a y^b)^{-ma} y; \end{aligned}$$

giving the identification

$$\mathcal{K}_{a\gamma+b\gamma'} = \theta_{(a,b),(1-(-1)^{mab}x^a y^b)^m}.$$

On the right hand side of (3.10) $\arg(Z_\gamma) > \arg(Z_{\gamma'})$ and so the phase ordered product is equivalent to ordering by increasing slope a/b from left to right. This completes the identification of (3.10) with (3.7). Matching the slope 1 terms in both equations,

$$\theta_{(1,1),f_{1,1}} = \prod_{n \geq 1} (\mathcal{K}_{n\gamma_c})^{\Omega(n\gamma_c)},$$

where $\gamma_c := \gamma + \gamma'$; in terms of generating functions, this is equivalent to the statement¹⁹

$$f_{1,1} = \prod_{n \geq 1} [(1 - (-1)^{mn} z^n)^m]^{n\Omega(n\gamma_c)}.$$

Equivalently, as $f_{1,1} = (\mathcal{P}_{m,m})^{m^2}$,

$$(\mathcal{P}_{m,m})^m = \prod_{n \geq 1} (1 - (-1)^{mn} z^n)^{n\Omega(n\gamma_c)}. \quad (3.16)$$

Now assume that the generating function P_m , derived in the context of spectral networks, is the generating function $\mathcal{P}_{m,m}$, derived in the context of wall crossing; then, given the exponents $\{\alpha_n\}_{n \geq 1}$ of the factorization of P_m (see (3.18)), (3.16) predicts spectral network techniques will show $\Omega(n\gamma_c) = m\alpha_n/n$. As we will see, this prediction is confirmed with Prop. 3.2.

¹⁸To make the identification with S_m and T_m we evaluate the formal (time) parameter at $t = -1$. Alternatively, we could set $-tx = Y_\gamma$ and $-ty = Y_{\gamma'}$.

¹⁹To see this, let $g_n = (1 - (-1)^{mn} (xy)^n)^m$, then $\mathcal{K}_{n\gamma_c} = \theta_{(n,n),g_n} = \theta_{(1,1),(g_n)^n}$; furthermore, as $\theta_{(1,1),(g_n)^n}$ fixes the product xy : $\theta_{(1,1),(g_n)^n} \circ \theta_{(1,1),(g_l)^l} = \theta_{(1,1),(g_n)^n (g_l)^l}$.

3.3 Herds of horses are wild (for $m \geq 3$)

Definition For each two-way street p , define the sequence of exponents $\{\alpha_n(p, l)\}_{n \geq 1} \subset \mathbb{Z}$ via

$$Q(p, l) = \prod_{n=1}^{\infty} (1 - (-1)^{mn} z^n)^{\alpha_n(p, l)}. \quad (3.17)$$

We also define the sequence of integers $\{\alpha_n\}_{n \geq 1}$ via

$$P_m = \prod_{n=1}^{\infty} (1 - (-1)^{mn} z^n)^{\alpha_n}. \quad (3.18)$$

By Prop. 3.1, we can express all $\alpha_n(p, l)$ as multiples of α_n .²⁰

Remark The choice of signs $(-1)^{mn}$ follows from our convention of factorization, defined by (2.15), in terms of formal variables in the image of $Y_\gamma \mapsto X_{\tilde{\gamma}}$ (which forms an embedding of the twisted algebra of Y_γ , $\gamma \in \Gamma$, as subalgebra of $\mathbb{Z}[\tilde{\Gamma}]$ as detailed in Appendix E). By Prop. 3.1, $z^n = (-1)^{mn} X_{n\tilde{\gamma}_c}$ for some $\gamma_c \in \Gamma$, leading to the choice of signs in (3.17).

Proposition 3.2.

$$[L(n\gamma_c)] = m\alpha_n\gamma_c \in H_1(\Sigma; \mathbb{Z}).$$

Proof (sketch). A rough argument goes as follows. Note that, using Prop. 3.1 and the definition of $L(n\gamma_c)$ in (2.16), we have

$$\begin{aligned} L(n\gamma_c) &= \sum_{l=1}^m \sum_{p^{(l)}} \alpha_n(p, l) \mathbf{p}^{(l)} \\ &= \alpha_n \sum_{l=1}^m \left\{ \mathbf{c}^{(l)} + (m-l) \left(\mathbf{a}_2^{(l)} + \mathbf{a}_3^{(l)} + \mathbf{b}_2^{(l)} + \mathbf{b}_3^{(l)} \right) \right. \\ &\quad \left. + (l-1) \left(\overline{\mathbf{a}}_2^{(l)} + \overline{\mathbf{a}}_3^{(l)} + \overline{\mathbf{b}}_2^{(l)} + \overline{\mathbf{b}}_3^{(l)} \right) + \right. \\ &\quad \left. + (m-l+1) \left(\mathbf{a}_1^{(l)} + \mathbf{b}_1^{(l)} \right) + l \left(\overline{\mathbf{a}}_1^{(l)} + \overline{\mathbf{b}}_1^{(l)} \right) \right\}. \end{aligned} \quad (3.19)$$

Each term in this sum can be split up into a sum of words of the form

$$\mathbf{a}_1^{(1)} + \mathbf{b}_1^{(1)} + (\dots) + \overline{\mathbf{a}}_1^{(m)} + \overline{\mathbf{b}}_1^{(m)},$$

Each such word represents a closed cycle on the lift of the m -herd to a graph on Σ , and is homologous²¹ to γ_c . As $\mathbf{a}_1^{(1)}, \mathbf{b}_1^{(1)}, \overline{\mathbf{a}}_1^{(m)}, \overline{\mathbf{b}}_1^{(m)}$ all come with multiplicity m in (3.19), then there are m such words and the proposition follows. A full proof, using brute-force homology calculations, can be found in Appendix C.8. \square

²⁰The radius of convergence R of the series in equation (3.2) is $\log R = -c_m$, where c_m is given in equation (3.23); in particular $R < 1$. Therefore, the product expansion is only a formal expansion and is not absolutely convergent; otherwise, it would predict that all the singularities of $d \log P$ sit on the unit circle.

²¹This homological equivalence can be shown using explicit calculations of the form shown in Appendix C.8. For the reader that wishes to avoid excruciating detail: sufficient staring at some simple examples will suffice.

Via (2.17), the immediate result of Prop. 3.2 is that

$$\Omega(n\gamma_c) = \frac{m\alpha_n}{n};$$

so all that remains is to compute α_n . For the cases $m = 1, 2$: using (3.4) and (3.5) we immediately have²²

$$\alpha_n = \begin{cases} \delta_{n,1}, & \text{if } m = 1 \\ -\delta_{n,1}, & \text{if } m = 2 \end{cases} \Rightarrow \Omega(n\gamma_c) = \begin{cases} \delta_{n,1}, & \text{if } m = 1 \\ -2\delta_{n,1}, & \text{if } m = 2 \end{cases}. \quad (3.20)$$

More generally, we can find an explicit form for α_n by taking the log of both sides of (3.18), matching powers of z , and applying Möbius inversion to derive

$$\alpha_n = \frac{1}{n} \sum_{d|n} (-1)^{md+1} \mu\left(\frac{n}{d}\right) \frac{1}{(d-1)!} \left[\frac{d^d}{dz^d} \log(P_m) \right]_{z=0},$$

where μ is the Möbius mu function. Using (3.6),

$$\alpha_n = \frac{1}{(m-1)^2 n} \sum_{d|n} (-1)^{md+1} \mu\left(\frac{n}{d}\right) \binom{(m-1)^2 d}{d}, \quad m \geq 2.$$

Corollary 3.3. *For $m \geq 2$,*

$$\Omega(n\gamma_c) = \frac{m}{(m-1)^2 n^2} \sum_{d|n} (-1)^{md+1} \mu\left(\frac{n}{d}\right) \binom{(m-1)^2 d}{d}. \quad (3.21)$$

This agrees with the result of Reineke²³ in the last section of [17]. A table of the values of $\Omega(n\gamma_c)$ is provided in Appendix C.9 for $1 \leq n, m \leq 7$. From this explicit result, we can deduce the large n asymptotics for the non-trivial²⁴ case $m \geq 3$.

Proposition 3.4. *Let $m \geq 3$, then as $n \rightarrow \infty$,*

$$\Omega(n\gamma_c) \sim (-1)^{mn+1} \left(\frac{1}{m-1} \sqrt{\frac{m}{2\pi(m-2)}} \right) n^{-5/2} e^{c_m n}, \quad (3.22)$$

where c_m is the constant

$$c_m = (m-1)^2 \log[(m-1)^2] - m(m-2) \log[m(m-2)]. \quad (3.23)$$

Proof. Restricting n to be an element of an infinite subsequence of primes, the sum over divisors simplifies and the claimed asymptotics (restricted to this subsequence) follow immediately using Stirling's asymptotics and (3.21). See Appendix D for a full proof. \square

²²The case $m = 1$ (i.e. the saddle) was also computed in [33].

²³Reineke showed (in our notation) $\Omega(n\gamma_c) = \frac{1}{(m-2)n^2} \sum_{d|n} (-1)^{md+1} \mu(n/d) \binom{(m-1)^2 d}{d}$. To translate between results, we use the observation that $\binom{(m-1)^2 d}{d} = \frac{(m-1)^2}{m(m-2)} \binom{(m-1)^2 d - 1}{d}$.

²⁴In the case $m = 2$, using the identity $\sum_{d|n} \mu(d) = \delta_{n,1}$ in (3.21) reproduces the result $\Omega(n\gamma_c) = -2\delta_{n,1}$ of (3.20).

3.4 Herds in the pure $SU(3)$ theory

Now, finally, let us exhibit some points of the Coulomb branch of the pure $SU(3)$ theory where m -herds actually occur in spectral networks \mathcal{W}_ϑ .

In the pure $SU(3)$ theory, the curve C is \mathbb{CP}^1 with two defects. It is natural to view it topologically as the cylinder $\mathbb{R} \times S^1$. Moreover, the spectral curve (4.1) has 4 branch points. Thus, the pictures of actual spectral networks in this theory look much like the “hypothetical” spectral networks we considered in Figures 1, 2.

In particular, consider the parameters

$$u_2 = -3, \quad u_3 = \frac{95}{10} \tag{3.24}$$

(in the notation of (4.1).) At this point, in accordance with the discussion of Section 3.1, we consider two charges γ, γ' supporting BPS hypermultiplets, represented simply by paths connecting pairs of branch points across the cylinder, as in the left side of Figure 2. In particular they have $\langle \gamma, \gamma' \rangle = 3$. By numerically computing the appropriate contour integrals we find that these charges have $Z_\gamma = 7.244 - 9.083i$, $Z_{\gamma'} = 20.980 - 40.148i$.

Now, our proposal in Section 3.1 was that when we have two such hypermultiplets, there will be a wall of marginal stability in the Coulomb branch when Z_γ and $Z_{\gamma'}$ become aligned, and on one side of that wall, the spectral network at the phase $\vartheta = \arg Z_{\gamma+\gamma'}$ will contain a 3-herd. So, we plot the spectral network at phase $\vartheta = \arg Z_{\gamma+\gamma'}$, and find Figure 5. Comparing with Figure 4, we see that the two-way streets in this network make up a 3-herd as desired.²⁵

Moving u_3 in the positive real direction, we have similarly found a 4-herd, a 5-herd and a 6-herd. It is natural to conjecture that one can similarly obtain m -herds for any m in this way. Of course, at a fixed point in the Coulomb branch it is in general possible that there could be m -herds for many different values of m at different values of ϑ .

In any case, the existence of 3-herds in the pure $SU(3)$ theory is already enough to show that the analysis of the last few sections is not only a theoretical exercise: the wild BPS degeneracies we found there indeed occur in the $\mathcal{N} = 2$ supersymmetric pure $SU(3)$ Yang-Mills theory!

4 Wild regions for pure $SU(3)$ theory from wall-crossing

In the previous section we exhibited an example of a class of spectral networks that lead to the m -wild degeneracies of slope $(1, 1)$. An explicit point on the Coulomb branch of the pure $SU(3)$ theory which produces such a spectral network for $m = 3$ was given in equation (3.24) above.

In the present section we start anew, and use wall crossing and quiver techniques to give an alternative demonstration that wild degeneracies exist on the Coulomb branch of the pure $SU(3)$ theory.

²⁵In particular, our point (3.24) is on the side of the wall where the 3-herd exists. The wall of marginal stability where the 3-herd disappears can be reached by moving u_3 in the negative real direction.

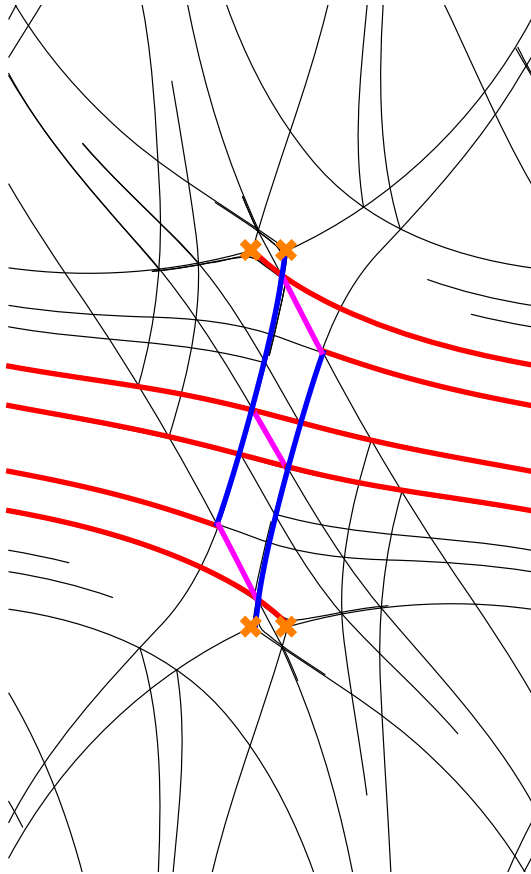


Figure 5. The spectral network \mathcal{W}_ϑ which occurs in the pure $SU(3)$ theory at the point (3.24) of the Coulomb branch. The phase ϑ has been chosen very close to the critical phase $\vartheta = \arg Z_{\gamma+\gamma'}$. Here we represent the cylinder C as the periodically identified plane, i.e., the left and right sides of the figure should be identified. Streets which become two-way at $\vartheta = \arg Z_{\gamma+\gamma'}$ are shown in thick red, blue and fuchsia. We do not show the whole network but only a cutoff version of it, as described in [33].

4.1 Strong Coupling Regime of the Pure $SU(3)$ Theory

The spectral curve Σ of pure $SU(3)$ SYM theory is

$$\lambda^3 - \frac{u_2}{z^2} \lambda + \left(\frac{1}{z^2} + \frac{u_3}{z^3} + \frac{1}{z^4} \right) = 0. \quad (4.1)$$

It is a branched three-sheeted covering of the cylinder C , with six ramification points. There are four branch points corresponding to two-cycles of S_3 , and there are also ramifications at the irregular singularities at $0, \infty$, with associated permutations of the sheets given by three-cycles.

In the strong coupling region, i.e. at small values of the moduli u_2, u_3 , the BPS spectrum is finite; so the spectral network evolves in a rather simple fashion. As a concrete example we

choose $u_2 = 0.7$, $u_3 = 0.4i$; then varying ϑ from 0 to π we encounter six degenerate networks containing finite webs, which are depicted in Figure 6.

We assign to these cycles the charges $\gamma_1, \gamma_2, \gamma_2 + \gamma_4, \gamma_1 + \gamma_3, \gamma_3, \gamma_4$, Figure 7 shows the

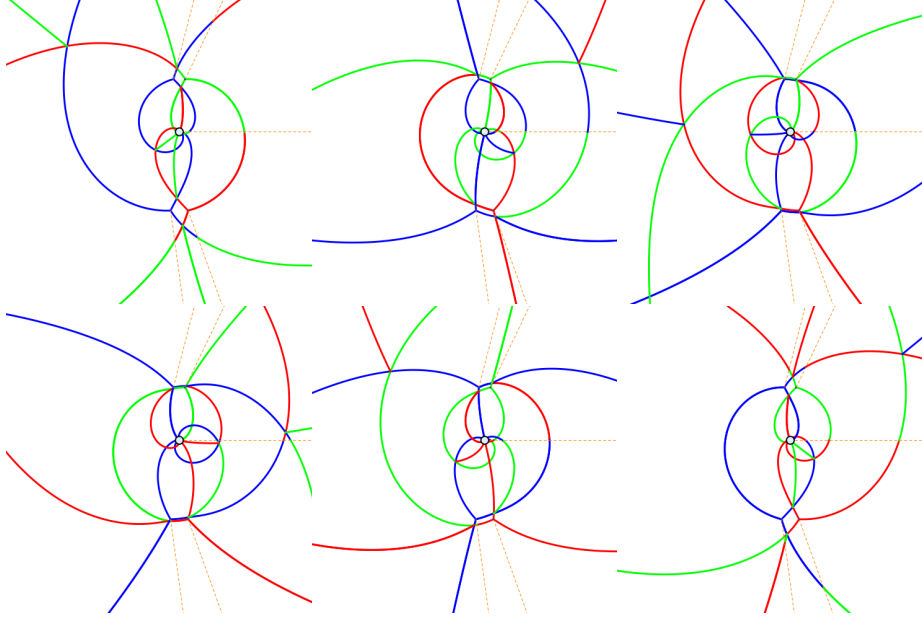


Figure 6. The six hypermultiplets in the strong coupling chamber: from the top left, the flips corresponding to $\gamma_1, \gamma_2, \gamma_1 + \gamma_3, \gamma_2 + \gamma_4, \gamma_3, \gamma_4$. $\text{Arg } Z_{\gamma_1} < \text{Arg } Z_{\gamma_2} < \text{Arg } Z_{\gamma_3} < \text{Arg } Z_{\gamma_4}$. Here we represent the cylinder C as the punctured plane.

charge assignments with the basis cycles resolved.

The mutual intersections of cycles can be read off Figure 7, and are summarized by the following pairing matrix $P_{ij} = \langle \gamma_i, \gamma_j \rangle$

$$P = \begin{pmatrix} 0 & -2 & 1 & 0 \\ 2 & 0 & -2 & 1 \\ -1 & 2 & 0 & -2 \\ 0 & -1 & 2 & 0 \end{pmatrix}. \quad (4.2)$$

For a video showing the evolution of the spectral network through an angle of π , see [43].

4.2 A path on the Coulomb branch

We now consider a straight path on the Coulomb branch of the pure $SU(3)$ theory, parameterized by

$$\begin{aligned} u_2(t) &= (u_2^{(f)} - u_2^{(i)})t + u_2^{(i)}, \\ u_3(t) &= (u_3^{(f)} - u_3^{(i)})t + u_3^{(i)}, \end{aligned} \quad (4.3)$$

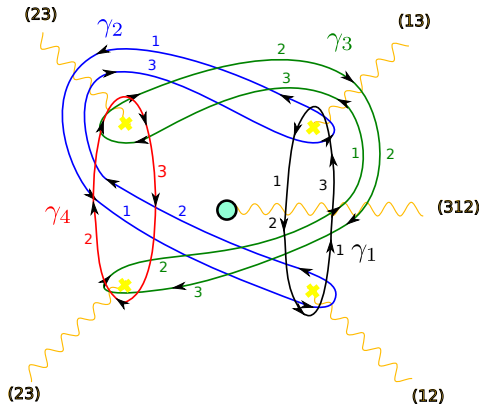


Figure 7. The labeling of finite networks. We only show the four basis hypermultiplets $\gamma_1, \dots, \gamma_4$. The trivialization is indicated by the branch cuts (wavy lines, the associated permutations of sheets are also specified), the sheets on which the cycles run are indicated explicitly. Here we represent the cylinder C as the punctured plane.

with $t \in [0, 1]$ and

$$\begin{aligned} u_2^{(i)} = 0.7, \quad u_3^{(i)} = 0.4i \quad (\text{strong coupling chamber}) \\ u_2^{(f)} = 0.56 - 0.75i, \quad u_3^{(f)} = 2 + 1.52i \quad (\text{wild chamber}) \end{aligned} \quad (4.4)$$

As discussed above, the spectrum in the strong coupling chamber is known (see for example [33]) to consist of six hypermultiplets. As we move along our path we cross several walls of marginal stability, with consequent jumps of the BPS spectrum. In order to study the evolution of the BPS spectrum, we must track explicitly the evolution of central charges. Variation of the moduli also induces changes in the geometry of the Seiberg-Witten curve Σ , therefore in computing the central charges at different points one must take care of deforming the cycles in a way compatible with the flat parallel transport of the local system $\widehat{\Gamma} \rightarrow \mathcal{B}^*$. Starting from the point studied in Section 4.1, the evolution of branch points can be tracked on C , as shown in Figure 8.

4.3 Cohorts in pure $SU(3)$

As the moduli cross walls of marginal stability, the BPS spectrum jumps according to a regular pattern. At a wall $\text{MS}(\gamma, \gamma')$ for two populated hypermultiplets, with $\langle \gamma, \gamma' \rangle = m > 0$, the KS wall crossing formula predicts

$$\mathcal{K}_{\gamma'} \mathcal{K}_{\gamma} =: \prod_{a, b \geq 0} \mathcal{K}_{a\gamma + b\gamma'}^{\Omega(a\gamma + b\gamma')} : \quad (4.5)$$

where the normal ordering symbols $: \ :$ on the right hand side indicate that factors are ordered according to the phases of central charges, phase-ordering on the right hand side is the opposite of that on the left-hand side. We refer to the spectrum on the right hand side

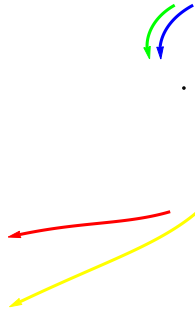


Figure 8. The picture shows the projection of the Seiberg-Witten curve on C . The four arrows show the progression of the four branch points as we vary $u_{2,3}$ along the path of equation (4.3). The black dot is the singularity at $z = 0$. The central charges have been computed numerically using Mathematica and, as a check, they evolve smoothly along the path (see [42]).

as the *cohort* generated by γ, γ' , and will occasionally denote it by $\mathcal{C}_m(\gamma, \gamma')$. An important fact to note about cohorts, following from the linearity of the central charge homomorphism, is that

$$\arg Z_{\gamma'} < \arg Z_{a\gamma+b\gamma'} < \arg Z_{\gamma}, \quad \forall a, b \geq 0 \quad (4.6)$$

for moduli corresponding to the right hand side of (4.5).

Quite generally, the wall-crossing of two hypermultiplet states with pairing m can be analyzed in terms of the corresponding m -Kronecker quiver (see [6, 30]), from this perspective the degeneracies of an m -cohort correspond to Euler characteristics of moduli spaces of (semi)stable quiver representations.

Cohort structures \mathcal{C}_m with $m = 1, 2$ are known exactly. Examples of such cohorts have been encountered a number of times in the literature [15, 19, 20, 23, 24], and are common in A_1 theories of class \mathcal{S} . For later convenience, we recall the structure of the $m = 2$ cohort in figure 9.

As we start moving along our path on the Coulomb branch, from $t = 0$ to $t = 1$, several cohorts are created. The first wall of marginal stability is $\text{MS}(\gamma_1 + \gamma_3, \gamma_2 + \gamma_4)$, with $\langle \gamma_1 + \gamma_3, \gamma_2 + \gamma_4 \rangle = 2$, thus a \mathcal{C}_2 cohort is generated. As we proceed along the path, other BPS states undergo wall-crossing, generating other \mathcal{C}_2 cohorts. As shown in Fig. 10, first γ_1 generates a cohort with γ_2 , then γ_3, γ_4 generate a similar cohort, finally another $m = 2$ cohort is generated by wall crossing of γ_1 and $\gamma_2 + \gamma_4$. At this point, *i.e.* within a chamber around $t = 0.95$, the spectrum can be schematically summarized as the union of four \mathcal{C}_2 cohorts

$$\mathcal{C}_2(\gamma_2 + \gamma_4, \gamma_1 + \gamma_3) \cup \mathcal{C}_2(\gamma_2, \gamma_1) \cup \mathcal{C}_2(\gamma_4, \gamma_3) \cup \mathcal{C}_2(\gamma_1, \gamma_2 + \gamma_4) \quad (4.7)$$

consisting of four vectormultiplets, and infinite towers of hypermultiplets.

Proceeding further along our path, we encounter another wall of marginal stability: $\gamma_2 + \gamma_4$ undergoes wall-crossing with $2\gamma_1 + \gamma_2$ generating a new cohort with $m = 3$. This phenomenon

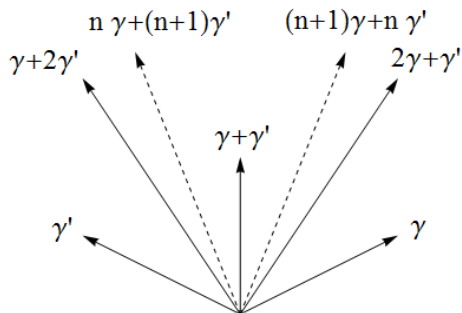


Figure 9. The populated BPS rays of the $m = 2$ cohort (a schematic depiction of central charges in the complex plane). The state with charge $\gamma + \gamma'$ is a BPS vectormultiplet ($\Omega = -2$), surrounded by two infinite towers of hypermultiplets ($\Omega = 1$), represented by dashed arrows.

has not been studied before, and deserves a detailed analysis. We anticipate here that this cohort contains distinctive new features, such as a wealth of higher spin states and a cone of densely populated BPS rays.

It is worth stressing that merely finding a point on the Coulomb branch where $Z_{\gamma_2+\gamma_4}$ approaches $Z_{2\gamma_1+\gamma_2}$ is hardly sufficient to claim that such wall-crossing happens. In addition one must make sure that such rays are populated. This is certainly the case in our example. Another important requirement is the absence of populated rays between $Z_{\gamma_2+\gamma_4}$ and $Z_{2\gamma_1+\gamma_2}$, as we approach their mutual wall of marginal stability. We claim that there aren't any, based on two independent facts. First, at values of the moduli just before $MS(\gamma_2 + \gamma_4, 2\gamma_1 + \gamma_2)$, the spectral network shows simple, smooth evolution for $\arg Z_{2\gamma_1+\gamma_2} < \vartheta < \arg Z_{\gamma_2+\gamma_4}$, see [44]. Second, our explicit path on the Coulomb branch – together with property (4.6) of cohorts – guarantees that all boundstates created so far fall outside of the cone bounded by the central charges of $2\gamma_1 + \gamma_2$, $\gamma_2 + \gamma_4$: indeed if a populated boundstate were between $\gamma_2 + \gamma_4$ and $2\gamma_1 + \gamma_2$, it would have to be one of the following

- a boundstate of $2\gamma_1 + \gamma_2$ with a charge counterclockwise of $\gamma_2 + \gamma_4$
- a boundstate of $\gamma_2 + \gamma_4$ with a charge clockwise of $2\gamma_1 + \gamma_2$
- a boundstate of two charges lying respectively counterclockwise of $\gamma_2 + \gamma_4$ and clockwise of $2\gamma_1 + \gamma_2$
- a boundstate due to one of the antiparticles

All these possibilities are clearly ruled out by our explicit choice of path. Our analysis relies on the numerical evaluation of central charges at several points on the Coulomb branch, video [42] shows the smooth evolution of central charges of basis hypermultiplets along the path, ensuring that integration contours have been adapted suitably. Another important check is the following: at fixed u_2 , u_3 we tune the spectral network to the phase of central charges (as predicted numerically), and we check that there are indeed degenerate networks.

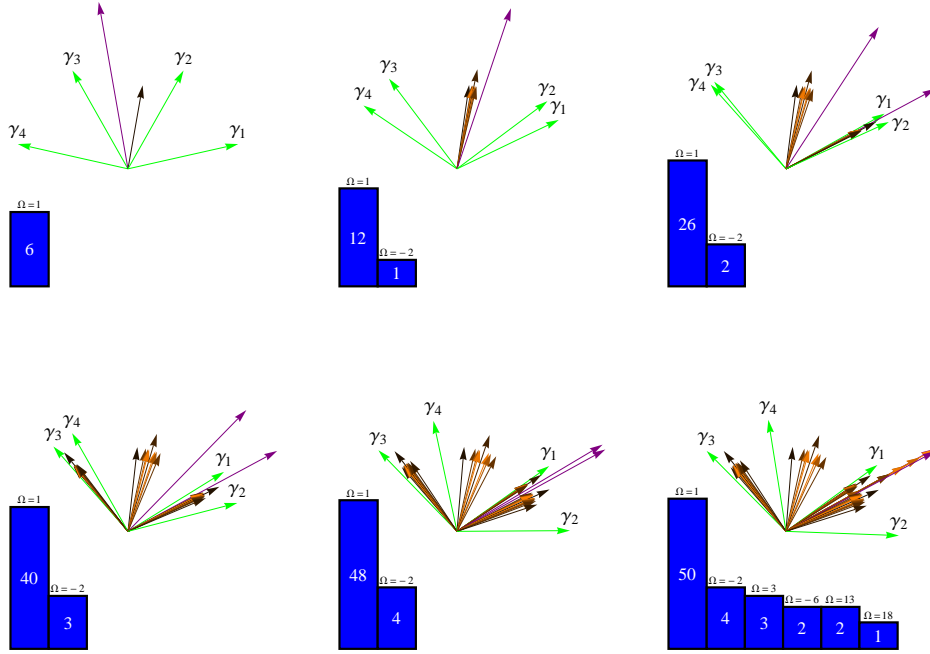


Figure 10. The evolution of the spectrum is illustrated. Green arrows represent the basis hypermultiplets, the purple arrows are $\gamma_2 + \gamma_4$ and $2\gamma_1 + \gamma_2$, the two states that generate the $m = 3$ cohort. For other charges, increasing length denotes higher $|\Omega|$ and lighter shades denote larger charges. First picture: the strong coupling chamber. Second picture: the states $\gamma_1 + \gamma_3$ and $\gamma_2 + \gamma_4$ have crossed and created a \mathcal{C}_2 cohort. Third picture: γ_2 and γ_1 cross and create another cohort. Fourth picture: the cohort generated by γ_3, γ_4 . Fifth picture: $\gamma_2 + \gamma_4$ and γ_1 have crossed and created a cohort. In the sixth picture $\gamma_2 + \gamma_4$ and $2\gamma_1 + \gamma_2$ have crossed, generating wild degeneracies.. For a video showing the full evolution of the spectrum along our path, see [45].

4.4 Wall-crossings with intersections $m > 3$

So far we have encountered an MS wall of two hypermultiplets with intersection pairing 3, but there is nothing special about $m = 3$. The path proposed in (4.3) can be extended through walls of marginal stability with $m = 4, 5$, and higher. The strategy is simply to look for a direction on the Coulomb branch, along which the ray $\gamma_2 + \gamma_4$ sweeps across the infinite tower of hypermultiplets with charges $(n + 1)\gamma_1 + n\gamma_2$.

For example, moving along a straight line from $(u_2^{(f)}, u_3^{(f)})$ to

$$u_2^{(4)} = 0.56 - 0.75i, \quad u_3^{(4)} = 2.00 + 1.99i \quad (4.8)$$

induces wall-crossing of $\gamma_2 + \gamma_4$ with $3\gamma_1 + 2\gamma_2$, with intersection $\langle \gamma_2 + \gamma_4, 3\gamma_1 + 2\gamma_2 \rangle = 4$. In this chamber the spectrum gains a new $m = 4$ cohort, described by the 4-Kronecker quiver.

Proceeding further, along a straight segment, to

$$u_2^{(5)} = 0.56 - 0.75i, \quad u_3^{(5)} = 2.00 + 2.52i \quad (4.9)$$

we cross the marginal stability wall of $\gamma_2 + \gamma_4$ and $4\gamma_1 + 3\gamma_2$, with intersection $\langle \gamma_2 + \gamma_4, 4\gamma_1 + 3\gamma_2 \rangle = 5$ generating an $m = 5$ cohort.

In the same spirit, we have checked numerically that there is a path along which $\gamma_2 + \gamma_4$ crosses all hypermultiplets with charges $(m - 1)\gamma_1 + (m - 2)\gamma_2$, with pairings

$$\langle \gamma_2 + \gamma_4, (m - 1)\gamma_1 + (m - 2)\gamma_2 \rangle = m \quad (4.10)$$

hence generating an infinite tower of cohorts. The situation gets very complicated, as these cohorts will widen and start overlapping with each other, inducing further wild wall crossing.²⁶ It is worth stressing that, by the same reasoning outlined for the wall-crossing of $\gamma_2 + \gamma_4$ with $2\gamma_1 + \gamma_2$, there are no populated states between $\gamma_2 + \gamma_4$ and $(m - 1)\gamma_1 + (m - 2)\gamma_2$ immediately before the point where they cross. This crucial fact guarantees that in this region of the Coulomb branch m -cohorts are generated, for arbitrarily high m .

Finally, we remark that a natural question arises as to whether analogous wall-crossings happen where the integer m is negative. In fact, there is a simple physical argument that such wall-crossings cannot happen on Coulomb branches of physical theories, it goes as follows. Let us consider two charges γ_1, γ_2 with $\langle \gamma_1, \gamma_2 \rangle < 0$; we would like to investigate whether there could be a chamber of the Coulomb branch, bounded by $MS(\gamma_1, \gamma_2)$, where

- $\arg Z_{\gamma_2} > \arg Z_{\gamma_1}$
- $\Omega(\gamma) = 1$ for $\gamma \in \{\pm\gamma_1, \pm\gamma_2\}$
- $\Omega(\gamma) = 0$ for all other combinations $\gamma = a\gamma_1 + b\gamma_2$.

If these conditions were realized, we would be in a situation in which the spectrum generator (defined below eq. (5.1)) contains a factor $\mathcal{K}_{\gamma_2}\mathcal{K}_{\gamma_1}$, and we stress that there would be no other \mathcal{K} factors between \mathcal{K}_{γ_2} and \mathcal{K}_{γ_1} .

We claim that this cannot happen: under sufficiently general conditions, near a wall $MS(\gamma_1, \gamma_2)$ we expect Denef's multicenter equations (for the case under consideration, they are reported below in (7.7)) to provide a reliable description of the boundstates. It is immediately evident from such description that, in the case of negative $\langle \gamma_1, \gamma_2 \rangle = m$, on the side of $MS(\gamma_1, \gamma_2)$ where $\arg Z_{\gamma_2} > \arg Z_{\gamma_1}$, there will be stable boundstates of γ_1 with γ_2 populating rays between those of Z_{γ_1} and Z_{γ_2} . In particular, inside the spectrum generator, the factors \mathcal{K}_{γ_2} and

²⁶As explained in the next section, the spectrum is best studied via the *spectrum generator* technique introduced in [19]. This technique is straightforwardly applicable whenever comparing two points on the Coulomb branch, such that the lattice basis vectors have corresponding central charges all contained within a half-plane. When instead one or more of the central charges exit the half-plane, one needs to account for that by suitably modifying the spectrum generator. While moving from strong coupling into these *wilder* regions, we actually incur in such a situation.

\mathcal{K}_{γ_1} are *necessarily* separated by other factors $\mathcal{K}_{a\gamma_1+b\gamma_2}$, for $a, b > 0$, violating the conditions formulated above.

Nevertheless, it makes sense to ask what the prediction of the KSWCF would be. To learn something interesting, it is actually sufficient to consider the motivic version of the primitive WCF (see [38]). From such formula, the protected spin character (see appendix A) associated to $\gamma_1 + \gamma_2$ has the simple expression

$$\Omega(\gamma_1 + \gamma_2; y) := \text{Tr}_{\mathfrak{h}_m}(y)^{2J_3}(-y)^{2I_3} = \frac{y^m - y^{-m}}{y - y^{-1}} \quad (4.11)$$

corresponding (not uniquely)²⁷ to the following exotic representations of $so(3) \oplus su(2)_R$

$$\mathfrak{h}_m = \begin{cases} \left(\frac{1}{2}, \frac{1}{2}\right) \oplus (1, 0) & m = -1 \\ \left(0, \frac{1}{2}\right) & m = -2 \\ \left(\frac{-m-2}{2}, \frac{1}{2}\right) \oplus \left(\frac{-m-3}{2}, 0\right) & m \leq -3 \end{cases} . \quad (4.12)$$

Since the no-exotics theorem is in fact fairly well established for pure $SU(K)$ gauge theories [39], this further supports the argument that such wall-crossings cannot occur on the Coulomb branch.

5 Some Numerical Checks on the $m = 3$ Wild Spectrum

The discussion of Section 4 is sufficient to prove that there are wild degeneracies on the Coulomb branch of the pure $SU(3)$ theory. However, since this phenomenon is somewhat novel, we have checked the results using the “spectrum generator” in some relevant regions of the Coulomb branch. This section explains those checks.

5.1 The spectrum generator technique

According to the KSWCF, the phase-ordered product

$$A(\triangleleft) = : \prod_{\gamma, \arg Z_\gamma \in \triangleleft} \mathcal{K}_\gamma^{\Omega(\gamma)} : \quad (5.1)$$

is invariant across walls of marginal stability provided no occupied BPS rays cross into or out of the angular sector \triangleleft . Considering an angle of π corresponds to a choice of the “half plane of particles”. Once this choice is made, $A(\pi)$ is called a ²⁸ *spectrum generator* and denoted \mathbb{S} [19].

The idea of the “spectrum generator technique” is that if - through some means or other - one can compute $A(\pi)$, then, by factorization one can deduce the spectrum (after computing the phase ordering of the Z_γ at that point). For example in [19] an algorithm is given for

²⁷Albeit necessarily involving exotic representations.

²⁸Several equivalent choices are related by how one chooses the half-plane in the complex plane of central charges.

computing $A(\pi)$ without an *a priori* knowledge of the spectrum. Here our strategy will be a little different. We will derive the spectrum generator in the strong coupling chamber, where the spectrum can be easily read off from the spectral network or from quiver techniques. We then use wall-crossing to argue that $A(\pi)$ is unchanged along a particular path in the Coulomb branch (described in Section 4) to the wild region. Then we factorize the spectrum generator at points along that path.

An effective technique for factorizing \mathbb{S} is the following. Let $\{\gamma_i\}_{i=1,\dots,k}$ be a basis for the lattice of charges Γ , and let $\gamma = \sum a_i \gamma_i$, with $a_i > 0$. Define the height $|\gamma| := \sum_i a_i$, and $\mathbb{S}^{(r)} := \prod_{\gamma, |\gamma| \leq r} \mathcal{K}_\gamma^{\Omega(\gamma)}$:²⁹ The full spectrum generator \mathbb{S} can then be factorized by studying its action on the basis formal variables³⁰ Y_{γ_i} for increasing values of r , by employing

$$Y_{-\gamma_i}(\mathbb{S} - \tilde{\mathbb{S}}^{(r)})Y_{\gamma_i} = - \sum_{|\gamma'|=r+1} \langle \gamma_i, \gamma' \rangle \Omega(\gamma') Y_{\gamma'} + \dots \quad (5.2)$$

where $\tilde{\mathbb{S}}$ represents the factorization of the spectrum generator under study. The ellipses contain terms with $Y_\gamma, |\gamma| > r + 1$.

5.2 Factorizing the spectrum generator

The spectrum in the strong coupling region can be obtained via spectral network techniques, as discussed in Section 4.1. According to the results presented there, the spectrum generator is

$$\mathbb{S} = \mathcal{K}_{\gamma_4} \mathcal{K}_{\gamma_3} \mathcal{K}_{\gamma_2 + \gamma_4} \mathcal{K}_{\gamma_1 + \gamma_3} \mathcal{K}_{\gamma_2} \mathcal{K}_{\gamma_1}, \quad (5.3)$$

in agreement with [30, 33].

We now fix a point on our path

$$u_2 = 0.56 - 0.73i, \quad u_3 = 1.94 + 1.49i, \quad (5.4)$$

corresponding to the situation exhibited in (4.7) immediately before the wall $\text{MS}(\gamma_2 + \gamma_4, 2\gamma_1 + \gamma_2)$. The central charges corresponding to the simple roots are

$$\begin{aligned} Z_{\gamma_1} &= 8.42972 + 6.00549i & Z_{\gamma_2} &= 4.83278 - 0.0226871i \\ Z_{\gamma_3} &= -7.30679 + 7.50651i & Z_{\gamma_4} &= -0.504898 + 2.53401i, \end{aligned} \quad (5.5)$$

²⁹Recall that the ordering depends crucially on the position u on the Coulomb branch, hence we should really write $\mathbb{S}^{(r)}(u)$. To lighten the notation we do not indicate the u -dependence.

³⁰i.e., it is sufficient to work with formal variables corresponding to a choice of simple roots for the lattice of charges. The choice of simple roots must be consistent with the choice of half-plane that comes with the spectrum generator.

the factorization of the spectrum generator up to $|\gamma| = 21$ reads³¹

$$\begin{aligned}
& \mathcal{K}_{\gamma_3} \mathcal{K}_{2\gamma_3+\gamma_4} \mathcal{K}_{3\gamma_3+2\gamma_4} \mathcal{K}_{4\gamma_3+3\gamma_4} \mathcal{K}_{5\gamma_3+4\gamma_4} \mathcal{K}_{6\gamma_3+5\gamma_4} \mathcal{K}_{7\gamma_3+6\gamma_4} \mathcal{K}_{8\gamma_3+7\gamma_4} \mathcal{K}_{9\gamma_3+8\gamma_4} \\
& \mathcal{K}_{10\gamma_3+9\gamma_4} \mathcal{K}_{11\gamma_3+10\gamma_4} \mathcal{K}_{\gamma_3+\gamma_4}^{-2} \mathcal{K}_{10\gamma_3+11\gamma_4} \mathcal{K}_{9\gamma_3+10\gamma_4} \mathcal{K}_{8\gamma_3+9\gamma_4} \mathcal{K}_{7\gamma_3+8\gamma_4} \mathcal{K}_{6\gamma_3+7\gamma_4} \\
& \mathcal{K}_{5\gamma_3+6\gamma_4} \mathcal{K}_{4\gamma_3+5\gamma_4} \mathcal{K}_{3\gamma_3+4\gamma_4} \mathcal{K}_{2\gamma_3+3\gamma_4} \mathcal{K}_{\gamma_3+2\gamma_4} \mathcal{K}_{\gamma_4} \mathcal{K}_{\gamma_1+\gamma_3} \mathcal{K}_{2\gamma_1+\gamma_2+2\gamma_3+\gamma_4} \\
& \mathcal{K}_{3\gamma_1+2\gamma_2+3\gamma_3+2\gamma_4} \mathcal{K}_{4\gamma_1+3\gamma_2+4\gamma_3+3\gamma_4} \mathcal{K}_{5\gamma_1+4\gamma_2+5\gamma_3+4\gamma_4} \mathcal{K}_{\gamma_1+\gamma_2+\gamma_3+\gamma_4}^{-2} \mathcal{K}_{4\gamma_1+5\gamma_2+4\gamma_3+5\gamma_4} \\
& \mathcal{K}_{3\gamma_1+4\gamma_2+3\gamma_3+4\gamma_4} \mathcal{K}_{2\gamma_1+3\gamma_2+2\gamma_3+3\gamma_4} \mathcal{K}_{\gamma_1+2\gamma_2+\gamma_3+2\gamma_4} \mathcal{K}_{\gamma_1} \mathcal{K}_{2\gamma_1+\gamma_2+\gamma_4} \mathcal{K}_{3\gamma_1+2\gamma_2+2\gamma_4} \\
& \mathcal{K}_{4\gamma_1+3\gamma_2+3\gamma_4} \mathcal{K}_{5\gamma_1+4\gamma_2+4\gamma_4} \mathcal{K}_{6\gamma_1+5\gamma_2+5\gamma_4} \mathcal{K}_{7\gamma_1+6\gamma_2+6\gamma_4} \mathcal{K}_{\gamma_1+\gamma_2+\gamma_4}^{-2} \mathcal{K}_{6\gamma_1+7\gamma_2+7\gamma_4} \\
& \mathcal{K}_{5\gamma_1+6\gamma_2+6\gamma_4} \mathcal{K}_{4\gamma_1+5\gamma_2+5\gamma_4} \mathcal{K}_{3\gamma_1+4\gamma_2+4\gamma_4} \mathcal{K}_{2\gamma_1+3\gamma_2+3\gamma_4} \mathcal{K}_{\gamma_1+2\gamma_2+2\gamma_4} \mathcal{K}_{\gamma_2+\gamma_4} \\
& \mathcal{K}_{2\gamma_1+\gamma_2} \mathcal{K}_{3\gamma_1+2\gamma_2} \mathcal{K}_{4\gamma_1+3\gamma_2} \mathcal{K}_{5\gamma_1+4\gamma_2} \mathcal{K}_{6\gamma_1+5\gamma_2} \mathcal{K}_{7\gamma_1+6\gamma_2} \mathcal{K}_{8\gamma_1+7\gamma_2} \mathcal{K}_{9\gamma_1+8\gamma_2} \\
& \mathcal{K}_{10\gamma_1+9\gamma_2} \mathcal{K}_{11\gamma_1+10\gamma_2} \mathcal{K}_{\gamma_1+\gamma_2}^{-2} \mathcal{K}_{10\gamma_1+11\gamma_2} \mathcal{K}_{9\gamma_1+10\gamma_2} \mathcal{K}_{8\gamma_1+9\gamma_2} \mathcal{K}_{7\gamma_1+8\gamma_2} \mathcal{K}_{6\gamma_1+7\gamma_2} \\
& \mathcal{K}_{5\gamma_1+6\gamma_2} \mathcal{K}_{4\gamma_1+5\gamma_2} \mathcal{K}_{3\gamma_1+4\gamma_2} \mathcal{K}_{2\gamma_1+3\gamma_2} \mathcal{K}_{\gamma_1+2\gamma_2} \mathcal{K}_{\gamma_2}
\end{aligned} \tag{5.6}$$

The spectrum exhibits four $m = 2$ cohorts, as expected from the discussion of Section 4.3: they include four vectormultiplets (with $\Omega = -2$), accompanied by infinite towers of hypermultiplets.

On the other side of the $m = 3$ wall, at

$$u_2 = 0.56 - 0.75i, \quad u_3 = 2.00 + 1.52i, \tag{5.7}$$

central charges read

$$\begin{aligned}
Z_{\gamma_1} &= 8.52337 + 6.18454i & Z_{\gamma_2} &= 4.89813 - 0.18347i \\
Z_{\gamma_3} &= -7.43876 + 7.53531i & Z_{\gamma_4} &= -0.410809 + 2.59321i.
\end{aligned} \tag{5.8}$$

³¹Color code: The factors in blue come from the hypermultiplets of the strong coupling chamber. The factors in red come from vectormultiplets. The remaining factors in black are hypermultiplets created by the wall-crossing from the strong coupling chamber.

The spectrum generator, up to $|\gamma| = 21$, is

$$\begin{aligned}
& \mathcal{K}_{\gamma_3} \mathcal{K}_{2\gamma_3+\gamma_4} \mathcal{K}_{3\gamma_3+2\gamma_4} \mathcal{K}_{4\gamma_3+3\gamma_4} \mathcal{K}_{5\gamma_3+4\gamma_4} \mathcal{K}_{6\gamma_3+5\gamma_4} \mathcal{K}_{7\gamma_3+6\gamma_4} \mathcal{K}_{8\gamma_3+7\gamma_4} \mathcal{K}_{9\gamma_3+8\gamma_4} \\
& \mathcal{K}_{10\gamma_3+9\gamma_4} \mathcal{K}_{11\gamma_3+10\gamma_4} \mathcal{K}_{\gamma_3+\gamma_4}^{-2} \mathcal{K}_{10\gamma_3+11\gamma_4} \mathcal{K}_{9\gamma_3+10\gamma_4} \mathcal{K}_{8\gamma_3+9\gamma_4} \mathcal{K}_{7\gamma_3+8\gamma_4} \mathcal{K}_{6\gamma_3+7\gamma_4} \\
& \mathcal{K}_{5\gamma_3+6\gamma_4} \mathcal{K}_{4\gamma_3+5\gamma_4} \mathcal{K}_{3\gamma_3+4\gamma_4} \mathcal{K}_{2\gamma_3+3\gamma_4} \mathcal{K}_{\gamma_3+2\gamma_4} \mathcal{K}_{\gamma_4} \mathcal{K}_{\gamma_1+\gamma_3} \mathcal{K}_{2\gamma_1+\gamma_2+2\gamma_3+\gamma_4} \\
& \mathcal{K}_{3\gamma_1+2\gamma_2+3\gamma_3+2\gamma_4} \mathcal{K}_{4\gamma_1+3\gamma_2+4\gamma_3+3\gamma_4} \mathcal{K}_{5\gamma_1+4\gamma_2+5\gamma_3+4\gamma_4} \mathcal{K}_{\gamma_1+\gamma_2+\gamma_3+\gamma_4}^{-2} \mathcal{K}_{4\gamma_1+5\gamma_2+4\gamma_3+5\gamma_4} \\
& \mathcal{K}_{3\gamma_1+4\gamma_2+3\gamma_3+4\gamma_4} \mathcal{K}_{2\gamma_1+3\gamma_2+2\gamma_3+3\gamma_4} \mathcal{K}_{\gamma_1+2\gamma_2+\gamma_3+2\gamma_4} \mathcal{K}_{\gamma_1} \mathcal{K}_{2\gamma_1+\gamma_2+\gamma_4} \mathcal{K}_{3\gamma_1+2\gamma_2+2\gamma_4} \\
& \mathcal{K}_{4\gamma_1+3\gamma_2+3\gamma_4} \mathcal{K}_{5\gamma_1+4\gamma_2+4\gamma_4} \mathcal{K}_{6\gamma_1+5\gamma_2+5\gamma_4} \mathcal{K}_{7\gamma_1+6\gamma_2+6\gamma_4} \mathcal{K}_{\gamma_1+\gamma_2+\gamma_4}^{-2} \mathcal{K}_{6\gamma_1+7\gamma_2+7\gamma_4} \\
& \mathcal{K}_{5\gamma_1+6\gamma_2+6\gamma_4} \mathcal{K}_{4\gamma_1+5\gamma_2+5\gamma_4} \mathcal{K}_{3\gamma_1+4\gamma_2+4\gamma_4} \mathcal{K}_{2\gamma_1+3\gamma_2+3\gamma_4} \mathcal{K}_{\gamma_1+2\gamma_2+2\gamma_4} \mathcal{K}_{2\gamma_1+\gamma_2} \\
& \mathcal{K}_{6\gamma_1+4\gamma_2+\gamma_4} \mathcal{K}_{10\gamma_1+7\gamma_2+2\gamma_4}^3 \mathcal{K}_{4\gamma_1+3\gamma_2+\gamma_4}^3 \mathcal{K}_{8\gamma_1+6\gamma_2+2\gamma_4}^{-6} \mathcal{K}_{10\gamma_1+8\gamma_2+3\gamma_4}^{68} \mathcal{K}_{6\gamma_1+5\gamma_2+2\gamma_4}^{13} \\
& \mathcal{K}_{8\gamma_1+7\gamma_2+3\gamma_4}^{68} \mathcal{K}_{6\gamma_1+6\gamma_2+3\gamma_4}^{18} \mathcal{K}_{2\gamma_1+2\gamma_2+\gamma_4}^3 \mathcal{K}_{4\gamma_1+4\gamma_2+2\gamma_4}^{-6} \mathcal{K}_{8\gamma_1+8\gamma_2+4\gamma_4}^{-84} \mathcal{K}_{6\gamma_1+7\gamma_2+4\gamma_4}^{68} \\
& \mathcal{K}_{4\gamma_1+5\gamma_2+3\gamma_4}^{13} \mathcal{K}_{6\gamma_1+8\gamma_2+5\gamma_4}^{68} \mathcal{K}_{6\gamma_1+9\gamma_2+6\gamma_4}^{18} \mathcal{K}_{2\gamma_1+3\gamma_2+2\gamma_4}^3 \mathcal{K}_{4\gamma_1+6\gamma_2+4\gamma_4}^{-6} \\
& \mathcal{K}_{4\gamma_1+7\gamma_2+5\gamma_4}^3 \mathcal{K}_{2\gamma_1+4\gamma_2+3\gamma_4} \mathcal{K}_{\gamma_2+\gamma_4} \mathcal{K}_{3\gamma_1+2\gamma_2} \mathcal{K}_{4\gamma_1+3\gamma_2} \mathcal{K}_{5\gamma_1+4\gamma_2} \mathcal{K}_{6\gamma_1+5\gamma_2} \mathcal{K}_{7\gamma_1+6\gamma_2} \\
& \mathcal{K}_{8\gamma_1+7\gamma_2} \mathcal{K}_{9\gamma_1+8\gamma_2} \mathcal{K}_{10\gamma_1+9\gamma_2} \mathcal{K}_{11\gamma_1+10\gamma_2} \mathcal{K}_{\gamma_1+\gamma_2}^{-2} \mathcal{K}_{10\gamma_1+11\gamma_2} \mathcal{K}_{9\gamma_1+10\gamma_2} \mathcal{K}_{8\gamma_1+9\gamma_2} \\
& \mathcal{K}_{7\gamma_1+8\gamma_2} \mathcal{K}_{6\gamma_1+7\gamma_2} \mathcal{K}_{5\gamma_1+6\gamma_2} \mathcal{K}_{4\gamma_1+5\gamma_2} \mathcal{K}_{3\gamma_1+4\gamma_2} \mathcal{K}_{2\gamma_1+3\gamma_2} \mathcal{K}_{\gamma_1+2\gamma_2} \mathcal{K}_{\gamma_2},
\end{aligned} \tag{5.9}$$

where \mathcal{K} -factors in green are those of the newborn $m = 3$ cohort. Notice the large values of Ω .

Both formulae (5.6), (5.9) can be recast in more suggestive forms by adopting the notation³²

$$\Pi^{(n,m)}(a,b) := \left(\prod_{k \nearrow n}^{\infty} \mathcal{K}_{(k+1)a+kb} \right) \mathcal{K}_{a+b}^{-2} \left(\prod_{\ell \searrow m}^{\infty} \mathcal{K}_{\ell a+(\ell+1)b} \right) \tag{5.10}$$

Expression (5.6) is then simply the truncation to $|\gamma| = 21$ of (cf. (4.7))

$$\Pi^{(0,0)}(\gamma_3, \gamma_4) \Pi^{(0,1)}(\gamma_1 + \gamma_3, \gamma_2 + \gamma_4) \Pi^{(0,0)}(\gamma_1, \gamma_2 + \gamma_4) \Pi^{(1,0)}(\gamma_1, \gamma_2) \tag{5.11}$$

Similarly, for (5.9) we have

$$\begin{aligned}
& \Pi^{(0,0)}(\gamma_3, \gamma_4) \Pi^{(0,1)}(\gamma_1 + \gamma_3, \gamma_2 + \gamma_4) \Pi^{(0,1)}(\gamma_1, \gamma_2 + \gamma_4) \\
& \Xi(2\gamma_1 + \gamma_2, \gamma_2 + \gamma_4) \Pi^{(2,0)}(\gamma_1, \gamma_2)
\end{aligned} \tag{5.12}$$

where $\Xi(2\gamma_1 + \gamma_2, \gamma_2 + \gamma_4)$ represents the contribution from the full $\mathcal{C}_3(2\gamma_1 + \gamma_2, \gamma_2 + \gamma_4)$ cohort, which we now analyze in greater detail.

5.3 Exponential growth of the BPS degeneracies

We now focus on the part of BPS spectrum within the cohort $\mathcal{C}_3(\gamma_2 + \gamma_4, 2\gamma_1 + \gamma_2)$. Let

$$\mathcal{K}_{(a,b)} \equiv \mathcal{K}_{a(2\gamma_1+\gamma_2)+b(\gamma_2+\gamma_4)}, \quad a, b \in \mathbb{Z}, \tag{5.13}$$

³²We adopt the following conventions: a product of noncommutative factors $\prod_{k \nearrow a}^b$ indicates that values of k increase from left to right between a and b , while $\prod_{k \searrow a}^b$ denotes decreasing values of k from left to right.

then, up to $a + b = 15$, $\Xi(2\gamma_1 + \gamma_2, \gamma_2 + \gamma_4)$ reads

$$\begin{aligned}
& \mathcal{K}_{(1,0)} \mathcal{K}_{(3,1)} \mathcal{K}_{(8,3)} \mathcal{K}_{(10,4)}^{-6} \mathcal{K}_{(5,2)}^3 \mathcal{K}_{(7,3)}^{13} \mathcal{K}_{(9,4)}^{68} \mathcal{K}_{(10,5)}^{465} \mathcal{K}_{(8,4)}^{-84} \mathcal{K}_{(6,3)}^{18} \\
& \mathcal{K}_{(4,2)}^{-6} \mathcal{K}_{(2,1)}^3 \mathcal{K}_{(9,5)}^{2530} \mathcal{K}_{(7,4)}^{399} \mathcal{K}_{(5,3)}^{68} \mathcal{K}_{(8,5)}^{4242} \mathcal{K}_{(9,6)}^{34227} \mathcal{K}_{(6,4)}^{-478} \mathcal{K}_{(3,2)}^{13} \mathcal{K}_{(7,5)}^{4242} \\
& \mathcal{K}_{(8,6)}^{-32050} \mathcal{K}_{(4,3)}^{68} \mathcal{K}_{(5,4)}^{399} \mathcal{K}_{(6,5)}^{2530} \mathcal{K}_{(7,6)}^{16965} \mathcal{K}_{(8,7)}^{118668} \mathcal{K}_{(7,7)}^{18123} \mathcal{K}_{(6,6)}^{-2808} \mathcal{K}_{(5,5)}^{465} \\
& \mathcal{K}_{(4,4)}^{-84} \mathcal{K}_{(3,3)}^{18} \mathcal{K}_{(2,2)}^{-6} \mathcal{K}_{(1,1)}^3 \mathcal{K}_{(7,8)}^{118668} \mathcal{K}_{(6,7)}^{16965} \mathcal{K}_{(5,6)}^{2530} \mathcal{K}_{(4,5)}^{399} \mathcal{K}_{(6,8)}^{-32050} \mathcal{K}_{(3,4)}^{68} \\
& \mathcal{K}_{(5,7)}^{4242} \mathcal{K}_{(6,9)}^{34227} \mathcal{K}_{(4,6)}^{-478} \mathcal{K}_{(2,3)}^{13} \mathcal{K}_{(5,8)}^{4242} \mathcal{K}_{(3,5)}^{68} \mathcal{K}_{(4,7)}^{399} \mathcal{K}_{(5,9)}^{2530} \mathcal{K}_{(5,10)}^{465} \mathcal{K}_{(4,8)}^{-84} \\
& \mathcal{K}_{(3,6)}^{18} \mathcal{K}_{(2,4)}^{-6} \mathcal{K}_{(1,2)}^3 \mathcal{K}_{(4,9)}^{68} \mathcal{K}_{(3,7)}^{13} \mathcal{K}_{(4,10)}^{-6} \mathcal{K}_{(2,5)}^3 \mathcal{K}_{(3,8)} \mathcal{K}_{(1,3)} \mathcal{K}_{(0,1)}
\end{aligned} \tag{5.14}$$

The BPS degeneracies appearing in (5.14) look rather *wild* at first sight. One way of looking at them is to consider sequences of charges $(a_0 + na, b_0 + nb)$ approaching different “slopes” a/b for $n \rightarrow \infty$, and study the asymptotics of Ω for large n . As illustrated in figure 11, the BPS index grows exponentially with n , the asymptotic exponential behavior depends entirely on a/b and not on a_0, b_0 .

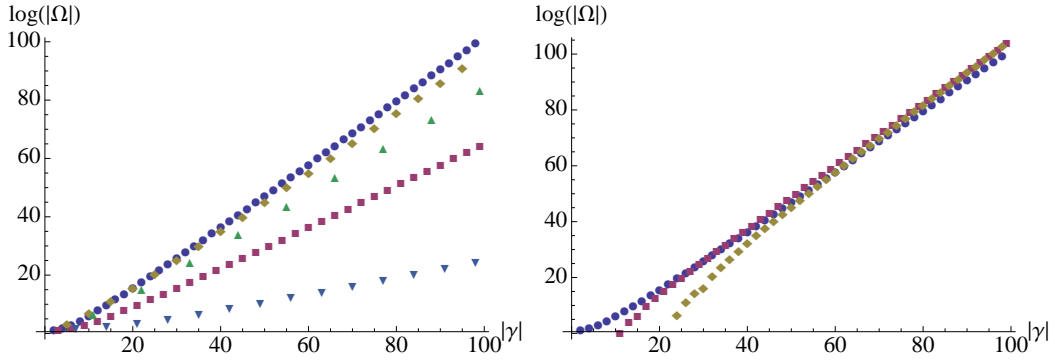


Figure 11. Left: values of $\log \Omega(an, bn)$ for several slopes a/b : 1 (circles), $3/2$ (diamonds), $7/4$ (up-triangles), 2 (squares), $5/2$ (down-triangles). Right: sequences of type $(a_0 + an, b_0 + bn)$ have the same asymptotics; here we show $a = b = 1$ with $a_0 - b_0 = 0, 5, 10$.

According to the positivity conjecture discussed below equation (A.4), BPS indices count dimensions of Hilbert subspaces, as stated more precisely in (7.19). Such exponential growth in the number of states may seem surprising in the context of a gauge theory. We will return to the physical implications below, in Section 7.

6 Relation to quivers

In addition to spectral networks, one alternative route to the BPS spectrum is the dual description in terms of quiver quantum mechanics [6, 29, 30]. The problem of counting BPS states gets mapped into that of counting cohomology classes of moduli spaces of quiver representations. These classes are organized into Lefschetz multiplets, which correspond to

the $\mathfrak{so}(3)$ multiplets. The PSC $\Omega(\gamma, u; y)$ is then given by the Poincaré polynomial associated to a certain quiver representation.

The basic observation here is that an isolated wall-crossing of hypermultiplets with charges γ, γ' such that $\langle \gamma, \gamma' \rangle = m$ will produce the spectrum of the Kronecker m -quiver in the wild stability region.

6.1 Derivation of the Kronecker m -quivers from the strong coupling regime

Here we briefly describe how the quiver description fits in our study of the BPS spectrum of this theory. We start in the strong coupling chamber: we choose a half-plane as shown in the first frame of figure 12, the corresponding BPS quiver is shown in the second frame of the same figure. As we move along the path (4.3), we come to the situation shown in the third frame of figure 12: three MS walls have been crossed, and the corresponding $m = 2$ cohorts are indicated (this corresponds to the situation shown in the fifth frame of figure 10 above.). Note that no walls of the second kind³³ have been crossed, hence the same BPS quiver is still valid.

Now, while keeping the moduli fixed, we rotate the half-plane clockwise inducing a mutation

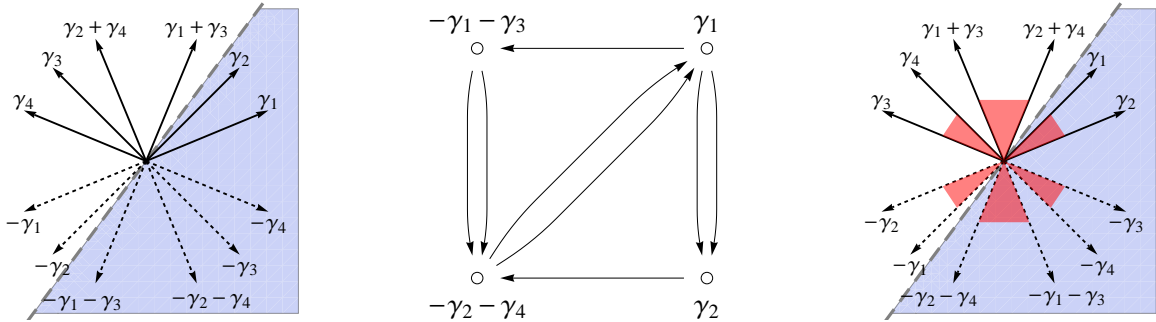


Figure 12. Left: the disposition of charges and choice of half plane in the strong coupling chamber. The depiction of the central charges is schematic. Center: the quiver at strong coupling. Right: central charges and cohorts after crossing the first three MS walls along our path.

on the quiver, as shown in the first two frames of figure 13. We then proceed a little further along our path on \mathcal{B} , until we cross the wall $MS(\gamma_1, \gamma_2 + \gamma_4)$, again this does not involve crossing walls of the second kind, and the same quiver is still valid. The charge disposition and cohorts are shown in the third frame of figure 13.

Finally, we rotate the half-plane counterclockwise, as shown in figure 14, inducing an inverse mutation on the node $-\gamma_2 - \gamma_4$, which results in the desired BPS quiver.

The two lower nodes of the quiver we just obtained manifestly exhibit the 3-Kronecker quiver involved in wild wall-crossing as a subquiver. In particular, it offers a convenient starting point for studying stable quiver representations on both sides of $MS(\gamma_2 + \gamma_4, 2\gamma_1 + \gamma_2)$: states with

³³In the physics literature, a wall of the second kind is, roughly speaking, the locus on the moduli space where the central charge of a populated state *exits* the half-plane associated with the quiver under study. When this happens, the quiver description changes by a mutation, for more details, see [30].

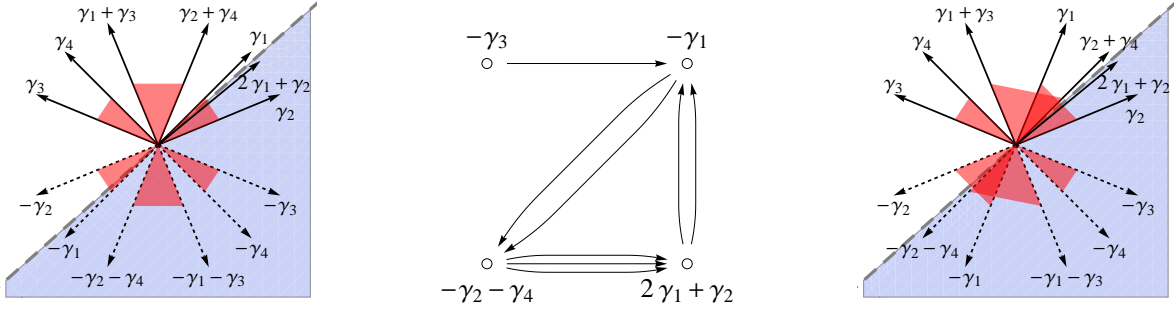


Figure 13. Left: a clockwise rotation of the half-plane past the ray Z_{γ_1} . Center: the corresponding BPS quiver. Right: after proceeding further on \mathcal{B} we cross $MS(\gamma_1, \gamma_2 + \gamma_4)$

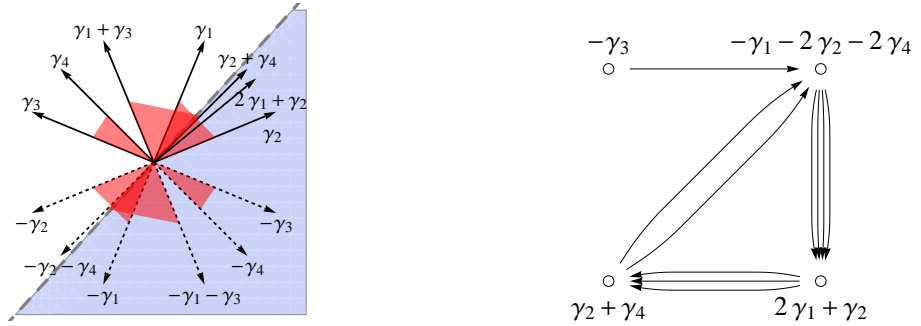


Figure 14. Left: a counterclockwise rotation past $Z_{\gamma_2 + \gamma_4}$. Right: the corresponding BPS quiver.

charge $a(\gamma_2 + \gamma_4) + b(2\gamma_1 + \gamma_2)$ correspond to particularly simple dimension vectors, in which the two upper nodes decouple leaving the pure 3-Kronecker quiver. We will not pursue the stability analysis in this paper, let us stress however that, since we have been working with stability parameters constrained by special geometry on the Coulomb branch (as opposed to working in \mathbb{C}^4), it should be possible to perform such analysis on both sides of the above-mentioned MS wall, thus recovering the related wild degeneracies.

The above construction generalizes easily to higher m . Consider indeed the situation in frame three of Figure 13: here one could rotate the half-plane clockwise up until crossing the ray of $\gamma^{(j+1,j)} := (j+1)\gamma_1 + j\gamma_2$, resulting in a sequence of mutations leading to the quiver of Figure 15. Then, without crossing walls of the second kind, one can move on \mathcal{B} on a continuation of our path, as discussed in Section 4.4, until getting past $MS((j+1)\gamma_1 + j\gamma_2, \gamma_2 + \gamma_4)$, the same quiver description still holds.

At this point, a counterclockwise rotation of the half-plane, corresponding to an inverse mutation on $-\gamma_2 - \gamma_4$ yields the quiver given in Figure 16. Again the two lower nodes exhibit the Kronecker subquiver of interest.

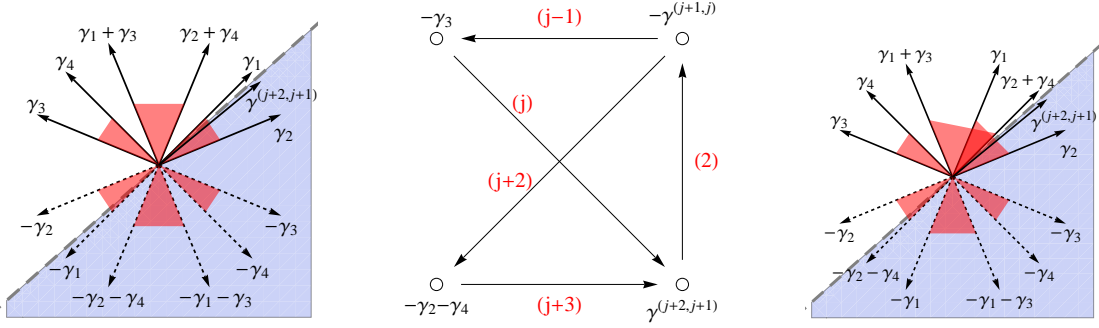


Figure 15. Left: a clockwise rotation of the half-plane past the ray $Z_{(j+1)\gamma_1 + j\gamma_2}$. Center: the corresponding BPS quiver, arrow multiplicities are indicated in red. Right: after proceeding further on \mathcal{B} we cross $MS((j+1)\gamma_1 + j\gamma_2, \gamma_2 + \gamma_4)$

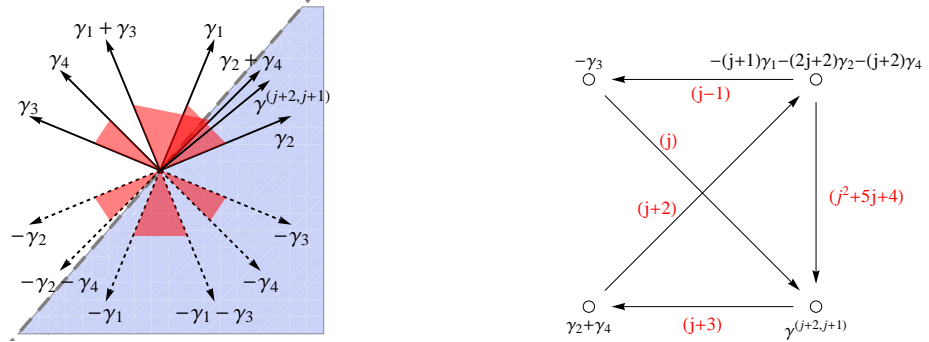


Figure 16. Left: a counter-clockwise rotation of the half-plane past the ray $Z_{\gamma_2 + \gamma_4}$. Right: the corresponding BPS quiver, with arrow multiplicities indicated in red.

6.2 A nontrivial symmetry of BPS degeneracies

One very nice application of the quiver approach is that it reveals an intriguing symmetry of BPS degeneracies which would be very hard to discover using spectral networks.

Our previous analysis of the \mathcal{C}_3 spectrum has focused on sequences of states $(na + a_0)\gamma_1 + (nb + b_0)\gamma_2$ with fixed slope a/b as $n \rightarrow \infty$. In this section we will instead consider sequences of states with the same BPS index.

In full generality, given two hypermultiplets with charges γ, γ' such that $\langle \gamma, \gamma' \rangle = m > 0$, we know already from the semi-primitive WCF that, across the wall $MS(\gamma, \gamma')$, a new hypermultiplet of charge $\gamma + m\gamma'$ will be a stable boundstate. The constituents γ, γ' , as well as their CPT conjugates will also be stable. Now, note that $\langle -\gamma', \gamma + m\gamma' \rangle = m$, moreover we have the following relation between stability parameters

$$\text{sign} \left(\text{Im} \frac{Z_\gamma}{Z_{\gamma'}} \right) \equiv \text{sign} \left(\text{Im} \frac{Z_{-\gamma'}}{Z_{\gamma + m\gamma'}} \right). \quad (6.1)$$

Thus, any boundstate of γ, γ' can *equivalently* be described as a boundstate of $-\gamma', \gamma + m\gamma'$.

Such change of *simple roots* for the $K(m)$ quiver simply corresponds³⁴ to a change of duality frame by

$$g_m = \begin{pmatrix} 0 & 1 \\ -1 & m \end{pmatrix} \in Sp(2, \mathbb{Z}) \quad (6.2)$$

in a basis where γ, γ' are represented by column vectors $(1, 0), (0, 1)$ respectively. That is, there is a mutation of the quiver corresponding to the change of basis g_m . Since this is detectable by the semiprimitive wall crossing formula there should be a halo interpretation, to which we return in Section §9, Remark 4.

The above is essentially an observation of [31] and it immediately implies some remarkable identities for BPS indices. The group

$$\mathcal{R} = \langle h, h' | h^2 = 1, h'^2 = 1 \rangle = \mathbb{Z}_2 \star \mathbb{Z}_2 \quad (6.3)$$

has an action on $\mathbb{Z}\gamma \oplus \mathbb{Z}\gamma'$ by

$$h = \begin{pmatrix} 0 & 1 \\ 1 & 0 \end{pmatrix}, \quad h' = \begin{pmatrix} -1 & m \\ 0 & 1 \end{pmatrix}, \quad g_m = h h', \quad (6.4)$$

then the BPS indices must have the symmetry:

$$\Omega(g \cdot \gamma) = \Omega(\gamma), \quad \forall g \in \mathcal{R}. \quad (6.5)$$

In other words, the spectrum can be organized into orbits of \mathcal{R} .

Remarks

- The identity (6.5) extends to the protected spin character

$$\Omega(g \cdot \gamma; y) = \Omega(\gamma; y). \quad (6.6)$$

- Consider for example $m = 3$, we call the *slope* of (a, b) the ratio a/b . The eigenvalues of g_3 are

$$\xi_{\pm} = \frac{3 \pm \sqrt{5}}{2} \quad (6.7)$$

corresponding to the slopes limiting the cone of dense states of Fig. 17. All g_3 orbits are confined to lie either inside or outside of the cone, and asymptote to the limiting rays.

- The only orbits falling outside of the cone are those of “pure” hypermultiplets i.e. states with $\Omega = 1$. All the other orbits are contained within the cone.

³⁴In the mathematics literature this correspondence is a known isomorphism among Kronecker moduli spaces, see for example [31], Remark 3.2.

- In the pure $SU(2)$ theory the limiting rays of the g_2 cone collapse into a single ray, which coincides with the slope of the gauge boson. In that context, the g_2 action has an interpretation in terms of a half-turn around the strong coupling chamber, combined with the residual R -symmetry, in a similar spirit to the approach of [4]. One can check that, in a suitable duality frame g_2 is a square root of the monodromy at infinity, up to an overall factor.

For the $m = 1$ Kronecker quiver, the g_1 action simply recovers the whole spectrum.

6.3 Asymptotics of BPS degeneracies

For physical reasons we are often interested in the asymptotics of BPS degeneracies for large charges. There is no known simple closed formula for the degeneracies $\Omega(a\gamma_1 + b\gamma_2)$ of the 3-Kronecker quiver. In this section we discuss some aspects of the large a, b asymptotics.

The Poincaré polynomial for quivers without closed loops has been found explicitly in a closed form, as a sum over constrained partitions of corresponding quiver dimension vectors [7]. Unfortunately Reineke’s formula does not lend itself well to an evaluation of the large charge asymptotics. On the other hand, use of localization techniques allows one to estimate asymptotic behavior of the Euler characteristic for moduli spaces of m -Kronecker quiver representations [18].

Weist conjectured the following. Consider a state $N\gamma + M\gamma'$ with $\langle \gamma, \gamma' \rangle = m$, in a wild region of the Coulomb branch. The corresponding BPS index equals the Euler characteristic of the moduli space of the quiver with m arrows between two nodes with spaces \mathbb{C}^N and \mathbb{C}^M in a wild region of stability parameters. Now consider a sequence of dimension vectors $N = an + a_0$, $M = bn + b_0$, with a, b, a_0, b_0 fixed. Weist conjectured that the asymptotic behavior of the Euler characteristic has the form

$$\log |\Omega(N\gamma + M\gamma')| \underset{n \rightarrow \infty}{\sim} n C_{a,b}(m)$$

$$C_{a,b}(m) = \frac{\sqrt{mab - a^2 - b^2}}{\sqrt{m - 2}} \left[(m - 1)^2 \log(m - 1)^2 - (m^2 - 2m) \log(m^2 - 2m) \right]. \quad (6.8)$$

Note that $C_{1,1}(m) = c_m$ of equation (3.23).

6.4 Numerical check of Weist’s conjecture

In section 5 we obtained BPS degeneracies by using an algorithmic approach, based on the KSWCF (4.5). The results are in agreement with [20]: in particular we found a sequence of degeneracies of slope 1 behaving as predicted by Reineke in [17], as well as a highly populated – suggesting dense – cone of “wild” BPS states in the complex Z_γ -plane. The region outside such cone is populated by hypermultiplets only, falling in sequences approaching the boundaries of the cone, as shown in figure 17.

Let $\gamma_{a,b}(n) = (na + a_0)\gamma_1 + (nb + b_0)\gamma_2$. Denoting by

$$\eta_{a,b} := \log |\Omega(\gamma_{a,b}(n))| \sqrt{\frac{m - 2}{mab - a^2 - b^2}}, \quad (6.9)$$

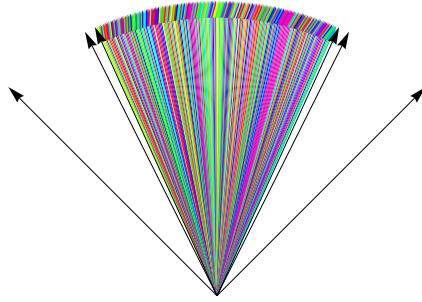


Figure 17. Schematic picture of BPS states charges for 3-Kronecker quiver. A dense cone is bounded by rays of slopes $a/b = (3 \pm \sqrt{5})/2$. Only hypermultiplets fall out of the cone.

Weist’s conjecture says that $\eta_{ab}/n \rightarrow c_m, \forall \gamma \in \text{dense cone}$ as n grows (c_m is defined by formula (3.23)). In Fig. 11 we already noticed this kind of behavior, to some extent. In order to establish a more precise match between our data and Weist’s conjecture, it is convenient to plot the behavior of $\eta_{a,b}/n$ versus the $|\gamma|$ filtration level, as in Fig. 18.

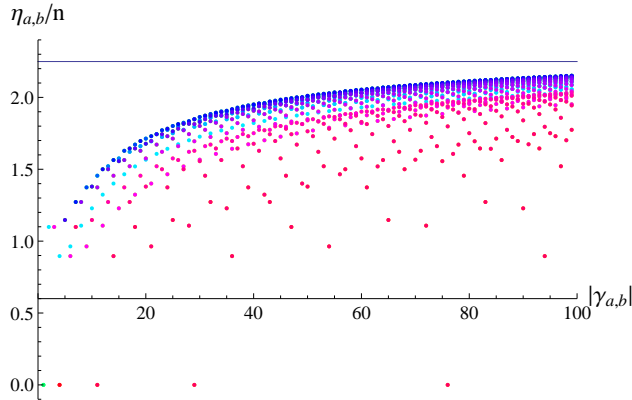


Figure 18. The data shown is for $m = 3$ with $(a_0, b_0) = (0, 0)$. The straight horizontal line represents the Weist coefficient $c_3 = 4 \log 4 - 3 \log 3$. For generic values of (a, b) the BPS degeneracies indeed approach the Weist asymptotics at large $|\gamma|$.

Different colors depict different slopes from the red for $a \gg b$ or $a \ll b$ to the blue for $a \sim b$. As the graph shows, the speed of convergence actually depends on the slope, so the degeneracies for BPS states nearest to the cone boundaries approach Weist’s asymptotics in the worst way. Note that there are some charges that do not obey the general asymptotic behavior. These give the horizontal data points at the bottom of Fig. 18. These charges indeed lie outside the dense cone. ³⁵

³⁵Note that, because of g_m symmetry, the figure would look rather different if we plotted the degeneracies as a function of n using $\gamma_{a,b}(n)$.

7 Physical estimates and expectations

7.1 An apparent paradox

In this section we first present a physical argument which seems to lead to a very general bound on the behavior of the BPS index in any supersymmetric field theory. The purported bound, however, is explicitly violated by the “wild” degeneracies we have just found in the pure $SU(3)$ theory. Thus, naïvely, there is a paradox. We first explain the paradox in more detail, and then explain how this paradox is resolved.³⁶

At very large energy our effective theory should approach a UV conformal fixed point. So consider a d -dimensional CFT put in a box of volume V and heated up to temperature T . Since we have only two dimensionful parameters and we assume the energy and the entropy of the system to be extensive quantities, simple dimensional analysis is enough to predict their form up to dimensionless constants (which will depend on the theory):

$$\begin{aligned} E(T, V) &= \alpha VT^d, \\ S(T, V) &= \beta VT^{d-1}. \end{aligned} \tag{7.1}$$

Eliminating the temperature dependence we derive the scaling of the entropy with the energy:

$$S(E, V) = \kappa V^{1/d} E^{(d-1)/d}. \tag{7.2}$$

This provides an estimate for the behavior of the number of microstates of energy E supported in a volume V , and gives the correct asymptotic dependence for $E \rightarrow \infty$.

In order to excite massive states we can increase the temperature, thus taking into account heavier BPS states. The BPS index, being a signed sum over the states in the theory, cannot exceed the overall number of states.³⁷ Thus we come to the following chain of inequalities (here we take $d = 4$ and set $E = |Z_\gamma|$):

$$|\Omega(\gamma)| = |\mathrm{Tr}_{\mathfrak{h}^\gamma} (-1)^{2J_3}| \leq \frac{1}{4} \mathrm{Tr}_{\mathcal{H}_{BPS, \gamma}} 1 \leq \frac{1}{4} \mathrm{Tr}_{\mathcal{H}, E} 1 = \frac{1}{4} e^{S(E)} \sim e^{\kappa V^{1/4} E^{3/4}}, \tag{7.3}$$

where the last estimate assumes large E . Thus the observed behavior $\log |\Omega(\gamma)| \sim E$ for large γ in the pure $SU(3)$ theory seems to give a contradiction.

The resolution of this paradox comes from taking into account the fact that our bound applies only to the theory in a finite volume. If the size of BPS states becomes large enough and they do not fit into the box of finite volume, then they do not contribute to the naïve counting of degrees of freedom. So we should instead consider a “truncated BPS index” $\check{\Omega}_V$, counting only the states which fit into a box of size V ; we should expect this index to satisfy the inequality

$$|\check{\Omega}_V| = |\mathrm{Tr}_{\mathcal{H}_{BPS, M=|E|, R \leq V^{1/3}}} (-1)^{2J_3}| \lesssim e^{\kappa V^{1/4} E^{3/4}} \tag{7.4}$$

³⁶We thank T. Banks and S. Shenker for crucial remarks on this matter.

³⁷In fact, the data for the Kronecker m -quiver suggest that in this case all the summands contributing to the BPS index have the same sign, so the BPS index actually counts the number of states up to an overall sign.

with R the average size of a BPS state.

The rest of this section is devoted to arguing that the above scenario is indeed correct. We will use the semiclassical picture of BPS states given by the Denef equations, reviewed in Section 7.2, to give a lower bound for the average size of the semiclassical BPS states. The resolution of the paradox is spelled out in some more detail in Section 7.3. We give some supporting evidence for the validity of the use of the Denef equations for describing the exponentially large number of BPS states in Section 7.4.

7.2 Denef equations

In order to estimate the size of the BPS states arising in the theory, we refer to the interpretation [29] of those BPS states that arise from wall-crossing as multi-centered solutions similar to those arising in $\mathcal{N} = 2$ supergravity [6]. We assume Denef’s multicentered picture has a good $\alpha' \rightarrow 0$ limit and can be applied to field theory. Suppose we have a set of elementary BPS states with charges $\{\gamma_A\}_{A=1}^n$ placed at corresponding points $\{r_A\}_{A=1}^n$ of \mathbb{R}^3 . This configuration is again BPS only if the following set of equations is satisfied:

$$\sum_{\substack{B=1 \\ B \neq A}}^n \frac{\langle \gamma_A, \gamma_B \rangle}{|r_A - r_B|} = 2\text{Im}(e^{-i\vartheta} Z_{\gamma_A}), \quad (7.5)$$

where $\vartheta = \arg \sum_{A=1}^n Z_{\gamma_A}$.

Now let us consider a BPS state of total charge $M\gamma_1 + N\gamma_2$, with $\langle \gamma_1, \gamma_2 \rangle = m$. Let us, *for the moment*, suppose that the dominant contribution to the entropy comes from a boundstate of M elementary constituents of charge γ_1 and N elementary constituents of charge γ_2 .

In the case where the charges are of the form

$$\underbrace{\{\gamma_1, \dots, \gamma_1\}}_M, \underbrace{\{\gamma_2, \dots, \gamma_2\}}_N \quad (7.6)$$

the equations simplify to

$$\begin{aligned} \sum_{a=1}^N \frac{m}{r_{ia}} &= \kappa_1 := 2\text{Im}(e^{-i\vartheta} Z_{\gamma_1}), & 1 \leq i \leq M \\ \sum_{i=1}^M \frac{-m}{r_{ia}} &= \kappa_2 := 2\text{Im}(e^{-i\vartheta} Z_{\gamma_2}), & 1 \leq a \leq N \end{aligned} \quad (7.7)$$

We can view the index a as running over “electrons” and i over “magnetic monopoles,” in an appropriate duality frame.

Now we are interested in the size of the boundstate. Therefore we consider the sum over the first equation in (7.7). (Doing the analogous sum over the second equation produces an equivalent result.) The result is that

$$\sum_{i,a} \frac{1}{r_{ia}} = \frac{NM}{|MZ_{\gamma_1} + NZ_{\gamma_2}|} \left(\frac{2\text{Im}(\bar{Z}_{\gamma_2} Z_{\gamma_1})}{m} \right) \quad (7.8)$$

We can rewrite this equation nicely in terms of the *harmonic average* of the distances r_{ia} :

$$\langle r_{ia} \rangle_h = \left(\frac{m}{2\text{Im}(\bar{Z}_{\gamma_2} Z_{\gamma_1})} \right) |MZ_{\gamma_1} + NZ_{\gamma_2}|. \quad (7.9)$$

On the other hand, we can use the well-known inequality that the harmonic average is a lower bound for the ordinary average, $\langle r_{ia} \rangle_h \leq \langle r_{ia} \rangle$, to conclude that

$$\left(\frac{m}{2\text{Im}(\bar{Z}_{\gamma_2} Z_{\gamma_1})} \right) |MZ_{\gamma_1} + NZ_{\gamma_2}| \leq \langle r_{ia} \rangle. \quad (7.10)$$

Equation (7.10) is a key result. It shows that if N or M goes to infinity then the size of the average BPS molecule grows linearly with N or M , respectively.

We have shown that boundstates of total charge $M\gamma_1 + N\gamma_2$ with constituents (7.6) become large when $N, M \rightarrow \infty$. However, other partitions of N, M can and do lead to BPS boundstates. In general, given a pair of partitions

$$M = \sum_{j=1}^M l_j j, \quad N = \sum_{k=1}^N s_k k \quad (7.11)$$

there can be other boundstates where there are l_j centers of charge $j\gamma_1$ and s_k centers of charge $k\gamma_2$. In order to deal with these cases, let us introduce, for any set of charges $\{\gamma_A\}$, the moduli space $\mathcal{M}(\{\gamma_A\})$ of solutions to the Denef equations (7.5). If there are n centers it is a subspace of \mathbb{R}^{3n} . Note that the moduli space for charges

$$\underbrace{\{\gamma_1, \dots, \gamma_1\}}_{l_1}, \underbrace{\{2\gamma_1, \dots, 2\gamma_1\}}_{l_2}, \dots, \underbrace{\{\gamma_2, \dots, \gamma_2\}}_{s_1}, \underbrace{\{2\gamma_2, \dots, 2\gamma_2\}}_{s_2}, \dots \quad (7.12)$$

is in fact a subspace of the moduli space for (7.6), where certain collections of centers r_i and r_a have (separately) collided. Nevertheless, the identity (7.9) applies uniformly throughout the moduli space and hence applies to all possible partitions. As an extreme example, the moduli space $\mathcal{M}(\{M\gamma_1, N\gamma_2\}) \cong \mathbb{R}^3 \times S^2$, where the \mathbb{R}^3 is the center of mass and the S^2 has a radius

$$R_{12} = \left(\frac{m}{2\text{Im}(\bar{Z}_{\gamma_2} Z_{\gamma_1})} \right) |MZ_{\gamma_1} + NZ_{\gamma_2}|. \quad (7.13)$$

In any case, we can conclude that for any partition of charges such as (7.12) the average BPS state has a size bounded below by a linear expression in N and M . We call these large semiclassical BPS states *BPS giants*.

7.3 Resolution and Revised Bound

The giant BPS states resolve the paradox explained in Section 7.1 above. Indeed we can adapt the bound (7.3) by adjusting the volume of the box V in such a way that states of mass E fit in a volume $V_E := R_E^3 := E^3$. From our estimate of the sizes of BPS molecules we know that the average size indeed scales linearly with E . Therefore the new bound is

$$\log |\Omega(E)| \sim \alpha E \lesssim \kappa E^{3/4} V_E^{1/4} \sim \kappa' E^{3/2} \quad (7.14)$$

and is indeed satisfied.

In equation (7.14) κ' is a dimensionful constant, it scales as $\kappa' \sim (\text{length})^{\frac{3}{2}}$. Let us give a physical interpretation for this scale. If we consider a sequence of charges $N(a\gamma_1 + b\gamma_2)$, with $N \rightarrow \infty$ and $\gamma_p := a\gamma_1 + b\gamma_2$ primitive, then the size of an average BPS molecule behaves as $R \sim r_0 N$, where r_0 is the size of a state with charge γ_p . The energy behaves as $E = |Z_0|N$, where Z_0 is a central charge of the state with charge γ_p . Thus we can give a formula accounting for the scaling dimension of κ' in (7.14) by using

$$V_E = R_E^3 \sim (r_0 N)^3 \sim (r_0 E / |Z_0|)^3 \quad (7.15)$$

to deduce

$$\begin{aligned} E^{3/4} V_E^{1/4} &\sim \left(\frac{r_0}{|Z_0|} \right)^{3/4} E^{3/2}, \\ \Rightarrow \kappa' &\sim \left(\frac{r_0}{|Z_0|} \right)^{3/4}. \end{aligned} \quad (7.16)$$

We remark that

1. The length scale $(r_0/|Z_0|)^{1/2}$ is a function of the moduli, since both r_0 and Z_0 are functions of the moduli.
2. The coefficient α in (7.14) is

$$\alpha = \frac{C_{a,b}(m)}{|Z(a\gamma_1 + b\gamma_2)|} \quad (7.17)$$

for the series of charges above eq. (6.9). As we noted in Section 4.4 there are points on the Coulomb branch with arbitrarily high m and

$$C_{a,b}(m) \sim \sqrt{ab} \log m^2 \quad (7.18)$$

for large m . Hence, somewhat surprisingly, the coefficient of the logarithmic growth is unbounded on the Coulomb branch.

7.4 Discussion of validity of the semiclassical picture

In this section we will address the question of how reliable the semiclassical approximation is. We will review some supporting evidence for the reliability of the semiclassical pictures based on the relation of an exact result for BPS degeneracies Ω to certain symplectic volumes.

As a side remark we note that numerical data for the 3-Kronecker quiver strongly suggest (cf. the discussion about positivity below (A.4)) that the BPS index actually measures the number of states

$$|\Omega(\gamma)| = \text{Tr}_{\mathfrak{h}_\gamma} 1. \quad (7.19)$$

This relation is not essential to our argument but it does nicely simplify the considerations.

Let us recall the symplectic structure on Denev moduli space $\mathcal{M}(\{\gamma_A\})$. Overall translation acts on this space and the reduced space $\overline{\mathcal{M}}(\{\gamma_A\}) = \mathcal{M}(\{\gamma_A\})/\mathbb{R}^3$ is generically $2n - 2$ dimensional. Moreover, the reduced space admits a symplectic form [14]:

$$\omega = \frac{1}{4} \sum_{i < j} \langle \gamma_i, \gamma_j \rangle \frac{\epsilon_{abc} dr_{ij}^a \wedge dr_{ij}^b r_{ij}^c}{r_{ij}^3}. \quad (7.20)$$

In the semiclassical approximation we identify a subspace of the space of BPS states with a set of BPS field configurations. We expect that the dimension of a subspace corresponding to a charge decomposition can be estimated, in the semiclassical approximation, by the symplectic volume

$$\text{Vol}(\{\gamma_A\}) := \frac{1}{(n-1)!} \int_{\overline{\mathcal{M}}} \left(\frac{\omega}{2\pi} \right)^{n-1}. \quad (7.21)$$

where n is the number of centers.

Now, thanks to a result of Manschot, Pioline, and Sen [26, 27], in the example of the m -Kronecker quiver the protected spin character in the wild chamber can in fact be expressed exactly as a sum over two partitions (7.11) so that

$$\begin{aligned} \Omega(M\gamma_1 + N\gamma_2; y) &= \\ &= \sum_{\{l_j\}, \{s_k\}} g_{\text{ref}}(\{l_j\}, \{s_k\}; y) \prod_{j,k} \frac{1}{l_j! j^{l_j} s_k! k^{s_k}} \left(\frac{y - y^{-1}}{y^j - y^{-j}} \right)^{l_j} \left(\frac{y - y^{-1}}{y^k - y^{-k}} \right)^{s_k} \end{aligned} \quad (7.22)$$

where g_{ref} refers to an equivariant Dirac index on the space of solutions to Denev's equations with distinguishable centers described by charge partitions $\{l_j\}, \{s_k\}$. If we specialize to the index at $y = 1$ ³⁸ then g_{ref} has a very nice interpretation as the symplectic volume (7.21) of the moduli space of solutions to Denev's equations (up to a sign):

$$\Omega(M\gamma_1 + N\gamma_2) = \sum_{\{l_j\}, \{s_k\}} (-1)^{mMN+1-\sum_j l_j - \sum_k s_k} \text{Vol}(\{l_j\}, \{s_k\}) \prod_{j,k} \frac{1}{l_j! j^{2l_j} s_k! k^{2s_k}}. \quad (7.23)$$

where $\text{Vol}(\{l_j\}, \{s_k\})$ is (7.21) for the charges (7.12).

We will take this relation of the exact number of BPS states to symplectic volumes as sufficient evidence for the validity of our resolution. There are, however, some further interesting aspects of this formula which we will comment on in the following Sections 7.4.1 and 7.4.2 below.

7.4.1 A toy example: the Hall halo

A very nice exactly solvable example of BPS configurations is provided by the Hall halo of [6]. Consider a configuration of N electric particles and a single magnetic monopole of charge m . This corresponds to the case $(M, N) = (1, N)$ in the notation above. In this case the

³⁸In the conventions of [26] we take $y \rightarrow 1$ rather than $y \rightarrow -1$ to get the index.

equations (7.7) imply that the N electric particles all lie on a single sphere centered on the magnetic particle and of radius:

$$R_{12} = \left(\frac{m}{2\text{Im}(\bar{Z}_{\gamma_2} Z_{\gamma_1})} \right) |Z_{\gamma_1} + NZ_{\gamma_2}|. \quad (7.24)$$

Now, in this case Denef argued that to get the spin character we can just apply the usual quantum mechanics of Landau levels on a sphere with a magnetic monopole inside. Counting the ground states gives the corresponding protected spin character [5]

$$\Omega(y) = (-y)^{-(m-N)N} \frac{\prod_{j=1}^m (1-y^{2j})}{\prod_{j=1}^N (1-y^{2j}) \prod_{j=1}^{m-N} (1-y^{2j})}, \quad (7.25)$$

in perfect agreement with Reineke's general formula (see eq. (5.3) of [6]).

There are two interesting lessons we can draw from (7.25):

1. First, naive physical intuition suggests that the large size of BPS states is due to large angular momentum. This example shows that in fact this is not necessarily the case. In this case the size of the configuration is given by formula (7.24). Nevertheless this configuration contains representations of many different spins.
2. Second, we can derive the number of states in a multiplet by taking $y \rightarrow -1$. Then $\Omega = \frac{m!}{N!(m-N)!}$. In the limit $N \ll m$ the number of allowed states is much greater than the number of populated states, so quantum statistics does not play an important role, and the semiclassical approximation should work. Indeed,

$$\Omega = \frac{m!}{N!(m-N)!} \underset{N \ll m}{\sim} \frac{m^N}{N!} + \dots \quad (7.26)$$

This confirms the semiclassical expectation that the number of states should be counted by the symplectic volume since the volume is proportional to m^N . Note however that, for fixed N the binomial coefficient is really a polynomial in m and (7.26) is only the leading term at large m . Since $1/m$ plays the role of \hbar we can interpret the subleading terms as quantum corrections to the naive semiclassical reasoning.

7.4.2 Estimating the contribution of the maximal partition

Let us consider the contribution to the BPS degeneracy of the maximal partition (7.6) in the formula (7.23). The symplectic volume for this partition is

$$\text{Vol}((N, M), \kappa_1, \kappa_2, m) := \frac{1}{(N+M-1)!} \int_{\mathcal{M}} \left(\frac{\omega}{2\pi} \right)^{N+M-1} \quad (7.27)$$

where we used the fact that there are $n = N + M$ centers. We would like to estimate this volume when N, M become large.

Rescaling both $\kappa_{1,2}$ in (7.7) by $\lambda \in \mathbb{R}$ together with $r_{ij} \mapsto r_{ij}\lambda^{-1}$ shows that solutions for rescaled values of $\kappa_{1,2}$ are obtained by simply rescaling the distances. Therefore the ratio

$$H((N, M), \kappa_1/\kappa_2) := \text{Vol}((N, M), \kappa_1, \kappa_2, m)/m^{N+M-1}$$

only depends on the ratio κ_1/κ_2 and on N, M . For simplicity, let us specialize to $M = N - 1$. In the limit $N \rightarrow \infty$ we have

$$\begin{aligned} & \lim_{N \rightarrow \infty} \frac{1}{N} \log (\text{Vol}((N - 1, N), \kappa_1, \kappa_2, m)) \\ & \sim \log m^2 + F\left(\frac{\kappa_1}{\kappa_2}\right). \end{aligned}$$

Note that the second piece is independent of m .

There are two important lessons we can draw from this computation:

1. This behavior nicely coincides with the Weist coefficient, but only in the large m limit when:

$$C_{1,1}(m) \sim \log m^2 + \mathcal{O}(m^{-1}) \tag{7.28}$$

The fact that we must take $m \rightarrow \infty$ is not terribly surprising in view of the Hall halo example discussed above.

2. It is interesting to note that at finite values of m the maximal partition does *not* fully account for the exponential growth coefficient, even in the large charge regime. Indeed, as pointed out in [31] we should take into account many other partitions to derive even the leading asymptotic behavior of the BPS index. One important (and subtle) aspect of (7.23) is that the different symplectic volumes are weighted with *signs*. This might imply some subtlety in applying the semiclassical pictures we have used, and should be understood better. In the meantime, as we discuss further in Remark 5 of Section 9: in the formula (7.23), considering the case where the BPS ray lies in the dense cone, there can be striking cancelations between volumes of different partitions.

8 Spectral Moonshine

In the course of these investigations we noticed some unusual and very intriguing features in our data. We mention these here, leaving a deeper analysis and conceptual understanding of these features to future work.

8.1 Scaling behavior of the spin degeneracies

An interesting pattern of the spectrum emerges when we consider the distribution of spin multiplets within $\mathcal{H}_\gamma^{\text{BPS}}$, the subspace of BPS states with gauge charge γ . For the definitions of the protected spin character and the spin decompositions see Appendix A.

Let $\delta_\gamma(j)$ be the number of times a spin- j multiplet³⁹ occurs within $\mathcal{H}_\gamma^{\text{BPS}}$, as in (A.3). Numerical data suggests that *all states within the dense cone* exhibit a common δ -distribution, as shown in Fig. 19 (the data are in Appendix A).

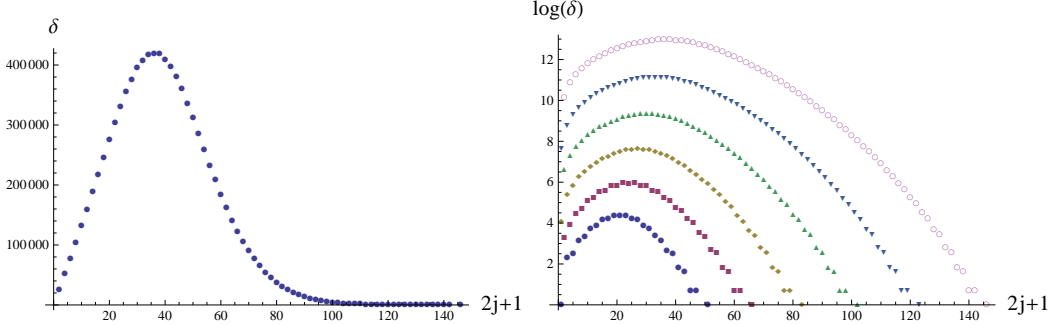


Figure 19. On the left: the distribution $\delta(j)$ for $\gamma = 12(\gamma_1 + \gamma_2)$. On the right: the same distribution for several states $\gamma = n(\gamma_1 + \gamma_2)$. This feature extends to other slopes as well, indeed all states within the dense cone exhibit such “Poisson” behavior.

More precisely, letting γ_n denote the sequence of charges $(na + a_0)\gamma_1 + (nb + b_0)\gamma_2$, data collected by computer experiments strongly suggest that there are functions $\kappa_1, \kappa_2, \kappa_3, \rho, \alpha$ ⁴⁰ of a, b, a_0, b_0 such that, if we define $j_n(s)$ by

$$s = (2j_n(s) + 1)/(\rho|\gamma_n|), \quad (8.1)$$

then the limit

$$u(s) := \lim_{n \rightarrow \infty} \kappa_3 |\gamma_n|^{-\kappa_1} e^{-\kappa_2 |\gamma_n|} \delta_{\gamma_n}(j_n(s)). \quad (8.2)$$

exists and is given by

$$u(s) = s^\alpha e^{-\alpha(s-1)} \quad (8.3)$$

(Recall that $|\gamma_n| = n(a + b) + a_0 + b_0$). The numerical evidence further suggests that for $m = 3$, $\alpha \approx 2$, regardless of the slope⁴¹.

If we assume that the above scaling law holds and the limiting behavior to the scaling function is sufficiently rapid, then one can relate the parameters κ_1, κ_2 of the scaling law to the leading terms in the $n \rightarrow \infty$ asymptotic expansion

$$\log |\Omega(\gamma_n)| \sim \kappa_2 |\gamma_n| + (\kappa_1 + 2) \log |\gamma_n| + \mathcal{O}(1) \quad (8.4)$$

where $\mathcal{O}(1)$ has a finite limit as $n \rightarrow \infty$. Indeed, comparing with the Weist asymptotics (6.8) we learn that $(a + b)\kappa_2 = C_{a,b}(m)$. Similarly, comparing with known asymptotics of $\Omega(\gamma_n)$ we can learn about the a, b, a_0, b_0 dependence of κ_1 .

³⁹Meaning a representation $\rho_{hh} \otimes (j, 0)$ of $\mathfrak{so}(3) \oplus \mathfrak{su}(2)_R$.

⁴⁰The κ_1, κ_2 employed here have nothing to do with those of section 7.4.2.

⁴¹This estimate is based on data collected for $|\gamma| < 30$.

Regardless of the validity of the scaling law, it is worthwhile stressing that the sub-leading behavior of $\log |\Omega(\gamma_n)|$ is interesting in its own right. It is often assumed that, at large n , the BPS index is a continuous function of the slope a/b , however – somewhat surprisingly – the sub-leading correction exhibits a dependence on a_0, b_0 too. To see this, consider two different sequences approaching slope 1, namely $\gamma^{(n)} = (n, n)$ and $\tilde{\gamma}^{(n)} = (n, n+1)$, we have

$$\begin{aligned}\log |\Omega(\gamma_n)| &= nC_{1,1}(m) - \frac{5}{2} \log n + \mathcal{O}(1) \\ \log |\Omega(\tilde{\gamma}_n)| &= nC_{1,1}(m) - 2 \log n + \mathcal{O}(1),\end{aligned}\tag{8.5}$$

where we used the known result⁴²

$$\Omega(n, n-1) = \frac{1}{(3n+2)(2n+1)} \binom{4n+2}{n+1}.\tag{8.6}$$

The subleading dependence on $a/b, a_0, b_0$ exhibited in (8.5) also occurs at the other slopes in the same g_m orbit.

8.2 Partitions and relation to modular functions

Interesting features of the pattern of spin decompositions lie in the tail of the distribution. First of all, for certain sequences $\gamma^{(\alpha)}$, $\alpha = 1, 2, \dots$ such that $|\gamma^{(\alpha)}| \xrightarrow{\alpha \rightarrow \infty} \infty$, we observe the asymptotic behavior of $J_{\max}(\gamma) := \max\{j | \delta_\gamma(j) \neq 0\}$, in particular

$$J_{\max}((n, n)) = \frac{n^2 + 1}{2}, \quad J_{\max}((n+1, n)) = \frac{n^2 + n}{2}.\tag{8.7}$$

We can compare this behavior, as well as that of all other sequences in our data, with a prediction deriving from Kac's theorem (see e.g. [13]) about the dimensionality of the quiver varieties. More precisely, for the Kronecker m -quiver $K(m)$, Kac's theorem asserts that the dimension of the quiver variety $M_{(a,b)}(K(m))$ for indecomposable representations with dimension vectors $\gamma = (a, b)$ is

$$\dim M_{(a,b)}(K(m)) = mab - a^2 - b^2 + 1,\tag{8.8}$$

therefore, noting that the Lefschetz multiplet of maximal spin must be

$$j_{\max}(\gamma = (a, b)) = \frac{1}{2} \dim M_{(a,b)}(K(m))\tag{8.9}$$

we find, as a nice check, that our data agrees with this prediction.

Now, while the overall size and shape of the distribution vary with the charge, the degeneracies $\delta_\gamma(j)$ on the tail of the distribution *stabilize* to a common pattern

γ	$\delta(J_{\max}), \delta(J_{\max} - 1), \dots$	
$4\gamma_1 + 3\gamma_2$	$1, 0, 2, 2, 3, 2, 2, 0, \dots$	
$7\gamma_1 + 6\gamma_2$	$1, 0, 2, 2, 5, 6, 13, 14, \dots$	(8.10)
$8\gamma_1 + 6\gamma_2$	$1, 0, 2, 2, 5, 6, 13, 16, \dots$	
$8\gamma_1 + 7\gamma_2$	$1, 0, 2, 2, 5, 6, 13, 16, \dots$	

⁴²Cf theorem 6.6 of [18]

As (8.10) shows, the length of the “saturated” subsequence $1,0,2,2,5,6,13,16,\dots$ increases with $|\gamma|$. Overall, the tail behavior seems to stabilize to the sequence generated by

$$g(\xi) = \prod_{m=2}^{\infty} (1 - \xi^m)^{-2} = 1 + 0\xi + 2\xi^2 + 2\xi^3 + 5\xi^4 + 6\xi^5 + 13\xi^6 + \dots \quad (8.11)$$

A slight modification yields the generating function which coefficients are the incremental sum of those in $g(\xi)$

$$\tilde{g}(\xi) = \frac{\prod_{m=2}^{\infty} (1 - \xi^m)^{-2}}{(1 - \xi)} = 1 + 1\xi + 3\xi^2 + 5\xi^3 + 10\xi^4 + 16\xi^5 + 29\xi^6 + \dots, \quad (8.12)$$

generating the number of planar partitions with at most two rows of the corresponding size, some examples are

No boxes		1 empty partition
1 box	1	1 partition
2 boxes	1 1, 2, $\frac{1}{1}$	3 partitions
3 boxes	3, 1 1 1, 2 1, $\frac{2}{1}, \frac{1}{1}$	5 partitions

This analogy suggests that the stabilized $\delta_\gamma(j)$ distribution counts some number of *constrained* partitions, only deviating from (8.11) at higher orders in ξ . This hypothesis is reminiscent of results of [7, 26].

Of course, $g(\xi)$ is also closely related to the Dedekind η -function. It is quite curious that the BPS degeneracies have some relation to modular functions. This has been long expected in supergravity [10, 12, 29] but the appearance in field theory is novel.

In fact, the above connection to the Dedekind η was noted before our work by Reineke [8], who offers a mathematical explanation. But the physical import of this strange behavior remains mysterious.

9 Open Problems

In conclusion we would like to mention a few open problems and questions raised by the current work.

1. It is natural to guess that wild degeneracies will be a common feature among higher rank theories of class S . Strictly speaking, the only examples we have given are for gauge group $SU(3)$, but we fully expect that the phenomenon will persist for $SU(K)$ with $K > 3$. This is strongly suggested by the quiver analysis of Section 6, but a fully rigorous proof would require that one demonstrate that the path exhibited in the moduli space of stability parameters of the the Fiol quiver, which leads to wild wall

crossing for $K > 3$, actually can be chosen in the moduli space of physical stability parameters. (While not fully mathematically rigorous, a compelling physical argument that this is indeed the case is that we could consider a hierarchy of symmetry breaking where $SU(K)$ is much more strongly broken to $SU(3) \times U(1)^{K-3}$ than the $SU(3)$ is broken to $U(1)^2$.)

2. Another open problem along similar lines is how the presence of, say, matter multiplets affects the existence of wild degeneracies.
3. It should be noted that the explicit point on the Coulomb branch illustrated in Figure 5 is in fact different from the region explored in Section 4.2. Nevertheless, using the techniques of Appendix C we have checked that the same crucial algebraic equation (3.2) governing the street factors of herds indeed appears in the spectral networks that arise in this region. These networks are very similar to but not quite the same as the m -herds. One might ask for a succinct test to see whether a degenerate spectral network leads to m -wild degeneracies.
4. It would be nice to understand better the physics of the curious invariance of the BPS degeneracies under the transformation by the g_m matrix discussed in Section 6.2 above. To the extent that the relation to quivers is physical, a physical understanding is indeed provided by the arguments in Section 6. However, we would like to suggest an alternative interpretation using the halo picture of BPS states. If we consider a core particle γ with halo particles of charge γ' then the replacement of the hypermultiplet of charge γ for the hypermultiplet $\gamma + m\gamma'$ is simply flipping the Fermi sea of the halo Fock space. (See, e.g. Section 3.5 of [32] for a similar transformation.) Perhaps then a physical derivation of the symmetry could proceed by using Fermi flips to establish such a symmetry for framed BPS states and then using recursion relations between framed and unframed BPS states to deduce it for general degeneracies. This symmetry also raises the interesting possibility that the mutation method for determining BPS degeneracies can be extended to higher spin states.
5. The g_m symmetry of Kronecker quivers makes a surprising prediction about two well-known formulae: Reineke's formula for Poincaré polynomials of quiver varieties [7], and the Manschot-Pioline-Sen wall-crossing formula [26, 27]. These formulae involve sums over certain partitions. For certain charges, there is rather extensive cancelation between terms in these formulae implied by the g_m symmetry of the BPS degeneracies. Since the individual terms in the sum in the MPS formulae have a simple geometrical interpretation [27] the g_m symmetry together with the MPS formula imply nontrivial identities on equivariant Dirac indices. For a simple and dramatic example we can choose $m = 3$ and note that that $(1, 1)$ has a very simple PSC, but

$$(g_3)^k \cdot \begin{pmatrix} 1 \\ 1 \end{pmatrix} = \begin{pmatrix} F_{2k-1} \\ F_{2k+1} \end{pmatrix} \quad (9.1)$$

(where F_n is the n^{th} Fibonacci number) involves arbitrarily large charges. Clearly there are many terms in the MPS formula (7.23) and, as we just said, their coefficients have a beautiful geometrical interpretation as equivariant indices of Dirac operators on the Denef moduli spaces. So the identity⁴³

$$\Omega((F_{2k-1}, F_{2k+1}); y) = \Omega((1, 1); y) = [3]_y \quad (9.2)$$

is a very remarkable set of identities for these indices. It would be interesting to understand better these identities (and their analogues for $m > 3$) from a geometrical point of view.

6. Returning to the key algebraic equation (3.2), a natural question is whether there is a physical interpretation of the other roots of this equation. We expect that there will be. For example, choose a small path \wp crossing a c -street in an m -herd. The corresponding supersymmetric interface has a vev when wrapped on the circle in $\mathbb{R}^3 \times S^1$ given by

$$\langle L_\zeta(\wp) \rangle_m = \begin{pmatrix} q(m, \zeta) & 0 & 0 \\ 0 & 1 & 0 \\ 0 & 0 & q(m, \zeta) \end{pmatrix} \quad (9.3)$$

where m is a point in Hitchin moduli space \mathcal{M} , $\zeta \in \mathbb{C}^*$ has phase $\arg \zeta = \arg Z(\gamma + \gamma')$, and $q(m, \zeta) = Q(c)|_{X_{\gamma_c} \rightarrow \mathcal{Y}_{\gamma_c}}$, where \mathcal{Y}_{γ_c} is a function on the twistor space of the Hitchin moduli space \mathcal{M} constructed in [15, 33]. It therefore makes sense to ask about the physical meaning of the analytic behavior of $\langle L_\zeta(\wp) \rangle$, and this might well involve the other roots of (3.2). Exploring this point further is beyond the scope of this paper.

7. A closely related point to the previous one is that the exponential growth of Ω for certain charges implies a similar exponential growth for μ and therefore for $\overline{\Omega}$. We expect this will have important implications for the construction of hyperkahler metrics of associated Hitchin systems proposed in [15] and for the definition of the nonabelianization map of [33, 34]. Again, we leave this important point for future work.

A Protected spin characters of the 3-Kronecker quiver

In this subsection we discuss some data for the “refined BPS degeneracies,” or, more properly, the “protected spin character.” First, we recall some definitions. Then we present the data.

A.1 Spin decompositions

Short irreducible representations of the $\mathcal{N} = 2$ superalgebra take the general form [1, 25]

$$\rho_{hh} \otimes \mathfrak{h} \quad (A.1)$$

⁴³We use the notation $[n]_y := \frac{y^n - y^{-n}}{y - y^{-1}}$

where $\rho_{hh} = (1/2, 0) \oplus (0, 1/2)$ is the *half-hypermultiplet* representation of $\mathfrak{so}(3) \oplus \mathfrak{su}(2)_R$, and \mathfrak{h} is the *Clifford vacuum*. It has been shown recently in [39] that the Clifford vacuum is actually a singlet of $\mathfrak{su}(2)_R$, this fact had been previously known as the *no-exotics conjecture*.

In order to extract information about the spin decomposition of the BPS index, we study a refinement known as the *protected spin character* (see e.g. [23, 35])

$$\begin{aligned}\Omega(\gamma, u; y) &= \text{Tr}_{\mathfrak{h}_\gamma} y^{2J_3} (-y)^{I_3} \\ &= \sum_m a_m(\gamma, u) (-y)^m,\end{aligned}\tag{A.2}$$

where J_3, I_3 are Cartan elements of $\mathfrak{so}(3), \mathfrak{su}(2)_R$ respectively, and the last line defines the coefficients a_m . The PSC reduces to the BPS index in the limit $y \rightarrow -1$.

For a given charge γ , \mathfrak{h}_γ has an isotypical decomposition into $\mathfrak{so}(3)$ reps:

$$\mathfrak{h}_\gamma = \bigoplus_j \left(D_j \otimes (j, 0) \right)\tag{A.3}$$

where the degeneracy space D_j is a complex vector space of dimension $\delta_\gamma(j)$. Therefore

$$\Omega(\gamma) = \sum_j (-1)^{2j} \delta_\gamma(j) (2j + 1).\tag{A.4}$$

The numerical evidence given below suggests that the degeneracies $\delta_\gamma(j)$ for the 3-Kronecker quiver satisfy the following property: for fixed γ , $\delta_\gamma(j) \neq 0$ only for $2j$ of a definite parity.⁴⁴ For such spin degeneracies note that

$$(-1)^{2j} \Omega(\gamma) = \dim \mathcal{H}_\gamma.\tag{A.5}$$

Of course, knowing $\Omega(\gamma)$ does not determine the isotypical decomposition. In order to determine that we need to employ a generalization of the KSWCF known in the physics literature as the “motivic” KSWCF [16, 21–24]. We introduce a set of non-commutative formal variables obeying

$$\hat{Y}_\gamma \hat{Y}_{\gamma'} = y^{\langle \gamma, \gamma' \rangle} \hat{Y}_{\gamma + \gamma'}, \quad \forall \gamma, \gamma' \in \Gamma.\tag{A.6}$$

The generalization of (3.13) is then (for details, see [23])

$$\hat{\mathcal{K}}_\gamma^{\Omega(\gamma; y)} : \hat{Y}_{\gamma_0} \mapsto \hat{Y}_{\gamma_0} \prod_{m \in \mathbb{Z}} \left(\Phi_{\langle \gamma_0, \gamma \rangle}((-y)^m \hat{Y}_\gamma) \right)^{a_m(\text{sign}\langle \gamma_0, \gamma \rangle)}\tag{A.7}$$

where the a_m are defined according to (A.2), and

$$\Phi_n(\xi) := \prod_{s=1}^{|n|} (1 + y^{-\text{sign}(n)(2s-1)} \xi).\tag{A.8}$$

⁴⁴Indeed the data suggests that $2j$ must be odd for $\gamma = a\gamma_1 + b\gamma_2$ with a, b both even and $2j$ must be even otherwise.

Let us now apply this formalism to the case at hand, namely the 3-Kronecker quiver. The motivic version of the wall crossing identity is

$$\hat{\mathcal{K}}_{\gamma_2} \hat{\mathcal{K}}_{\gamma_1} = : \prod_{\substack{a\gamma_1 + b\gamma_2 \\ a, b \geq 0}} \hat{\mathcal{K}}_{\gamma}^{\Omega(a\gamma_1 + b\gamma_2; y)} : \quad (\text{A.9})$$

The RHS admits a *unique* decomposition with the required charge orderings and hence this equation fully determines the $\Omega(a\gamma_1 + b\gamma_2; y)$.

In practical terms the protected spin characters can be extracted from this formula as follows. First, acting with the operator on the LHS of (A.9) on the formal variable \hat{Y}_{γ_1} , yields⁴⁵

$$\hat{Y}_{\gamma_1} + (y^{-2} + 1 + y^2) \hat{Y}_{\gamma_1 + \gamma_2} + (y^{-2} + 1 + y^2) \hat{Y}_{\gamma_1 + 2\gamma_2} + \hat{Y}_{\gamma_1 + 3\gamma_2}. \quad (\text{A.10})$$

with a similar formula for the action on \hat{Y}_{γ_2} . Then, we apply an inductive procedure directly analogous to that used in (5.2) for the ordinary BPS indices.

We report the resulting PSCs in A.2, for charges up to $a + b \leq 15$.

A.2 The data

The following tables report the content of BPS boundstates corresponding to the 3-Kronecker quiver, only a quarter of the spectrum is given⁴⁶, the rest is determined by symmetry. For convenience, boundstates are ordered according to the phase of the central charge. Here j labels the $\mathfrak{so}(3)$ irrep of the Clifford vacuum, while δ counts the number of occurrences of such irreps.

⁴⁵As a side note, this implies that a line defect with charge γ_1 would support halo configurations of vanilla hypermultiplets, with overall halo charges $\gamma_h = k\gamma_2$, $k = 0, 1, 2, 3$. The $\mathfrak{so}(3)$ representations of the respective framed BPS states would have spin $j = 0, 1, 1, 0$ (see [23, 35]). These can also be thought of as the Hall-halo configurations of [6].

⁴⁶I.e. one half of the *particle* spectrum, namely dimension vectors with non-negative entries.

γ	j	δ
γ_1	0	1
$3\gamma_1 + \gamma_2$	0	1
$8\gamma_1 + 3\gamma_2$	0	1
$10\gamma_1 + 4\gamma_2$	5/2	1
$5\gamma_1 + 2\gamma_2$	1	1
$7\gamma_1 + 3\gamma_2$	3	1
	5	1
$9\gamma_1 + 4\gamma_2$	0	2
	1	2
	2	3
	3	2
	4	2
	6	1
$2\gamma_1 + \gamma_2$	1	1
$4\gamma_1 + 2\gamma_2$	5/2	1
$6\gamma_1 + 3\gamma_2$	3	1
	5	1
$8\gamma_1 + 4\gamma_2$	5/2	1
	9/2	2
	11/2	1
	13/2	2
	17/2	1
$10\gamma_1 + 5\gamma_2$	1	1
	3	2
	4	2
	5	4
	6	4
	7	5
	8	4
	9	4
	10	2
	11	2
	13	1

γ	j	δ
$9\gamma_1 + 5\gamma_2$	0	7
	1	25
	2	30
	3	38
	4	32
	5	31
	6	23
	7	21
	8	12
	9	11
	10	6
	11	5
	12	2
	13	2
	15	1
$7\gamma_1 + 4\gamma_2$	0	5
	1	5
	2	11
	3	7
	4	9
	5	4
	6	5
	7	2
	8	2
	10	1
$5\gamma_1 + 3\gamma_2$	0	2
	1	2
	2	3
	3	2
	4	2
	6	1

γ	j	δ
$8\gamma_1 + 5\gamma_2$	0	17
	1	32
	2	55
	3	55
	4	61
	5	48
	6	44
	7	30
	8	25
	9	15
	10	12
	11	6
	12	5
	13	2
	14	2
	16	1
$3\gamma_1 + 2\gamma_2$	1	2
	3	1
$6\gamma_1 + 4\gamma_2$	1/2	4
	3/2	7
	5/2	11
	7/2	7
	9/2	10
	11/2	5
	13/2	5
	15/2	2
	17/2	2
	21/2	1

γ	j	δ
$9\gamma_1 + 6\gamma_2$	0	31
	1	125
	2	173
	3	241
	4	251
	5	279
	6	255
	7	244
	8	201
	9	177
	10	129
	11	109
	12	74
	13	58
	14	37
	15	29
	16	15
	17	13
	18	16
	19	5
	20	2
	21	2
	23	1
$7\gamma_1 + 5\gamma_2$	0	17
	1	32
	2	55
	3	55
	4	61
	5	48
	6	44
	7	30
	8	25
	9	15
	10	12
	11	6
	12	5
	13	2
	14	2
	16	1

γ	j	δ
$4\gamma_1 + 3\gamma_2$	0	2
	1	2
	2	3
	3	2
	4	2
	6	1
$8\gamma_1 + 6\gamma_2$	1/2	94
	3/2	171
	5/2	242
	7/2	263
	9/2	291
	11/2	263
	13/2	252
	15/2	203
	17/2	179
	19/2	128
	21/2	109
	23/2	71
	25/2	58
	27/2	35
	29/2	29
	31/2	15
	33/2	13
	35/2	6
	37/2	5
	39/2	2
	41/2	2
	45/2	1
$5\gamma_1 + 4\gamma_2$	0	5
	1	5
	2	11
	3	7
	4	9
	5	4
	6	5
	7	2
	8	2
	10	1

γ	j	δ
$6\gamma_1 + 5\gamma_2$	0	7
	1	25
	2	30
	3	38
	4	32
	5	31
	6	23
	7	21
	8	12
	9	11
	10	6
	11	5
	12	2
	13	2
	15	1
$7\gamma_1 + 6\gamma_2$	0	23
	1	95
	2	119
	3	160
	4	150
	5	157
	6	131
	7	124
	8	91
	9	83
	10	57
	11	49
	12	31
	13	26
	14	14
	15	13
	16	6
	17	5
	18	2
	19	2
	21	1

γ	j	δ
$8\gamma_1 + 7\gamma_2$	0	135
	1	353
	2	562
	3	677
	4	765
	5	762
	6	752
	7	679
	8	619
	9	522
	10	455
	11	363
	12	304
	13	231
	14	188
	15	135
	16	109
	17	73
	18	57
	19	36
	20	28
	21	16
	22	13
	23	6
	24	5
	25	2
	26	2
	28	1

γ	j	δ
$\gamma_1 + \gamma_2$	1	1
$2\gamma_1 + 2\gamma_2$	5/2	1
$3\gamma_1 + 3\gamma_2$	3	1
	5	1
$4\gamma_1 + 4\gamma_2$	5/2	1
	9/2	2
	11/2	1
	13/2	2
	17/2	1
$5\gamma_1 + 5\gamma_2$	1	1
	3	2
	4	2
	5	4
	6	4
	7	5
	8	4
	9	4
	10	2
	11	2
	13	1
$6\gamma_1 + 6\gamma_2$	1/2	1
	3/2	2
	5/2	5
	7/2	5
	9/2	11
	11/2	9
	13/2	18
	15/2	15
	17/2	20
	19/2	15
	21/2	18
	23/2	9
	25/2	11
	27/2	5
	29/2	5
	31/2	2
	33/2	2
	37/2	1

γ	j	δ
$7\gamma_1 + 7\gamma_2$	0	1
	1	10
	2	12
	3	23
	4	28
	5	41
	6	48
	7	63
	8	68
	9	79
	10	77
	11	79
	12	68
	13	63
	14	48
	15	41
	16	29
	17	23
	18	14
	19	12
	20	6
	21	5
	22	2
	23	2
	25	1

B The Six-Way Junction

For reference, we present some basic conditions on soliton generating functions as enforced by the homotopy invariance of the framed 2D-4D generating functions $F(\varphi, \vartheta)$. First, using the

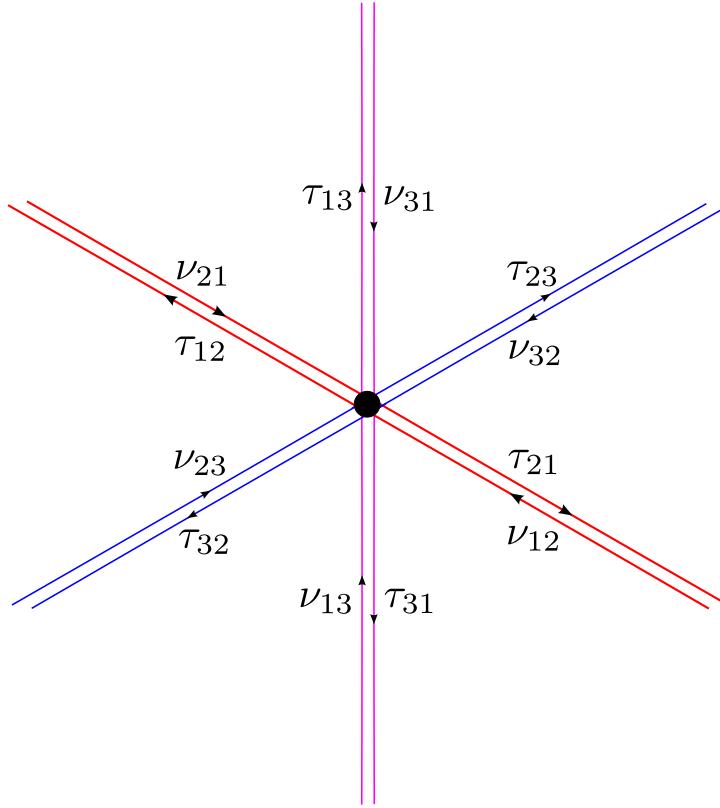


Figure 20. A six-way junction. Two-way streets are resolved into one-way constituent streets using the British resolution. Streets of type 12 are red, type 23 are blue, and type 13 are fuchsia. A soliton generating function attached to a (one-way constituent) street is shown adjacent to its respective street. Subscripts on the soliton generating functions are ordered pairs $ij \in \{1, 2, 3\}^2$ denoting the type of solitons that the generating function “counts”.

convention described in Section 2.2.1, we assign every two-way street an orientation. If the network in question is degenerate, we resolve all two-way streets into “constituent one-way streets” using the *British resolution*: let p be a two-way street; using the orientation on p , we resolve p into two one-way streets running in opposite directions, infinitesimally displaced from one another, and such that the street pointing along the orientation of p is to the *left* of the street running against the orientation. If p is a two-way street of type ij (i.e. composed of coincident streets of type ij and type ji), then (after resolving) the street on the left is of type ij and the street on the right is of type ji .

Just as with Kirchoff’s circuit laws it is most convenient to express our equations locally around each joint (or branch point). Hence, rather than expressing them in terms of the

street-dependent Υ/Δ notation introduced in (2.13)-(2.14), we will temporarily adopt a joint-dependent notation.

Definition Let $v \in C$ be a joint or branch point, then τ_{ij} will denote the soliton generating function attached to a constituent one-way street of type ij running *out* of v , and ν_{ij} will denote the soliton generating function attached to a constituent one-way street of type ij running *into* v .

In a full spectral network, the joint dependent τ, ν notation can become redundant; so we will eventually revert back to the Υ/Δ notation in Appendix C.

To define products of soliton generating functions properly we introduce the following.

Definition Let η be a formal variable that acts on each formal variable X_a in the homology path algebra via

$$\eta X_a = X_{a^{\text{tw}}},$$

where, at the level of 1-chains, a^{tw} is the 1-chain produced by inserting a half-twist along the circle fiber of $\tilde{\Sigma} \rightarrow \Sigma$ at some point⁴⁷ along a .

Remark It is immediate that $\forall G \in \mathcal{A}$

$$\eta^2 G = X_H G = -G.$$

We now consider a general type of joint, that can occur for a spectral network subordinate to a branched cover with $K \geq 3$ sheets, where six (possibly two-way) streets meet. The situation is shown in Fig. 20: the (relevant) sheets of the cover are labeled from 1 to 3, and the soliton generating functions attached to a constituent one-way street (under the British resolution of all possible two-way streets) are shown adjacent to their corresponding sheet. Using homotopy invariance of $F(\wp, \vartheta)$, one arrives at the six-way junction equations:⁴⁸

$$\begin{aligned} \tau_{12} &= \nu_{12} + \eta \tau_{13} \nu_{32}, & \tau_{21} &= \nu_{21} + \eta^{-1} \nu_{23} \tau_{31}, \\ \tau_{23} &= \nu_{23} + \eta \tau_{21} \nu_{13}, & \tau_{32} &= \nu_{32} + \eta^{-1} \nu_{31} \tau_{12}, \\ \tau_{31} &= \nu_{31} + \eta \tau_{32} \nu_{21}, & \tau_{13} &= \nu_{13} + \eta^{-1} \nu_{12} \tau_{23}. \end{aligned} \tag{B.1}$$

At a branch point of type ij , we will assume that there is at most one two-way street, of type ij , emanating from the branch point; on this two-way street we will take

$$\tau_{ij} = X_{a_{ij}}$$

⁴⁷Up to homotopy (rel endpoints) the insertion point does not matter; hence, it is irrelevant for relative homology.

⁴⁸In [33] these equations were erroneously written without the factors η, η^{-1} .

where a_{ij} is the charge of a simpleton.⁴⁹ As described at the end of Section 2.2, fixing a point z near the branch point, such a simpleton is represented by a path which runs from the lift of z on sheet i to the lift of z on sheet j . In [33] one can find a more general rule accommodating the situation of three two-way streets emanating from the branch point; however, we will not need this generalized rule for m -herds.

C m -Herds in Detail

C.1 Notational Definitions

We will consider four distinct branch points of a branched cover $\Sigma \rightarrow C$ of degree $K \geq 3$. On any local region on C' , where the cover may be trivialized, only three sheets will be relevant and we will label the relevant sheets from 1 to 3. Label the branch points from 1 to 4 such that branch points 1 and 3 are branch points of type 12, while branch points 2 and 4 are branch points of type 23. For each branch point $i \in \{1, \dots, 4\}$ we will choose a simpleton (cf. the end of Section 2.2) s_i with endpoints on distinct lifts of some $z_i \in C'$ close to the i th branch point. s_1 and s_2 will be simpletons of type 12 and 23, respectively, while s_3 and s_4 will be of type 21 and 32, respectively. We denote the charges of these simpletons by

$$\begin{aligned} a_* &= [s_1] \in \Gamma_{12}(z_1, z_1) \\ b_* &= [s_2] \in \Gamma_{23}(z_2, z_2) \\ \bar{a}_* &= [s_3] \in \Gamma_{21}(z_3, z_3) \\ \bar{b}_* &= [s_4] \in \Gamma_{32}(z_4, z_4). \end{aligned} \tag{C.1}$$

More often, however, computations are performed in the “ $\mathbb{Z}/2\mathbb{Z}$ -extended” sets $\tilde{\Gamma}(\tilde{z}, -\tilde{z})$, $\tilde{z} \in \tilde{C}'$ where we define

$$\begin{aligned} a &= [\hat{s}_1] \in \tilde{\Gamma}_{12}(\tilde{z}_1, -\tilde{z}_1) \\ b &= [\hat{s}_2] \in \tilde{\Gamma}_{23}(\tilde{z}_2, -\tilde{z}_2) \\ \bar{a} &= [\hat{s}_3] \in \tilde{\Gamma}_{21}(\tilde{z}_3, -\tilde{z}_3) \\ \bar{b} &= [\hat{s}_4] \in \tilde{\Gamma}_{32}(\tilde{z}_4, -\tilde{z}_4). \end{aligned} \tag{C.2}$$

where $\widehat{(\cdot)}$ denotes the *tangent framing lift* (first discussed in Section 2.2.3) and the $\tilde{z}_i \in \tilde{C}'$ are the unit tangent vectors at the starting points of the tangent framing lifts.

In a slight abuse of notation, horse streets⁵⁰ (which may be two-way), will be denoted by decorated latin letters: a_i, \bar{a}_i are streets of type 12, b_i, \bar{b}_i are of type 23, and c is of type 13. The subscripts, denoted by $i \in \{1, 2, 3\}$, denote which street is in question and the use of overlines are just a notational exploit of the duality operation described below in C.2.

Furthermore, in contrast with the “joint-dependent” τ, ν notation of Appendix B, we will (more naturally) denote soliton generating functions⁵¹ “streetwise.” The point $z \in p \subset C$ in

⁴⁹The coefficient of $\mu(a_{ij}) = 1$ in front of $X_{a_{ij}}$ is a result of the soliton input data (2.12).

⁵⁰See the definition in Section 3.1.

⁵¹We refer to Section 2.2.2 for the detailed definitions of generating functions and formal variables.

the definition of soliton generating functions will be dropped for notational convenience. As mentioned in a remark at the end of Section 2.2.2: for any $z, z' \in p$ the generating functions $\Upsilon_z(p)$ and $\Upsilon_{z'}(p)$ are related by parallel transport (similarly for $\Delta_z(p)$ and $\Delta_{z'}(p)$).

For the sake of readability, we will modify our notation slightly from Section 2.2.2 and write streets as subscripts.

Definition Let p be a street, the generating function of solitons on p which *agree* with the orientation of p is denoted Υ_p , the generating function of solitons which *disagree* with the orientation of p is denoted Δ_p . In all figures in this paper streets are oriented in an upward direction (upsilon is for “up” and delta is for “down”).

We now wish to associate the street factor (a generating function) Q_p to each street p . To do so, it is convenient to pass through the definition of a closely related auxiliary function.

Definition

For each street p , we define the function

$$Q_p := 1 + \Upsilon_p \Delta_p \in \mathcal{A}_C \tag{C.3}$$

To produce a formal series in the X_γ , $\gamma \in \Gamma$, we use the “basepoint-forgetting” closure map.

Definition

$$Q_p := \text{cl}[Q_p] \in \mathbb{Z}[\tilde{\Gamma}].$$

We now make some important technical remarks about the use of Q_p vs. Q_p .

Remarks If p is a street of type ij , then Q_p is a formal series in formal variables over Γ_{ii} . In particular, let $a \in \Gamma_{kl}$, then this means

$$\begin{aligned} Q_p X_a &= \begin{cases} 0 & \text{if } k \neq i \\ Q_p X_a = X_a Q_p & \text{if } k = i \end{cases}, \\ X_a Q_p &= \begin{cases} 0 & \text{if } l \neq i \\ X_a Q_p = Q_p X_a & \text{if } l = i \end{cases}. \end{aligned}$$

Hence, if the (left or right) action of Q_p on a soliton function of type kl is nonvanishing, then it can be replaced with the (commutative) action of Q_p . In the following derivations, the action of Q_p happens to be always nonvanishing; hence, it will almost always be replaced by Q_p , except in cases where we resist such replacements for the sake of precision and pedagogy.

Terminology Occasionally we will use the term *spectral data* to refer to the collection of soliton generating functions, street factors, and the functions Q_p supported on a particular collection of streets.

C.2 Duality

As an oriented graph embedded in a disk, Fig. 3 is invariant under an involution given by rotating the diagram 180 degrees, and reversing all orientations; we denote this involution on streets p via an overline

$$p \mapsto \bar{p}, \tag{C.4}$$

for $p \in \{a_i, \bar{a}_i, b_i, \bar{b}_i, c : i = 1, 2, 3\}$. As the terminology suggests, this involution satisfies $\bar{\bar{p}} = p$ for every street p and $\bar{c} = c$. We claim that this geometric involution actually induces a duality operation on all spectral data, i.e. generating functions. In particular, on any equations involving soliton generating functions, the replacements

$$\begin{aligned} \Upsilon_p &\leftrightarrow \Delta_{\bar{p}} \\ \eta &\leftrightarrow \eta^{-1}, \end{aligned} \tag{C.5}$$

with all products taken in reverse order, will also yield a valid equation. This claim can be verified by brute-force checking. Note, in particular, applying the duality operation to the definition of \mathcal{Q}_p in (C.3) will yield $\mathcal{Q}_{\bar{p}}$.

C.3 The Horse as a Machine

Recall the definition of a horse is given as a condition on the subset of two-way streets of a spectral network in an open disk region (see Section 3.1). For convenience we restate the definition.

Definitions

1. A *horse street* $p \in \{a_1, a_2, a_3, b_1, b_2, b_3, c, \bar{a}_1, \bar{a}_2, \bar{a}_3, \bar{b}_1, \bar{b}_2, \bar{b}_3\}$ is one of the streets of Fig. 3 (left frame).
2. Let N be a spectral network (subordinate to some branched cover $\Sigma \rightarrow C$) and $U \subset C'$ be an open disk region. Then $U \cap N$ is a horse if a subset of its streets can be identified with Fig. 3 in a way such that
 - (a) Every two-way street is a horse street.
 - (b) There is always a two-way street identified with the street labeled c .

It may happen, however, that on a horse there are “background” non-horse streets that cannot be identified with those of Fig. 3; by definition, these are one-way streets. The following claim ensures that the computation of soliton generating functions on the streets of a horse are independent of the details of the non-horse streets.

Claim The equations for soliton generating functions on horse streets, induced by (B.1), close on themselves. I.e., the equations for the soliton generating functions on a given horse street can be written entirely in terms of the soliton generating functions on horse streets.

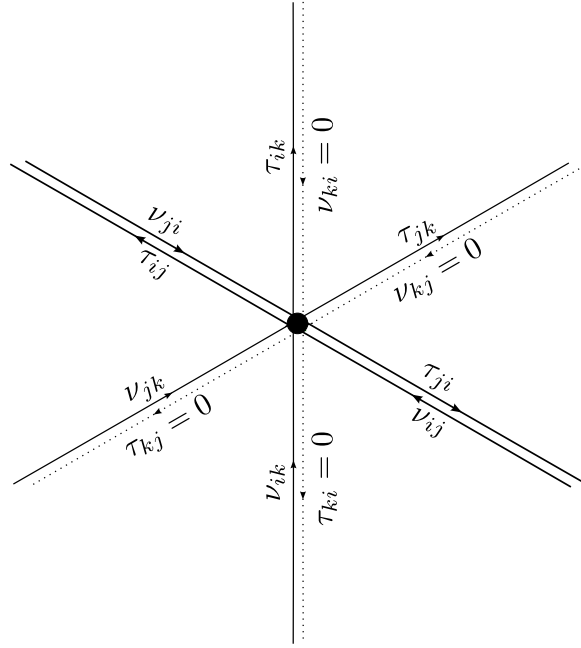


Figure 21. The most general type of joint where non-horse streets of class (A) meets a horse street (which may be two-way). As in Fig. 20, streets are resolved into one-way constituents using the British resolution. Soliton generating functions vanish on the dotted streets. The labels i, j, k are a permutation of the sheets 1, 2, 3.

Proof. Let us temporarily denote the four joints in Fig. 3 (left frame) as *horse joints*. We split non-horse streets into two classes:

- (A) Streets that have no endpoints on a horse joint.
- (B) Streets that have a single endpoint on a horse joint.

Let us first consider streets of class (A). The claim is trivial for (A)-streets that do not intersect a horse street. Thus, we turn our attention to a joint where an (A)-street meets a horse street. The most general picture of such a joint⁵² is depicted in Fig. 21. In this figure: i, j, k label any permutation of the sheets 1, 2, 3, the streets of type jk and ki label background one-way streets, and the streets of type ij compose the horse street (after being split into two streets by the joint). The soliton generating functions on the horse street are (in the “joint-wise” notation of Section B) $\tau_{ji}, \nu_{ij}, \tau_{ij}$, and ν_{ji} . The claim (for (A)-streets)

⁵²By the “most general picture” we mean a six-way junction equipped with the weakest possible constraints on incoming soliton degeneracy functions, compatible with the condition that only the streets of type ij (for some fixed pair ij) are two-way. Using (B.1), one finds that the most general picture is Fig. 21.

is then equivalent to the statement that $\tau_{ij} = \nu_{ij}$, $\tau_{ji} = \nu_{ji}$; we will show this is the case. Indeed, by the six-way joint equations (B.1):

$$\begin{aligned}\tau_{ij} &= \nu_{ij} + \begin{cases} \eta\tau_{ik}\nu_{kj}, & \text{if } ij \in \{12, 23, 31\} \\ \eta^{-1}\nu_{ik}\tau_{kj}, & \text{if } ij \in \{21, 32, 13\} \end{cases} \\ \tau_{ji} &= \nu_{ji} + \begin{cases} \eta^{-1}\nu_{jk}\tau_{ki}, & \text{if } ij \in \{12, 23, 31\} \\ \eta\tau_{jk}\nu_{ki}, & \text{if } ij \in \{21, 32, 13\} \end{cases}\end{aligned}$$

but $\nu_{kj} = 0$, $\tau_{kj} = 0$, $\nu_{ki} = 0$, and $\tau_{ki} = 0$. Hence,

$$\begin{aligned}\tau_{ij} &= \nu_{ij} \\ \tau_{ji} &= \nu_{ji}.\end{aligned}$$

Now, via inspection of Fig. 3, streets of class (B) are of type 13. If a (B)-street meets a horse street at a non-horse joint, then we apply the same argument used for (A)-streets to see that the (equations for) soliton generating functions on horse streets do not depend on the (B)-street soliton generating function. Thus, we focus our attention on the horse joint.

If a (B)-street meets a horse joint, then (B.1) requires the equations for soliton generating functions, on the horse streets meeting the joint, to depend on the soliton generating function of the (B)-street. We will show that the soliton generating function on the (B) street can be rewritten in terms of generating functions on the horse streets. First, note that if a (B)-street meets the horse joint where a_1 and b_1 meet, or the joint where \bar{a}_1 and \bar{b}_1 meet, then it must be outgoing with respect to the horse joint. Indeed, the constraint that c is two-way requires the presence of outgoing streets of type 13 at the horse joints meeting c ; if the (B)-street were incoming, it would combine with one of these outgoing streets to form a two-way street, violating the horse condition. Without loss of generality, assume the (B) street meets the horse joint where a_1 and b_1 meet; denote the soliton generating function on the (B)-street by $\Upsilon_{(B)}$. Then, using (B.1), it follows that $\Upsilon_{(B)} = \eta^{-1}\Upsilon_{a_1}\Upsilon_{b_1}$; so its soliton generating function is a function of the soliton generating functions on horse streets.

If a (B)-street meets one of the other two horse joints (where b_3 and \bar{a}_3 meet or where a_3 and \bar{b}_3 meet), then there are two situations: the horse streets at the horse joint are both two-way, or only one of the horse streets at the horse joint is two-way. The former situation is equivalent to the situation where the (B)-street meets the horse joint where a_1 and b_1 meet. To resolve the latter situation we repeat the same argument used for (A)-streets. \square

We divide the soliton generating functions supported on horse streets into elements of three subspaces: incoming data, outgoing data, and internal data.

Incoming data

Incoming data is defined as the spectral data which flows into the internal joints of the horse and is supported on the external streets. Here, the space of such data is composed of four

soliton generating functions and their duals:

$$\text{Incoming-Data} = \left\{ \left(\begin{array}{cccc} \Upsilon_{a_1}, & \Upsilon_{b_1}, & \Delta_{a_3}, & \Delta_{b_3}, \\ \Delta_{\bar{a}_1}, & \Delta_{\bar{b}_1}, & \Upsilon_{\bar{a}_3}, & \Upsilon_{\bar{b}_3} \end{array} \right) \in \mathcal{A}_S^{\times 8} \right\}. \quad (\text{C.6})$$

It will prove useful to subdivide this space of data further into generating functions of solitons that agree with the orientation of the diagram, Incoming-Data^+ , and those that disagree, Incoming-Data^- :

$$\begin{aligned} \text{Incoming-Data}^+ &= \left\{ \left(\Upsilon_{a_1}, \Upsilon_{b_1}, \Upsilon_{\bar{a}_3}, \Upsilon_{\bar{b}_3} \right) \in \mathcal{A}_S^{\times 4} \right\}, \\ \text{Incoming-Data}^- &= \left\{ \left(\Delta_{\bar{a}_1}, \Delta_{\bar{b}_1}, \Delta_{a_3}, \Delta_{b_3} \right) \in \mathcal{A}_S^{\times 4} \right\}. \end{aligned}$$

Outgoing data

Similarly, outgoing data is defined as the spectral data which flows out of the internal joints and is supported on external streets. This consists of the space of soliton generating functions,

$$\text{Outgoing-Data} = \left\{ \left(\begin{array}{cccc} \Delta_{a_1}, & \Delta_{b_1}, & \Upsilon_{a_3}, & \Upsilon_{b_3}, \\ \Upsilon_{\bar{a}_1}, & \Upsilon_{\bar{b}_1}, & \Delta_{\bar{a}_3}, & \Delta_{\bar{b}_3} \end{array} \right) \in \mathcal{A}_S^{\times 8} \right\}. \quad (\text{C.7})$$

As with the incoming data, we can similarly subdivide this data into generating functions of solitons that agree or disagree with the overall orientation:

$$\begin{aligned} \text{Outgoing-Data}^+ &= \left\{ \left(\Upsilon_{\bar{a}_1}, \Upsilon_{\bar{b}_1}, \Upsilon_{a_3}, \Upsilon_{b_3} \right) \in \mathcal{A}_S^{\times 4} \right\}, \\ \text{Outgoing-Data}^- &= \left\{ \left(\Delta_{a_1}, \Delta_{b_1}, \Delta_{\bar{a}_3}, \Delta_{\bar{b}_3} \right) \in \mathcal{A}_S^{\times 4} \right\}. \end{aligned} \quad (\text{C.8})$$

Internal/Bound data

The internal data of the diagram is composed of the ten soliton generating functions defined on the internal streets $a_2, b_2, \bar{a}_2, \bar{b}_2$:

$$\text{Internal-Data} = \left\{ \left(\begin{array}{ccccc} \Upsilon_{a_2}, & \Upsilon_{b_2}, & \Upsilon_{\bar{a}_2}, & \Upsilon_{\bar{b}_2}, & \Upsilon_c, \\ \Delta_{\bar{a}_2}, & \Delta_{\bar{b}_2}, & \Delta_{a_2}, & \Delta_{b_2}, & \Delta_c. \end{array} \right) \in \mathcal{A}_S^{\times 10} \right\} \quad (\text{C.9})$$

However, as far as the results of this paper are concerned, all that is relevant are the street factors Q_p , for p an internal street, which are derived from the soliton generating functions above:

$$\text{Internal-Data} \rightsquigarrow \left\{ \left(Q_{a_2}, Q_{b_2}, Q_{\bar{a}_2}, Q_{\bar{b}_2}, Q_c \right) \in \mathbb{Z}[\tilde{\Gamma}]^{\times 5} \right\}. \quad (\text{C.10})$$

We then view a horse as a scattering-matrix machine that eats incoming solitons and spits out outgoing solitons + ‘‘bound’’/internal solitons:

$$\text{Horse} : \text{Incoming-Data} \rightarrow \text{Outgoing-Data} \times \text{Internal-Data},$$

or in other words, we can determine **Outgoing-Data** and **Internal-Data** as a function of **Incoming-Data**; to do so we utilize the six-way junction equations (B.1) to give⁵³

$$\begin{aligned}
\Upsilon_{a_2} &= \Upsilon_{a_1} + \eta \Upsilon_c \Delta_{b_2} \\
\Upsilon_{a_3} &= \Upsilon_{a_2} + \eta \left(\eta^{-1} \Upsilon_{a_2} \Upsilon_{\bar{b}_2} \right) \Delta_{\bar{b}_2} \\
&= \Upsilon_{a_2} \mathcal{Q}_{\bar{b}_2} \\
\Upsilon_{b_2} &= \Upsilon_{b_1} \\
\Upsilon_{b_3} &= \Upsilon_{b_2} \\
\Upsilon_c &= \eta^{-1} \Upsilon_{a_1} \Upsilon_{b_1} \\
\Delta_{a_1} &= \Delta_{a_2} + \eta^{-1} \Upsilon_{b_1} \left(\Delta_c + \eta \Delta_{b_1} \Delta_{a_2} \right) \\
&= \mathcal{Q}_{b_1} \Delta_{a_2} + \eta^{-1} \Upsilon_{b_1} \Delta_c \\
\Delta_{a_2} &= \Delta_{a_3} + \eta^{-1} \Upsilon_{\bar{b}_3} \left(\eta \Delta_{\bar{b}_3} \Delta_{a_3} \right) \\
&= \mathcal{Q}_{\bar{b}_3} \Delta_{\bar{a}_3} \\
\Delta_{b_1} &= \Delta_{b_2} + \eta^{-1} \Delta_c \Upsilon_{a_2} \\
\Delta_{b_2} &= \Delta_{b_3}.
\end{aligned} \tag{C.11}$$

By applying the duality operation of Section C.2 to each equation above, we produce the rest of the six-way junction equations.

We wish to solve for the outgoing and internal (blue) quantities in terms of the incoming (red) quantities.

C.3.1 Outgoing Soliton Generating Functions

Starting from a_1 and moving counter-clockwise around the edge of Fig. 3, we have

$$\begin{aligned}
\Delta_{a_1} &= \left(1 + \Upsilon_{b_1} \Delta_{\bar{b}_1} \Delta_{\bar{a}_1} \Upsilon_{a_1} \right) \left(1 + \Upsilon_{b_1} \Delta_{b_3} \right) \left(1 + \Upsilon_{\bar{b}_3} \Delta_{\bar{b}_1} \right) \Delta_{a_3} + \Upsilon_{b_1} \Delta_{\bar{b}_1} \Delta_{\bar{a}_1} \\
\Delta_{b_1} &= \Delta_{b_3} + \Delta_{\bar{b}_1} \Delta_{\bar{a}_1} \Upsilon_{a_1} \left(1 + \Upsilon_{b_1} \Delta_{b_3} \right) \\
\Delta_{\bar{b}_3} &= \Delta_{\bar{b}_1} \\
\Upsilon_{a_3} &= \Upsilon_{a_1} \left(1 + \Upsilon_{b_1} \Delta_{b_3} \right) \left(1 + \Upsilon_{\bar{b}_3} \Delta_{\bar{b}_1} \right) \\
\Upsilon_{\bar{a}_1} &= \Upsilon_{\bar{a}_3} \left(1 + \Delta_{\bar{a}_1} \Upsilon_{a_1} \Upsilon_{b_1} \Delta_{\bar{b}_1} \right) \left(1 + \Upsilon_{\bar{b}_3} \Delta_{\bar{b}_1} \right) \left(1 + \Upsilon_{b_1} \Delta_{b_3} \right) + \Upsilon_{a_1} \Upsilon_{b_1} \Delta_{\bar{b}_1} \\
\Upsilon_{\bar{b}_1} &= \Upsilon_{\bar{b}_3} + \left(1 + \Upsilon_{\bar{b}_3} \Delta_{\bar{b}_1} \right) \Delta_{\bar{a}_1} \Upsilon_{a_1} \Upsilon_{b_1} \\
\Upsilon_{b_3} &= \Upsilon_{b_1} \\
\Delta_{\bar{a}_3} &= \left(1 + \Upsilon_{\bar{b}_3} \Delta_{\bar{b}_1} \right) \left(1 + \Upsilon_{b_1} \Delta_{b_3} \right) \Delta_{\bar{a}_1}.
\end{aligned}$$

⁵³When using the six-way junction equations on the four relevant joints of a horse, pictured in the left panel of Fig. 3, one must take into account one-way streets of type 13 that flow out of these joints. However, as shown in the proof of the claim of Section C.3, the soliton generating functions on these one-way streets can be written in terms of soliton generating functions on the horse streets.

C.3.2 Outgoing Street Factors

We remark that all outgoing street factors can be expressed in terms of the internal street factors. Hence, starting from a_1 and moving counter-clockwise around the edge of the diagram, we have

$$\begin{aligned}
Q_{a_1} &= Q_c Q_{a_2} \\
Q_{b_1} &= Q_c Q_{b_2} \\
Q_{b_3} &= Q_{b_2} \\
Q_{a_3} &= Q_{a_2} \\
Q_{a_1} &= Q_c Q_{a_2} \\
Q_{b_1} &= Q_c Q_{b_2} \\
Q_{b_3} &= Q_{b_2} \\
Q_{a_3} &= Q_{a_2}.
\end{aligned}$$

C.3.3 Internal Street Factors

We now state the internal street factors in terms of the incoming soliton generating functions. These equations follow from (C.11) and are:

$$\begin{aligned}
Q_c &= 1 + \Upsilon_{a_1} \Upsilon_{b_1} \Delta_{b_1} \Delta_{a_1} \\
Q_{a_2} &= 1 + \Upsilon_{a_1} Q_{b_2} Q_{b_2} \Delta_{a_3} \\
Q_{b_2} &= 1 + \Upsilon_{b_3} \Delta_{b_1} \\
Q_{a_2} &= 1 + \Upsilon_{a_3} Q_{b_2} Q_{b_2} \Delta_{a_1} \\
Q_{b_2} &= 1 + \Upsilon_{b_1} \Delta_{b_3}.
\end{aligned}$$

By applying the closure map cl one produces the corresponding Q_p functions.

Remark We note that in all the equations of sections C.3.1 - C.3.2 there is an almost magical cancellation of the half-twists η ; this cancellation will ultimately ensure that the coefficients of the degeneracy generating functions Q_p (as polynomials in some formal variable $X_{\widehat{\gamma}_c}$, yet to be identified) are all positive.

Special Cases

We now cite two important special cases of incoming data for a horse.

Definitions

1. A lower-sourced horse is a horse along with exactly “two-sources from below,” i.e. it is a horse restricted to the subset of **Incoming-Data** where a point in **Incoming-Data**⁺ is

specified:

$$\text{Incoming-Data}_{\text{LSH}}^+ = \left\{ \left(\begin{array}{l} \Upsilon_{a_1} = X_a \\ \Upsilon_{b_1} = X_b \\ \Upsilon_{\bar{a}_3} = 0 \\ \Upsilon_{\bar{b}_3} = 0. \end{array} \right) \right\} \subset \text{Incoming-Data}^+. \quad (\text{C.12})$$

2. An upper-sourced horse is dual to a lower-sourced horse, i.e. it is a horse restricted to the subset of **Incoming-Data** where a point in **Incoming-Data**⁻ is specified:

$$\text{Incoming-Data}_{\text{USH}}^- = \left\{ \left(\begin{array}{l} \Delta_{\bar{a}_1} = X_{\bar{a}} \\ \Delta_{\bar{b}_1} = X_{\bar{b}} \\ \Delta_{a_3} = 0 \\ \Delta_{b_3} = 0. \end{array} \right) \right\} \subset \text{Incoming-Data}^-. \quad (\text{C.13})$$

Remark Inserting the lower-sourced horse conditions into the equations of Section C.3.3, the most important of the resulting equations are

$$Q_{\bar{a}_2} = Q_{\bar{b}_2} = 1; \quad (\text{C.14})$$

which, furthermore, via (C.3.2) require

$$Q_{\bar{a}_3} = Q_{\bar{b}_3} = 1. \quad (\text{C.15})$$

The upper-sourced horse conditions yield the dual equations,

$$Q_{a_2} = Q_{a_3} = Q_{b_2} = Q_{b_3} = 1. \quad (\text{C.16})$$

With this technology, we can define an m -herd on an arbitrary oriented real surface C as a collection of m -horses glued together using the relations (3.1), beginning with a lower-sourced horse coming from a pair of branch points, and ending with an upper-sourced horse near another pair of branch points (which, for the purposes of this paper, we will take to be disjoint from the lower-sourced branch points).

Definition Let N be a spectral network subordinate to some branched cover $\Sigma \rightarrow C$ and let $H \subset N$ be the set of two-way streets of N . Then N is an m -herd if the following conditions are satisfied.

Horses: There exists a collection of open embedded disks $\{U_l\}_{l=1}^m \subset C'$ forming a covering of H , with $U_l \cap U_k \neq \emptyset$ iff $l = k \pm 1$, and each $N \cap U_l$ is:

- a lower-sourced horse if $l = 1$,
- a horse if $1 < l < m$,

- an upper-sourced horse if $l = m$.

Gluing: Each horse satisfies particular gluing conditions: let $p^{(l)}$ denote a horse street⁵⁴ on $N \cap U_l$. Then, for $l = 2, \dots, m - 1$, we have the conditions

$$\begin{aligned}
a_1^{(l)} &= a_3^{(l-1)} \\
b_1^{(l)} &= b_3^{(l-1)} \\
\bar{a}_1^{(l)} &= \bar{a}_3^{(l+1)} \\
\bar{b}_1^{(l)} &= \bar{b}_3^{(l+1)}.
\end{aligned} \tag{3.1}$$

No Holes: For $l = 1, \dots, m - 1$, the oriented loops traced out by the words

- $(\bar{a}_2^{(l)}) (\bar{b}_1^{(l)}) (a_2^{(l+1)})^{-1} (b_3^{(l)})^{-1}$,
- $(\bar{b}_2^{(l)}) (\bar{a}_1^{(l)}) (b_2^{(l+1)})^{-1} (a_3^{(l)})^{-1}$

are each the oriented boundary of (separate) disks on C' (see Fig. 22).

Remarks

- Note that a 1-herd is the spectral network for a saddle: indeed, via the above definition it consists of a single horse which is both lower and upper-sourced. The picture of a saddle is formed by viewing only the two-way streets remaining after “removing” the horse streets constrained to be one-way according to (C.14) - (C.16).
- Let **Incoming-Data** $^\pm(l)$ (**Outgoing-Data** $^\pm(l)$) be the domain of incoming (range of outgoing) data associated to the l th horse of an m -herd. Via the definition, **Incoming-Data** $^+(1)$ and **Incoming-Data** $^+(m)$ are specified by the lower sourced horse conditions (C.12) and upper-sourced horse conditions (C.13) respectively:

$$\begin{aligned}
\text{Incoming-Data}^+(1) &= \left\{ \left(\begin{array}{l} \Upsilon_{a_1}^{(1)} = X_a \\ \Upsilon_{b_1}^{(1)} = X_b \\ \Upsilon_{\bar{a}_3}^{(1)} = 0 \\ \Upsilon_{\bar{b}_3}^{(1)} = 0. \end{array} \right) \right\}, \\
\text{Incoming-Data}^-(m) &= \left\{ \left(\begin{array}{l} \Delta_{\bar{a}_1}^{(m)} = X_{\bar{a}} \\ \Delta_{\bar{b}_1}^{(m)} = X_{\bar{b}} \\ \Delta_{a_3}^{(m)} = 0 \\ \Delta_{b_3}^{(m)} = 0. \end{array} \right) \right\}.
\end{aligned} \tag{C.17}$$

⁵⁴Using our previous naming convention: $p \in \{a_1, a_2, a_3, b_1, b_2, b_3, c, \bar{a}_1, \bar{a}_2, \bar{a}_3, \bar{b}_1, \bar{b}_2, \bar{b}_3\}$.

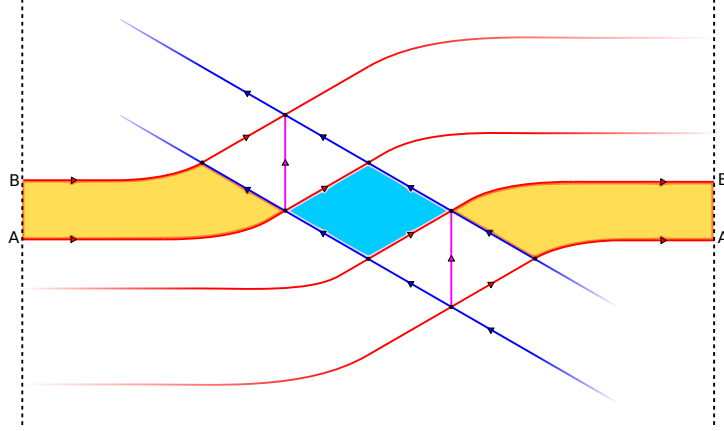


Figure 22. A picture of two horses (cf. Fig. 3) glued together using the *Gluing* conditions and satisfying the *No Holes* condition; the dotted lines are identified, and we assign the “horse-indices” l and $l+1$ to the bottom and top horses respectively. The aqua-blue region is a disk with boundary traced out by the word $(\bar{a}_2^{(l)}) (\bar{b}_1^{(l)}) (a_2^{(l+1)})^{-1} (b_3^{(l)})^{-1}$; the yellow region is a disk with boundary traced out by the word $(\bar{b}_2^{(l)}) (\bar{a}_1^{(l)}) (b_2^{(l+1)})^{-1} (a_3^{(l)})^{-1}$. Two examples for which the *No Holes* condition fails can be pictured by either inserting a puncture, or connect summing with a torus (inserting a “handle”), inside of the colored regions.

Further, for $l = 2, \dots, m - 1$, the gluing conditions (3.1) force⁵⁵

$$\begin{aligned} \text{Incoming-Data}^+(l) &= \text{Outgoing-Data}^+(l - 1), \\ \text{Incoming-Data}^-(l) &= \text{Outgoing-Data}^-(l + 1). \end{aligned} \tag{C.18}$$

In fact, as we will discover, all spectral data on an m -herd can be determined recursively from (C.18) using the initial conditions (C.17).

- The technical *No Holes* condition excludes cases where there are “holes” between adjacent streets when gluing together horses. This condition is essential for our proof of Prop. 3.2, as such holes create obstructions to auxiliary streets introduced in the proof. Furthermore, the *No Holes* condition is utilized in Prop. 3.1 in order to produce an explicit expression for the charge $\hat{\gamma}_c$ (defined in (C.45)) that appears in the formal variable z , but the condition is not necessary to derive the algebraic equation (3.2).⁵⁶

⁵⁵We have omitted the parallel transport map (on the RHS of (C.18)), detailed in Section C.4, that transports spectral data on the $(l - 1)$ th horse to the l th horse.

⁵⁶In particular, the *No Holes* condition is used in the definition of the parallel transport maps $\rho_*^{(l, l \pm 1)}$ of Section C.4. One could use a more general notation for parallel transport in a situation without the *No Holes* condition and the proof of the algebraic equation would follow similarly, although, the final expression for z would be modified.

C.4 A Global Interlude

The following is a technical subsection dedicated to a proper definition of the symbols $\rho_*^{(k,l)}$ that appear throughout the proof of Prop. 3.1. Readers who wish to avoid this technical detour may skip this section and interpret the symbols $\rho_*^{(l,l\pm 1)}$ as parallel transport maps along an appropriate path, from the l th horse to the $(l \pm 1)$ th horse, along the graph of the m -herd living on C' ; further, the $R^{(k,l)}$ can be replaced by parallel transport maps from the l th horse to the k th horse.

First, we will define the local system of soliton charges over \widetilde{C}' .

Definition Let $\mathfrak{s} : \bigcup_{\tilde{z} \in \widetilde{C}'} \widetilde{\Gamma}(\tilde{z}, -\tilde{z}) \rightarrow \widetilde{C}'$ be the projection map with fibers $\mathfrak{s}^{-1}(\tilde{z}) = \widetilde{\Gamma}(\tilde{z}, -\tilde{z})$.

Remark \mathfrak{s} defines a local system of $\widetilde{\Gamma}$ -sets (a locally constant sheaf of $\widetilde{\Gamma}$ -sets) over \widetilde{C}' , when equipped with a parallel transport map defined by a lifted version of the parallel transport of solitons (2.6). More explicitly, for any path $\ell : [0, 1] \rightarrow \widetilde{C}'$, the parallel transport map $\widetilde{P}_\ell : \widetilde{\Gamma}(\ell(0), -\ell(0)) \rightarrow \widetilde{\Gamma}(\ell(1), -\ell(1))$ is given by

$$\widetilde{P}_\ell s = (s' + [\ell\{j\}] - [\ell\{i\}]) \bmod 2H, \quad s \in \widetilde{\Gamma}_{ij}(\ell(0), -\ell(0)). \quad (\text{C.19})$$

where

- s' is a lift of s to a relative homology cycle⁵⁷ on $\widetilde{\Sigma}$,
- $\ell\{n\}$ is the lift of ℓ to a path on $\widetilde{\Sigma}$ given by lifting $\ell(0)$ to sheet n ,
- $[\ell\{n\}]$ is the relative homology class of $\ell\{n\}$
- $(\cdot) \bmod 2H : G(\ell(1), -\ell(1)) \rightarrow \widetilde{\Gamma}(\ell(1), -\ell(1))$ is the quotient map (where the subset of relative homology classes $G(\ell(1), -\ell(1))$ is defined in (2.7)).

By construction, \widetilde{P}_ℓ only depends on the homotopy class of ℓ (rel endpoints).

Let $\xi : \widetilde{C}' \rightarrow C'$ be the unit tangent bundle projection map (previously denoted $\xi^{C'}$). We now make an important observation.

Observation The monodromy of \widetilde{P}_ℓ around any loop that wraps the circle fibers of ξ is trivial. I.e., let $z \in C'$ and choose $\ell : S^1 \rightarrow (\xi)^{-1}(z) \subset \widetilde{C}'$ to be a closed loop supported on the circle fiber $\xi^{-1}(z)$, then the monodromy \widetilde{P}_ℓ is the identity map.

Proof. The proof is immediate: if ℓ is such a loop, then for any sheet n , we have $\text{cl}([\ell\{n\}]) = H$; the result follows from (C.19). \square

Definition Let S be any topological space; $\pi_1(S; z_1, z_2)$ is the set of homotopy (rel endpoints) classes of paths $p : [0, 1] \rightarrow S$ with $p(0) = z_1$ and $p(1) = z_2$.

⁵⁷Recall from (2.8): $\widetilde{\Gamma}(\tilde{z}, -\tilde{z})$ is defined as a quotient of the the subset $G(\tilde{z}, -\tilde{z})$ (consisting of relative homology classes on $\widetilde{\Sigma}$).

Corollary C.1. *Let $\ell : [0, 1] \rightarrow \widetilde{C}'$ be a path. Then $\widetilde{P}_\ell : \widetilde{\Gamma}(\ell(0), -\ell(0)) \rightarrow \widetilde{\Gamma}(\ell(1), -\ell(1))$ is completely specified by the homotopy class (rel endpoints) of the projected path $\xi \circ \ell : [0, 1] \rightarrow C'$.*

In particular, given $q \in \pi_1(C', z_1, z_2)$ along with lifts $\widetilde{z}_1 \in \xi^{-1}(z_1)$, $\widetilde{z}_2 \in \xi^{-1}(z_2)$, we may associate a parallel transport map $\widetilde{P}_\ell : \widetilde{\Gamma}(\widetilde{z}_1, -\widetilde{z}_1) \rightarrow \widetilde{\Gamma}(\widetilde{z}_2, -\widetilde{z}_2)$ where $\ell : [0, 1] \rightarrow \widetilde{C}'$ is a lift of any path representative of the class q such that $\ell(0) = \widetilde{z}_1$, $\ell(1) = \widetilde{z}_2$. By the corollary this association $(q, \widetilde{z}_1, \widetilde{z}_2) \rightsquigarrow \widetilde{P}_\ell$ is well-defined.

Definition Let $q \in \pi_1(C'; z_1, z_2)$ and $\widetilde{z}_1 \in \xi^{-1}(z_1)$, $\widetilde{z}_2 \in \xi^{-1}(z_2)$, then $\widetilde{P}_{(q, \widetilde{z}_1, \widetilde{z}_2)} : \widetilde{\Gamma}(\widetilde{z}_1, -\widetilde{z}_1) \rightarrow \widetilde{\Gamma}(\widetilde{z}_2, -\widetilde{z}_2)$ is the unique parallel transport map assigned to $(q, \widetilde{z}_1, \widetilde{z}_2)$.

To simplify matters of computation, without ignoring global issues, we will develop a notation, suitable to combinatorics, for parallel transport on an m -herd. As each horse is embedded in a contractible region of C , it suffices to keep track of parallel transport of paths *between the horses* of an m -herd: our notation need not keep track of parallel transport between points in an individual horse as suggested by the following remark.

Remark Let $\{U_l\}_{l=1}^m$ be an open cover of disks (on C') satisfying the *Horses* condition for an m -herd, then all paths running between points $z_1, z_2 \in U_l$ and contained within U_l are homotopic (rel endpoints). Thus, by Cor. C.1, for each pair of points $\widetilde{z}_1 \in \xi^{-1}(z_1)$, $\widetilde{z}_2 \in \xi^{-1}(z_2)$, there is a unique parallel transport map assigned to all paths running from \widetilde{z}_1 to \widetilde{z}_2 and contained in $\xi^{-1}(U_l)$.

Now, let us turn our attention to parallel transport of paths running between horses; in particular, paths contained in $U_l \cup U_{l+1}$ for some $l = 1, \dots, m-1$. First, note that each non-vanishing intersection $U_l \cap U_{l+1}$, $l = 1, \dots, m-1$, will consist of some number of disconnected disks. However, on an m -herd, the *No Holes* condition allows us to modify our cover such that $U_l \cap U_{l+1}$ contains exactly *two* components:

$$U_l \cap U_{l+1} = D_{12}^{(l)} \sqcup D_{23}^{(l)}, \quad (\text{C.20})$$

where the $D_{ij}^{(l)}$ are disks such that for $l = 1, \dots, m-1$

$$\begin{aligned} \left(\bar{a}_1^{(l)} = \bar{a}_3^{(l+1)} \right) \cap (U_l \cap U_{l+1}) &\subset D_{12}^{(l)}, \quad \left(a_3^{(l)} = a_1^{(l+1)} \right) \cap (U_l \cap U_{l+1}) \subset D_{12}^{(l)} \\ \left(\bar{b}_1^{(l)} = \bar{b}_3^{(l+1)} \right) \cap (U_l \cap U_{l+1}) &\subset D_{23}^{(l)}, \quad \left(b_3^{(l)} = b_1^{(l+1)} \right) \cap (U_l \cap U_{l+1}) \subset D_{23}^{(l)}; \end{aligned} \quad (\text{C.21})$$

an example of such a cover is shown in Fig. 23 for the case of a 3-herd on $\mathbb{C} = \mathbb{R} \times S^1$. Thus, fixing a pair of points $\widetilde{z}_1 \in \xi^{-1}(U_l)$, $\widetilde{z}_2 \in \xi^{-1}(U_{l+1})$, our interest lies in two homotopy classes (rel endpoints) of paths that run from \widetilde{z}_1 to \widetilde{z}_2 , and are contained in $U_l \cup U_{l+1}$. In particular, denoting these two classes by $q_{12}, q_{23} \in \pi_1(U_l \cup U_{l+1}; z_1, z_2)$,

1. q_{12} has a path representative given by a simple curve running from \widetilde{z}_1 to \widetilde{z}_2 and passing through $D_{12}^{(l)}$ (but not $D_{23}^{(l)}$) exactly once,

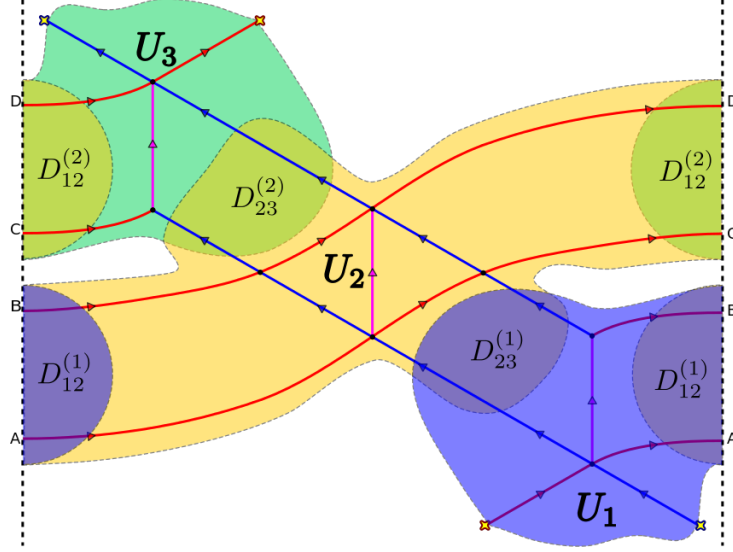


Figure 23. A 3-herd, on $C = \mathbb{R} \times S^1$, equipped with a (two-way street) cover $\{U_l\}_{l=1}^3$ satisfying the *Horses* condition along with (C.20)-(C.21).

2. q_{23} has a path representative given by a simple curve running from \tilde{z}_1 to \tilde{z}_2 and passing through $D_{23}^{(l)}$ (but not $D_{12}^{(l)}$) exactly once.

Definition Let $z_1 \in U_l$, $z_2 \in U_{l+1}$, and take q_{ij} ($ij \in \{12, 23\}$) to be the homotopy classes described above. Then, for a choice of lifts $\tilde{z}_1 \in \xi^{-1}(z_1)$ and $\tilde{z}_2 \in \xi^{-1}(z_2)$,

$$\begin{aligned} \rho_{ij}^{(l,l+1)}(\tilde{z}_1, \tilde{z}_2) &:= \tilde{P}_{(q_{ij}, \tilde{z}_1, \tilde{z}_2)} : \tilde{\Gamma}(\tilde{z}_1, -\tilde{z}_1) \rightarrow \tilde{\Gamma}(\tilde{z}_2, -\tilde{z}_2), \\ \rho_{ij}^{(l+1,l)}(\tilde{z}_1, \tilde{z}_2) &:= \tilde{P}_{(q_{ij}^{-1}, \tilde{z}_2, \tilde{z}_1)} : \tilde{\Gamma}(\tilde{z}_2, -\tilde{z}_2) \rightarrow \tilde{\Gamma}(\tilde{z}_1, -\tilde{z}_1) = \left[\rho_{ij}^{(l,l+1)}(\tilde{z}_1, \tilde{z}_2) \right]^{-1}. \end{aligned} \quad (\text{C.22})$$

Notation In the following computations we will just write $\rho_{ij}^{(l,l+1)}$, dropping the explicit dependence on the endpoints $\tilde{z}_1 \in \xi^{-1}(U_l)$ and $\tilde{z}_2 \in \xi^{-1}(U_{l+1})$; this notation will be sufficiently unambiguous for our purposes. Indeed, let $\tilde{w}_1 \in \xi^{-1}(U_l)$, $\tilde{w}_2 \in \xi^{-1}(U_{l+1})$ be another choice of endpoints with projections $w_i = \xi(\tilde{w}_i)$, $i = 1, 2$; then, by a remark above, $\exists!$ homotopy classes $q_1 \in \pi_1(U_l; w_1, z_1)$ and $q_2 \in \pi_1(U_{l+1}, z_2, w_2)$ such that

$$\rho_{ij}^{(l,l+1)}(\tilde{w}_1, \tilde{w}_2) = \tilde{P}_{(q_2, \tilde{z}_2, \tilde{w}_2)} \left(\rho_{ij}^{(l,l+1)}(\tilde{z}_1, \tilde{z}_2) \right) \tilde{P}_{(q_1, \tilde{w}_1, \tilde{z}_1)}, \quad ij \in \{12, 23\}.$$

Now, on an m -herd, (C.21) indicates that only solitons of type 12 or 21 will be transported via $\rho_{12}^{(l,l+1)}$, and only solitons of type 23 or 32 will be transported via $\rho_{23}^{(l,l+1)}$. With this in mind, for the sake of readability, it will prove convenient to make further notation simplifying definitions.

Definitions

1. Let $\tilde{z} \in \xi^{-1}(U_l)$, then

$$\rho_*^{(l,l+1)} a := \begin{cases} \rho_{12}^{(l,l+1)} a & \text{if } a \in \tilde{\Gamma}_{12}(\tilde{z}, -\tilde{z}) \cup \tilde{\Gamma}_{21}(\tilde{z}, -\tilde{z}) \\ \rho_{23}^{(l,l+1)} a & \text{if } a \in \tilde{\Gamma}_{23}(\tilde{z}, -\tilde{z}) \cup \tilde{\Gamma}_{32}(\tilde{z}, -\tilde{z}) \end{cases}, \quad (\text{C.23})$$

$$\text{and } \rho_*^{(l-1,l)} := \left(\rho_*^{(l-1,l)} \right)^{-1}.$$

- 2.

$$R^{(k,n)} := \begin{cases} \rho_*^{(n-1,n)} \cdots \rho_*^{(k+1,k+2)} \rho_*^{(k,k+1)} & \text{if } k < n \\ \rho_*^{(n+1,n)} \cdots \rho_*^{(k-1,k-2)} \rho_*^{(k,k-1)} & \text{if } n < k. \end{cases} \quad (\text{C.24})$$

Remarks

1. The $\rho_*^{(l,k)}$ extend their action to formal variables X_a via

$$\rho_*^{(l,k)} X_a = X_{\rho_*^{(l,k)} a}.$$

2. $R^{(k,n)}$ is a parallel transport map, on the local system \mathfrak{s} , from the k th horse to the n th horse associated to a path that passes through each l -horse between k and n exactly once. If $R^{(k,n)}$ acts on a soliton of charge 12 or 21, this path passes through the sets $D_{12}^{(l)}$ (but never $D_{23}^{(l)}$) for $\min\{k, n\} < l < \max\{k, n\}$; if $R^{(k,n)}$ acts on a soliton of charge 23 or 32 the path passes through the sets $D_{23}^{(l)}$ (but never $D_{12}^{(l)}$) for $\min\{k, n\} < l < \max\{k, n\}$.

We make one final observation that will be of use in Section C.7.

Remark Let $\mathfrak{r} : \bigcup_{z \in C} \Gamma(z, z) \rightarrow C'$ be the projection map with $\mathfrak{r}^{-1}(z) = \Gamma(z, z)$; this forms a local system over C' when equipped with the parallel transport map

$$P_q s_* = s_* + [q\{j\}] - [q\{i\}], \quad s_* \in \Gamma_{ij}(q(0), q(0)). \quad (\text{C.25})$$

The parallel transport on \mathfrak{r} is compatible with the parallel transport (C.19) on the local system \mathfrak{s} in the sense that for any $q \in \pi_1(C', z_1, z_2)$ and $\tilde{z}_1 \in \xi^{-1}(z_1)$, $\tilde{z}_2 \in \xi^{-1}(z_2)$, we have

$$\xi_*^\Sigma \left(\tilde{P}_{(q, \tilde{z}_1, \tilde{z}_2)} s \right) = P_q \left(\xi_*^\Sigma s \right), \quad (\text{C.26})$$

where, recall, $\xi^\Sigma : \tilde{\Sigma} \rightarrow \Sigma$ is the unit tangent bundle projection map.

Now, we may define the analog of the parallel transport operators $R^{(k,n)}$ for \mathfrak{r} .

Definition Let $s_* \in \bigsqcup_{ij \in \{12, 21, 23, 32\}} \Gamma_{ij}(z, z)$ for some $z \in U_k$, then

$$R_{\mathfrak{r}}^{(k,n)} s_* := \xi_*^\Sigma R^{(k,n)} s, \quad (\text{C.27})$$

where $s \in \bigsqcup_{ij \in \{12, 21, 23, 32\}} \tilde{\Gamma}_{ij}(\tilde{z}, -\tilde{z})$ is any lift of s_* (i.e. $s_* = \xi_*^\Sigma s$).

(C.26) ensures that (C.27) is a well-defined (lift-independent) statement.

C.5 Identifications of Generating Functions

Using the notation developed in Section C.4, we can express (C.18) explicitly as

$$\begin{aligned}
\Upsilon_{a_1}^{(l)} &= \rho_*^{(l-1,l)} \Upsilon_{a_3}^{(l-1)}, & \Delta_{a_1}^{(l)} &= \rho_*^{(l+1,l)} \Delta_{a_3}^{(l+1)}, \\
\Upsilon_{b_1}^{(l)} &= \rho_*^{(l-1,l)} \Upsilon_{b_3}^{(l-1)}, & \Delta_{b_1}^{(l)} &= \rho_*^{(l+1,l)} \Delta_{b_3}^{(l+1)}, \\
\Upsilon_{a_3}^{(l)} &= \rho_*^{(l-1,l)} \Upsilon_{a_1}^{(l-1)}, & \Delta_{a_3}^{(l)} &= \rho_*^{(l+1,l)} \Delta_{a_1}^{(l+1)}, \\
\Upsilon_{b_3}^{(l)} &= \rho_*^{(l-1,l)} \Upsilon_{b_1}^{(l-1)}, & \Delta_{b_3}^{(l)} &= \rho_*^{(l+1,l)} \Delta_{b_1}^{(l+1)}.
\end{aligned} \tag{C.28}$$

In particular,

$$\begin{aligned}
Q_{a_1}^{(l)} &= Q_{a_3}^{(l-1)}, & Q_{a_1}^{(l)} &= Q_{a_3}^{(l+1)}, \\
Q_{b_1}^{(l)} &= Q_{b_3}^{(l-1)}, & Q_{b_1}^{(l)} &= Q_{b_3}^{(l+1)}.
\end{aligned} \tag{C.29}$$

C.6 Proof of Proposition 3.1

C.6.1 Proof of Equations (3.3)

Using the recursion relations (C.29), in conjunction with the equations listed in Sections C.3.3 and C.3.2, we first solve for the internal street factors $Q_{a_2}^{(l)}$, $Q_{a_2}^{(l)}$, $Q_{b_2}^{(l)}$, $Q_{b_2}^{(l)}$ in terms of street factors on the lower/upper-sourced horses at $l = 1$ or $l = m$. As we noticed in Section C.3.2, all other street factors can be written in terms of the internal ones.

Now, via (C.29), and the equations of Section (C.3.2),

$$\begin{aligned}
Q_{a_2}^{(l)} &= Q_{a_3}^{(l)} \\
&= Q_{a_1}^{(l+1)} \\
&= Q_c^{(l+1)} Q_{a_2}^{(l+1)}.
\end{aligned} \tag{C.30}$$

Similarly, we find

$$Q_{a_2}^{(l)} = Q_c^{(l-1)} Q_{a_2}^{(l-1)} \tag{C.31}$$

$$Q_{b_2}^{(l)} = Q_c^{(l+1)} Q_{b_2}^{(l+1)} \tag{C.32}$$

$$Q_{b_2}^{(l)} = Q_c^{(l-1)} Q_{b_2}^{(l-1)}. \tag{C.33}$$

This leads us to the following.

Lemma C.2. *For $l = 1, \dots, m$, we have*

$$Q_{a_2}^{(l)} = Q_{b_2}^{(l)} = \prod_{r=l+1}^{m+1} Q_c^{(r)} \tag{C.34}$$

$$Q_{a_2}^{(l)} = Q_{b_2}^{(l)} = \prod_{r=0}^{l-1} Q_c^{(r)}. \tag{C.35}$$

with the convention that $Q_c^{(m+1)} = Q_c^{(0)} = 1$.

Proof. From the upper-sourced horse conditions (C.13) we have

$$Q_{a_2}^{(m)} = Q_{b_2}^{(m)} = 1; \quad (\text{C.16})$$

so (C.34) follows via (C.30) and (C.32). Similarly, from the lower-sourced horse conditions (C.12) we have

$$Q_{a_2}^{(1)} = Q_{b_2}^{(1)} = 1; \quad (\text{C.14})$$

so (C.35) follows via (C.31) and (C.33). \square

To reduce (C.34) - (C.35) further, we must compute some soliton generating functions.

Computing $\Upsilon_{b_1}^{(l)}$

Via (C.28)

$$\begin{aligned} \Upsilon_{b_1}^{(l)} &= \rho_*^{(l-1,l)} \Upsilon_{b_3}^{(l-1)} \\ &= \rho_*^{(l-1,l)} \Upsilon_{b_1}^{(l-1)}. \end{aligned} \quad (\text{C.36})$$

Thus, propagating the lower sourced horse conditions (C.12) through this recursion relation,

$$\Upsilon_{b_1}^{(l)} = \left(\prod_{r=1}^l \rho_*^{(r-1,r)} \right) X_b \quad (\text{C.37})$$

$$= R^{(1,l)} X_b. \quad (\text{C.38})$$

Computing $\Delta_{b_1}^{(l)}$

The idea is dual to above; indeed

$$\begin{aligned} \Delta_{b_1}^{(l)} &= \rho_*^{(l+1,l)} \Delta_{b_3}^{(l+1)} \\ &= \rho_*^{(l+1,l)} \Delta_{b_1}^{(l+1)}. \end{aligned} \quad (\text{C.39})$$

Using the upper-sourced horse conditions (C.13),

$$\begin{aligned} \Delta_{b_1}^{(l)} &= \left(\prod_{r=l}^m \rho_*^{(r+1,r)} \right) X_{\bar{b}} \\ &= R^{(m,l)} X_{\bar{b}}. \end{aligned} \quad (\text{C.40})$$

Computing $\Upsilon_{a_1}^{(l)}$

Via (C.28) and the equation for Υ_{a_3} in Section C.3.1,

$$\begin{aligned} \Upsilon_{a_1}^{(l)} &= \rho_*^{(l-1,l)} \Upsilon_{a_3}^{(l-1)} \\ &= \rho_*^{(l-1,l)} \Upsilon_{a_1}^{(l-1)} \left(1 + \Upsilon_{b_3}^{(l-1)} \Delta_{b_1}^{(l-1)} \right) \left(1 + \Upsilon_{b_1}^{(l-1)} \Delta_{b_3}^{(l-1)} \right) \\ &= \rho_*^{(l-1,l)} \Upsilon_{a_1}^{(l-1)} Q_{b_2}^{(l-1)} Q_{b_2}^{(l-1)}. \end{aligned} \quad (\text{C.41})$$

Using the lower-sourced horse conditions (C.12),

$$\begin{aligned}\Upsilon_{a_1}^{(l)} &= \left(\prod_{r=1}^l \rho_*^{(r-1,r)} X_a \right) \left(\prod_{r=1}^l \rho_*^{(r-1,r)} Q_{\frac{b_2}{b_2}}^{(r-1)} Q_{b_2}^{(r-1)} \right) \\ &= R^{(1,l)} X_a \left(\prod_{r=0}^{l-1} Q_{\frac{b_2}{b_2}}^{(r)} Q_{b_2}^{(r)} \right).\end{aligned}\tag{C.42}$$

Computing $\Delta_{a_1}^{(l)}$

Again, the computation is dual to that for $\Upsilon_{a_1}^{(l)}$,

$$\begin{aligned}\Delta_{a_1}^{(l)} &= \rho_*^{(l+1,l)} \Delta_{a_3}^{(l+1)} \\ &= \rho_*^{(l+1,l)} \left[\left(1 + \Upsilon_{\frac{b_3}{b_3}}^{(l+1)} \Delta_{\frac{b_1}{b_1}}^{(l+1)} \right) \left(1 + \Upsilon_{b_1}^{(l+1)} \Delta_{b_3}^{(l+1)} \right) \Delta_{a_1}^{(l+1)} \right] \\ &= \rho_*^{(l+1,l)} Q_{\frac{b_2}{b_2}}^{(l+1)} Q_{b_2}^{(l+1)} \Delta_{a_1}^{(l+1)}.\end{aligned}\tag{C.43}$$

So, using the upper-sourced horse conditions (C.13),

$$\begin{aligned}\Delta_{a_1}^{(l)} &= \left(\prod_{r=l}^m \rho_*^{(r+1,l)} Q_{\frac{b_2}{b_2}}^{(r+1)} Q_{b_2}^{(r+1)} \right) X_a \\ &= \left(\prod_{r=l+1}^{m+1} Q_{\frac{b_2}{b_2}}^{(r)} Q_{b_2}^{(r)} \right) R^{(m,l)} X_a.\end{aligned}\tag{C.44}$$

These computations lead us to the following key lemma that allows all street factors Q_p to be reduced to powers of a single function.

Lemma C.3.

$$Q_c^{(l)} = Q_c^{(1)}, \forall l = 1, \dots, m.$$

Proof. Recall (C.36), (C.39), (C.41), and (C.43)

$$\begin{aligned}\Upsilon_{b_1}^{(l)} &= \rho_*^{(l-1,l)} \Upsilon_{b_1}^{(l-1)} \\ \Delta_{b_1}^{(l)} &= \rho_*^{(l+1,l)} \Delta_{b_1}^{(l+1)} \\ \Upsilon_{a_1}^{(l)} &= \rho_*^{(l-1,l)} Q_{\frac{b_2}{b_2}}^{(l-1)} Q_{b_2}^{(l-1)} \Upsilon_{a_1}^{(l-1)} \\ \Delta_{a_1}^{(l)} &= \rho_*^{(l+1,l)} Q_{\frac{b_2}{b_2}}^{(l+1)} Q_{b_2}^{(l+1)} \Delta_{a_1}^{(l+1)};\end{aligned}$$

we can rewrite the equations for $\Delta_{b_1}^{(l)}$ and $\Delta_{a_1}^{(l)}$ as

$$\begin{aligned}\Delta_{b_1}^{(l)} &= \rho_*^{(l-1,l)} \Delta_{b_1}^{(l-1)} \\ \Delta_{a_1}^{(l)} &= \rho_*^{(l-1,l)} \frac{\Delta_{a_1}^{(l-1)}}{Q_{\frac{b_2}{b_2}}^{(l)} Q_{b_2}^{(l)}}.\end{aligned}$$

Using the equation for Q_c in Section C.3.3

$$\begin{aligned}
Q_c^{(l)} &= 1 + \Upsilon_{a_1}^{(l)} \Upsilon_{b_1}^{(l)} \Delta_{b_1}^{(l)} \Delta_{a_1}^{(l)} \\
&= 1 + \left(\rho_*^{(l-1,l)} Q_{b_2}^{(l-1)} Q_{b_2}^{(l-1)} \Upsilon_{a_1}^{(l-1)} \right) \left(\rho_*^{(l-1,l)} \Upsilon_{b_1}^{(l-1)} \right) \left(\rho_*^{(l-1,l)} \Delta_{b_1}^{(l-1)} \right) \left(\rho_*^{(l-1,l)} \frac{\Delta_{a_1}^{(l-1)}}{Q_{b_2}^{(l)} Q_{b_2}^{(l)}} \right) \\
&= 1 + \left(Q_c^{(l-1)} - 1 \right) \left(\frac{Q_{b_2}^{(l-1)} Q_{b_2}^{(l-1)}}{Q_{b_2}^{(l)} Q_{b_2}^{(l)}} \right);
\end{aligned}$$

where, on the last line, the cancellation of the $\rho_*^{(l-1,l)}$ (parallel transport) actions⁵⁸ can be seen by working through its definition in equations (C.19), (C.22), and (C.23). Applying the closure map we obtain

$$Q_c^{(l)} = 1 + \left(Q_c^{(l-1)} - 1 \right) \left(\frac{Q_{b_2}^{(l-1)} Q_{b_2}^{(l-1)}}{Q_{b_2}^{(l)} Q_{b_2}^{(l)}} \right).$$

Using (C.34) and (C.35), then

$$\begin{aligned}
Q_c^{(l)} &= 1 + \left(Q_c^{(l-1)} - 1 \right) \left(\frac{\prod_{r \neq l-1} Q_c^{(r)}}{\prod_{r \neq l} Q_c^{(r)}} \right) \\
&= 1 + \left(Q_c^{(l-1)} - 1 \right) \frac{Q_c^{(l)}}{Q_c^{(l-1)}} \\
&= 1 + Q_c^{(l)} - \frac{Q_c^{(l)}}{Q_c^{(l-1)}}.
\end{aligned}$$

Hence,

$$Q_c^{(l)} = Q_c^{(l-1)}, \quad l = 2, \dots, m.$$

□

The above proposition motivates the following simplified notation.

Definition

$$P_m := Q_c^{(1)}.$$

Now, when lemmata C.2 and C.3 are combined, we have

Corollary C.4.

$$\begin{aligned}
Q_{a_2}^{(l)} &= Q_{b_2}^{(l)} = (P_m)^{m-l} \\
Q_{a_2}^{(l)} &= Q_{b_2}^{(l)} = (P_m)^{l-1}.
\end{aligned}$$

⁵⁸This is consistent with the fact that, according to (C.19), parallel transport acts trivially on charges of type *ii*.

The above corollary, combined with the equations of Section C.3.2, is enough to express the remainder of the street factors in terms of P_m ,

$$\begin{aligned}(P_m)^{m-l} &= Q_{a_3}^{(l)} = Q_{b_3}^{(l)} \\ (P_m)^{l-1} &= Q_{a_3}^{(l)} = Q_{b_3}^{(l)} \\ (P_m)^{m-l+1} &= Q_{a_1}^{(l)} = Q_{b_1}^{(l)} \\ (P_m)^l &= Q_{a_1}^{(l)} = Q_{b_1}^{(l)}.\end{aligned}$$

This completes the proof of (3.3) in Prop. 3.1.

C.6.2 Proof of the Algebraic Equation (3.2)

Via the equation for \mathcal{Q}_c in Section C.3.3 along with (C.38)-(C.42),

$$\begin{aligned}\mathcal{Q}_c^{(l)} &= 1 + \Upsilon_{a_1}^{(l)} \Upsilon_{b_1}^{(l)} \Delta_{b_1}^{(l)} \Delta_{a_1}^{(l)} \\ &= 1 + \left[\left(\prod_{r=0}^{l-1} Q_{b_2}^{(r)} Q_{b_2}^{(r)} \right) R^{(1,l)} X_a \right] \left[R^{(1,l)} X_b \right] \left[R^{(m,l)} X_{\bar{b}} \right] \left[\left(\prod_{r=l+1}^{m+1} Q_{b_2}^{(r)} Q_{b_2}^{(r)} \right) R^{(m,l)} X_a \right] \\ &= 1 + \left(\prod_{r \neq l} Q_{b_2}^{(r)} Q_{b_2}^{(r)} \right) \left(R^{(1,l)} X_a \right) \left(R^{(1,l)} X_b \right) \left(R^{(m,l)} X_{\bar{b}} \right) \left(R^{(m,l)} X_a \right) \\ &= 1 + (P_m)^{(m-1)^2} \left(R^{(1,l)} X_a \right) \left(R^{(1,l)} X_b \right) \left(R^{(m,l)} X_{\bar{b}} \right) \left(R^{(m,l)} X_a \right); \end{aligned}$$

where, on the last line we utilized Corollary C.4.

Remark We note that,

$$R^{(1,l)} a + R^{(1,l)} b + R^{(m,l)} \bar{b} + R^{(m,l)} \bar{a}$$

represents a soliton charge of type 11 on the open set $\xi^{-1}(U_l) \subset \widetilde{C}'$. Thus, we may apply the map cl to this expression to produce an element of $\widetilde{\Gamma}$.

This leads us to the following definition.

Definition We define

$$\widehat{\gamma}_c := \text{cl} \left[R^{(1,l)} a + R^{(1,l)} b + R^{(m,l)} \bar{b} + R^{(m,l)} \bar{a} \right] \in \widetilde{\Gamma} \quad (\text{C.45})$$

and corresponding formal variable

$$z := X_{\widehat{\gamma}_c}. \quad (\text{C.46})$$

(We will show below that, in fact, (C.45) does not depend on l ; thus, this definition is sensible.)

With the above definitions we have

$$\mathcal{Q}_c^{(l)} = 1 + z P_m^{(m-1)^2}$$

hence, by Lemma C.3, P_m satisfies the algebraic equation

$$P_m = 1 + zP_m^{(m-1)^2}. \quad (3.2)$$

This completes the proof of the algebraic equation in Prop. 3.1.

Remark As we will show in Section C.7, $\widehat{\gamma}_c$ is the sum of two tangent framing lifts of simple closed curves with corresponding homology classes $\gamma, \gamma' \in \Gamma$. In fact, we will show that (C.46) can be rewritten in the form stated in Prop. 3.1: $z = (-1)^m X_{\widetilde{\gamma} + \widetilde{\gamma}'}$, where $\widetilde{(\cdot)} : \Gamma \rightarrow \widetilde{\Gamma}$ is defined in Section (2.2.3) and discussed further in Section E.

C.7 Proof of the Decomposition of $\widehat{\gamma}_c$

We begin with an example (which may be skipped for the more general proof below).⁵⁹

C.7.1 Example: $\widehat{\gamma}_c$ for m -herds on the cylinder

We consider generalizations (to arbitrary m) of the herds shown in Fig. 4 for $m = 1, \dots, 4$. Assume we are equipped with a branched 3-cover of the cylinder $C = S^1 \times \mathbb{R}$ with four branch points. Now, consider an m -herd such that it is contained in a presentation of the cylinder as an identification space of $[0, 1] \times \mathbb{R}$: the streets of type 23 lie entirely in the interior of $(0, 1) \times \mathbb{R}$, while the streets of type 12 involved in the identifications (3.1) pass through the identified boundary. First, each of the charges a, b, \bar{a}, \bar{b} can be thought of as flat sections of the local system $\mathfrak{s} : \bigcup_{\widetilde{z} \in \widetilde{C}'} \widetilde{\Gamma}(\widetilde{z}, -\widetilde{z}) \rightarrow \widetilde{C}'$, locally defined around their respective branch points. The two-way streets are contained within the open set $U := \bigcup_{l=1}^m U_l$, which is homeomorphic to $S^1 \times I$ for $I \cong (0, 1)$ an open interval. Let $U^c \cong (0, 1)^2$ be the open set formed by removing the vertical line⁶⁰ $(\{0\} \times \mathbb{R}) \cap U \sim (\{1\} \times \mathbb{R}) \cap U$ from U . \mathfrak{s} is trivial over the open set $\xi^{-1}(U^c) \cong (0, 1)^2 \times S^1$ in \widetilde{C}' ; so, we can extend a, b, \bar{a}, \bar{b} to flat sections over all of $\xi^{-1}(U^c)$.

Now, let $q_{\text{cyl}} : [0, 1] \rightarrow U \subset C'$ denote a loop winding once around the S^1 direction of U , and oriented such that the upper-sourced horse branch points sit to its “left,” while the lower-sourced horse branch points sit to its “right”; $\widehat{q}_{\text{cyl}} : [0, 1] \rightarrow \widetilde{C}'$ will denote the tangent framing lift of q_{cyl} .

Working through the definition of the parallel transport maps $R^{(k,l)}$ in (C.19), (C.22)-(C.24), we have

$$\widehat{\gamma}_c = \text{cl}(a + b + \bar{b} + \bar{a}) + (m-1)([\widehat{q}_{\text{cyc}}\{2\}] - [\widehat{q}_{\text{cyc}}\{1\}]);$$

the expression in the closure map is defined by evaluating the sections a, b, \bar{a}, \bar{b} at some point $\widetilde{z} \in \xi^{-1}(U^c \cap U_l)$ and taking their sum to define an element in $\widetilde{\Gamma}_{11}(\widetilde{z}, -\widetilde{z})$.

Observe that we can decompose $\widehat{\gamma}_c$ as $\widehat{\gamma}_c = \widehat{\gamma} + \widehat{\gamma}'$ where,

$$\begin{aligned} \widehat{\gamma} &= \text{cl}(b + \bar{b}) \\ \widehat{\gamma}' &= \text{cl}(a + \bar{a}) + (m-1)([\widehat{q}_{\text{cyc}}\{2\}] - [\widehat{q}_{\text{cyc}}\{1\}]). \end{aligned}$$

⁵⁹The following sections rely on the ideas of Section C.4.

⁶⁰Here \sim denotes the identification of the boundary of $[0, 1] \times \mathbb{R}$ to form the cylinder. The removed vertical line is given by the (identified) dotted lines in Fig. 4.

Now, note that we can realize $\widehat{\gamma}$ the tangent framing lift of a simple closed curve on Σ . Indeed, consider an auxiliary street of type 23, realized as a straight line on $U \cup \{\text{branch pts.}\}$, running between the two branch points of type 23 (beginning at the branch point emitting the charge b and ending at the branch point emitting the charge \bar{b}). The lift of this street to Σ is a simple closed curve; the tangent framing lift is a representative of $\text{cl}(b + \bar{b})$. Similarly, we can realize $\text{cl}(a + \bar{a})$ with the tangent framing lift of a simple closed curve ℓ_a on $U \cup \{\text{branch pts.}\}$ and so $\widehat{\gamma}'$ can be realized as a modification of ℓ_a by smoothly “detouring” along the lifts (to sheets 1 and 2) of a curve that winds $m - 1$ times around the S^1 direction of U . The resulting curve is the tangent framing lift of a simple closed curve. Furthermore, project these simple-closed curves to Σ ; then letting γ and γ' be the homology classes of our projections, with their representative curves it is clear that $\langle \gamma, \gamma' \rangle = m$.

Now, using different techniques, let us proceed on with the general proof of the decomposition $\widehat{\gamma}_c = \widehat{\gamma} + \widehat{\gamma}'$, described in the example above, for an m -herd on a general oriented curve C .

C.7.2 General Proof

Let $\xi^\Sigma : \widetilde{\Sigma} \rightarrow \Sigma$ be the unit tangent bundle projection.

Definition

$$\gamma_c := \xi_*^\Sigma \widehat{\gamma}_c \in \Gamma.$$

To derive an explicit expression for γ_c in terms of simpleton charges (C.1) in $\bigcup_{z \in C} \Gamma(z, z)$, we “pushforward” the expression (C.45) via ξ^Σ . From the definitions (C.1), (C.2), and (C.45) it follows that

$$\gamma_c = \text{cl} \left[R_{\mathfrak{r}}^{(1,l)} a_* + R_{\mathfrak{r}}^{(1,l)} b_* + R_{\mathfrak{r}}^{(m,l)} \bar{b}_* + R_{\mathfrak{r}}^{(m,l)} \bar{a}_* \right] \quad (\text{C.47})$$

where $R_{\mathfrak{r}}^{(k,n)}$ are the “pushforward” of the parallel transport operators $R^{(k,n)}$ defined in (C.27).

We will construct a decomposition $\gamma_c = \gamma + \gamma'$ with $\langle \gamma, \gamma' \rangle = m$ roughly by shrinking the $c^{(l)}$ streets of the herd to points. To be precise, we introduce some definitions.

Definitions

1. A pony is a partial spectral network as shown in Fig. 24. Upper and lower-sourced ponies are defined similar to upper and lower sourced horses.
2. The string of ponies S_m associated to an m -herd H_m is the spectral network constructed by placing
 - (a) A lower sourced pony on U_1
 - (b) Ponies on U_l , $1 < l < m$
 - (c) An upper-sourced pony on U_m ,

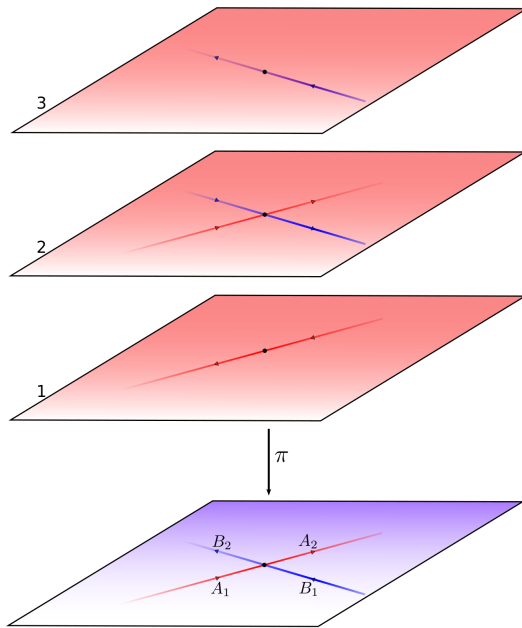


Figure 24. A pony and its lift to Σ . Red streets are of type 12, blue streets are of type 23.

where the U_m are a good open cover satisfying the *Horses* condition for H_m , and forcing the identifications

$$\begin{aligned} A_1^{(l+1)} &= A_2^{(l)} \\ B_1^{(l+1)} &= B_2^{(l)} \end{aligned}$$

on each $U_l \cap U_{l+1}$.

Remarks

1. S_m is only defined up to homotopy on each disk U_l .
2. The interpretation of S_m as a spectral network is overkill for our discussion and we introduce it as such mainly for notational convenience: all that will be necessary is the graph of the lift $\text{Lift}(S_m) \subset \Sigma$. However, in the wall-crossing interpretation of m -herds discussed in Section 3.1, the spectral network S_m is expected to appear on the wall of marginal stability where two hypermultiplets of intersection number m have coincident central charge phase. In fact, the procedure of deforming such a picture is what motivated the construction of m -herds.

Definition Let $p^{(l)}$ be a street of type ij , then $\mathbf{p}^{(l)} \in C_1(\Sigma; \mathbb{Z})$ is the 1-chain on Σ representing the lift⁶¹ of $p^{(l)}$ as a street of type ij (using the orientation discussed in Section 2.2).

⁶¹If $p^{(l)}$ connects two joints, this lift has two components. If $p^{(l)}$ connects a joint to a branch point of type ij , then the two components combine to form a connected 1-chain between sheets i and j .

If we define,

$$\begin{aligned}\gamma &= \left[\sum_{l=1}^m (\mathbf{B}_1^{(l)} + \mathbf{B}_2^{(l)}) \right] \in H_1(\Sigma; \mathbb{Z}) \\ \gamma' &= \left[\sum_{l=1}^m (\mathbf{A}_1^{(l)} + \mathbf{A}_2^{(l)}) \right] \in H_1(\Sigma; \mathbb{Z}),\end{aligned}$$

then, as shown in Fig. 24, γ and γ' intersect once in each $\pi^{-1}(U_l)$, $l = 1, \dots, m$; hence,

$$\langle \gamma, \gamma' \rangle = m.$$

Now

- $\sum_{l=1}^{m-1} (\mathbf{A}_1^{(l)} + \mathbf{A}_2^{(l)})$ is a 1-chain representative of the parallel transported charge $R_{\mathfrak{r}}^{(1, m-1)} a_*$.
- $\sum_{l=1}^{m-1} (\mathbf{B}_1^{(l)} + \mathbf{B}_2^{(l)})$ is a 1-chain representative of $R_{\mathfrak{r}}^{(1, m-1)} b_*$.
- $\mathbf{A}_1^{(m)} + \mathbf{A}_2^{(m)}$ is a 1-chain representative of \bar{a}_* .
- $\mathbf{B}_1^{(m)} + \mathbf{B}_2^{(m)}$ is a 1-chain representative of \bar{b}_* .

Hence,

$$\gamma_c = \gamma + \gamma'.$$

Now, each of the 1-chains $\mathbf{A}_i^{(l)}$, $\mathbf{B}_i^{(l)}$ have well-defined tangent framing lifts $\widehat{\mathbf{A}}_i^{(l)}$, $\widehat{\mathbf{B}}_i^{(l)}$ when thought of as oriented paths on $\text{Lift}(S_m) \subset \Sigma$. Similarly, γ and γ' have obvious representative curves on $\text{Lift}(S_m)$ that allow us to produce tangent framing lifts $\widehat{\gamma}$, $\widehat{\gamma}'$. In fact,

$$\begin{aligned}\widehat{\gamma} &= \left[\sum_{l=1}^m (\widehat{\mathbf{B}}_1^{(l)} + \widehat{\mathbf{B}}_2^{(l)}) \right] \in H_1(\widetilde{\Sigma}; \mathbb{Z}) \\ \widehat{\gamma}' &= \left[\sum_{l=1}^m (\widehat{\mathbf{A}}_1^{(l)} + \widehat{\mathbf{A}}_2^{(l)}) \right] \in H_1(\widetilde{\Sigma}; \mathbb{Z}).\end{aligned}$$

Via similar arguments to above, along with the definition of $\widehat{\gamma}_c$ in (C.45), we have

$$\widehat{\gamma}_c = \widehat{\gamma} + \widehat{\gamma}'.$$

Alternatively, we can lift $\gamma_c = \gamma + \gamma'$ using the map $\widetilde{(\cdot)} : \Gamma \rightarrow \widetilde{\Gamma}$ defined in (E.1) of Appendix E. Indeed, as the curves representing γ and γ' intersect m times, we have

$$\widetilde{\gamma}_c = \widehat{\gamma} + \widehat{\gamma}' + mH = \widehat{\gamma}_c + mH.$$

Thus,

$$z = X_{\widehat{\gamma}_c} = (-1)^m X_{\widetilde{\gamma}_c}.$$

C.8 Proof of Proposition 3.2

We wish to compute the homology class of the 1-chain $L(n\gamma_c)$. First we introduce a few notational definitions that differ slightly from the main body of the paper.

Definition $\mathbf{p}^{(l,r)} \in C_1(\Sigma; \mathbb{Z})$ is the component of $\mathbf{p}^{(l)} \in C_1(\Sigma; \mathbb{Z})$ on the r th sheet. If $\mathbf{p}^{(l)}$ is a street of type ij , then

$$\mathbf{p}^{(l,r)} = \begin{cases} + (\text{1-chain representing the lift of } \mathbf{p}^{(l)} \text{ to the } r\text{th sheet}), & \text{if } r = j \\ - (\text{1-chain representing the lift of } \mathbf{p}^{(l)} \text{ to the } r\text{th sheet}), & \text{if } r = i \\ 0 & \text{otherwise} \end{cases}.$$

Now,

$$\begin{aligned} L(n\gamma_c) &= \sum_{l=1}^m \sum_{p^{(l)}} \alpha_n(p, l) \mathbf{p}^{(l)} \\ &= \alpha_n \sum_{l=1}^m \left\{ \mathbf{c}^{(l)} + (m-l) \left(\mathbf{a}_2^{(l)} + \mathbf{a}_3^{(l)} + \mathbf{b}_2^{(l)} + \mathbf{b}_3^{(l)} \right) \right. \\ &\quad + (l-1) \left(\overline{\mathbf{a}_2}^{(l)} + \overline{\mathbf{a}_3}^{(l)} + \overline{\mathbf{b}_2}^{(l)} + \overline{\mathbf{b}_3}^{(l)} \right) + \\ &\quad \left. + (m-l+1) \left(\mathbf{a}_1^{(l)} + \mathbf{b}_1^{(l)} \right) + l \left(\overline{\mathbf{a}_1}^{(l)} + \overline{\mathbf{b}_1}^{(l)} \right) \right\}. \end{aligned} \tag{3.19}$$

after using the results of Prop. 3.1 and the definition of α_n given in equation (3.18).

For the sake of readability we introduce some simplifying notation.

Notational Definition We denote,

$$\begin{aligned} \mathbf{a}_{12} &:= \mathbf{a}_1^{(l)} + \mathbf{a}_2^{(l)} \\ \mathbf{a}_{23} &:= \mathbf{a}_2^{(l)} + \mathbf{a}_3^{(l)} \\ \mathbf{a}_{123} &:= \mathbf{a}_1^{(l)} + \mathbf{a}_2^{(l)} + \mathbf{a}_3^{(l)}; \end{aligned}$$

and similarly, for $\overline{\mathbf{a}}_i$, \mathbf{b}_i , and $\overline{\mathbf{b}}_i$.

Using this notation, we can rewrite our sum in slightly more illuminating form,

$$\begin{aligned} L(n\gamma_c) &= \alpha_n \sum_{l=1}^m \left\{ (m-l) \left(\mathbf{a}_{123}^{(l)} + \mathbf{b}_{123}^{(l)} \right) + l \left(\overline{\mathbf{a}}_{123}^{(l)} + \overline{\mathbf{b}}_{123}^{(l)} \right) \right. \\ &\quad \left. + \mathbf{a}_1^{(l)} + \mathbf{b}_1^{(l)} + \mathbf{c}^{(l)} - \overline{\mathbf{a}}_{23}^{(l)} - \overline{\mathbf{b}}_{23}^{(l)} \right\}. \end{aligned}$$

This form suggests we should try to find a homological equivalence taking the terms multiplying the factor l , to the terms multiplying the factor $(m-l)$. We introduce extra 1-chains to aid in our computation. To define them, it is helpful to think of them as lifts of auxiliary streets. However, the interpretation as lifts of streets on C is only a notational tool: these streets are not part of any spectral network.

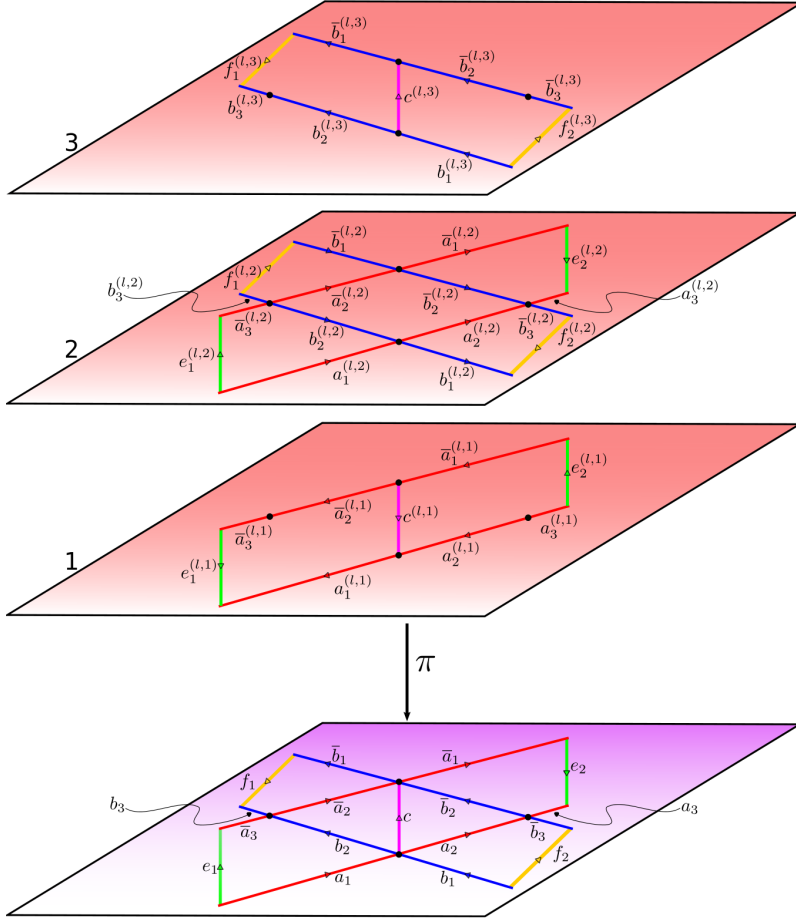


Figure 25. Lift of a horse with extra 1-chains, pictured here as the lift of some auxiliary streets on C . For the sake of readability, the “horse label” (l) is suppressed on the base C .

Definition Let $\{U_l\}_{l=1}^m$ be an open covering satisfying the *Horses* condition for an m -herd. On each horse we define auxiliary streets as in Fig. 25: $e_1^{(l)}, e_2^{(l)} \subset U_l$ of type 12, and $f_1^{(l)}, f_2^{(l)} \subset U_l$, of type 23 ; such that,

(C1):

$$\begin{aligned} e_1^{(l+1)} &= -e_2^{(l)} \\ f_2^{(l+1)} &= -f_1^{(l)}, \end{aligned}$$

where “ $-$ ” indicates orientation reversal.

(C2): $e_1^{(1)}$ and $f_2^{(1)}$ end on the branch points of type 12 and 23 (respectively) of the lower-sourced horse, while $e_2^{(m)}$ and $f_1^{(m)}$ end on the branch points of type 12 and 23 (respectively) of the upper-sourced horse.

Remark The *No Holes* condition removes any obstruction to condition (C1).

The 1-chains that will aid in our proof are the lifts of the auxiliary streets.

Remark Keeping with the (previously defined) convention for lifts of streets, there are 1-chains (on Σ) $e_1^{(l)}$, $e_2^{(l)}$, $f_1^{(l)}$, and $f_2^{(l)}$ (also depicted in Fig. 25). It follows that, via (C1),

$$\begin{aligned} e_1^{(l+1)} &= -e_2^{(l)} \\ f_2^{(l+1)} &= -f_1^{(l)}. \end{aligned} \tag{C.48}$$

for $l = 1, \dots, m-1$.

Lemma C.5. *Let \sim denote homological equivalence. Then for each $l = 1, \dots, m$: on the first (locally defined) sheet,*

$$0 \sim \bar{a}_{23}^{(l,1)} + e_1^{(l,1)} - a_1^{(l,1)} - c^{(l,1)} \tag{C.49}$$

$$0 \sim \bar{a}_1^{(l,1)} + c^{(l,1)} - a_{23}^{(l,1)} + e_2^{(l,1)}. \tag{C.50}$$

On the second sheet,

$$0 \sim \bar{a}_{123}^{(l,2)} + e_2^{(l,2)} - a_{123}^{(l,2)} + e_1^{(l,2)} \tag{C.51}$$

$$0 \sim \bar{b}_{123}^{(l,2)} + f_2^{(l,2)} - b_{123}^{(l,2)} + f_1^{(l,2)} \tag{C.52}$$

$$0 \sim \bar{a}_3^{(l,2)} + b_2^{(l,2)} - a_1^{(l,2)} + e_1^{(l,2)} \tag{C.53}$$

$$0 \sim a_2^{(l,2)} + \bar{b}_3^{(l,2)} + f_2^{(l,2)} - b_1^{(l,2)} \tag{C.54}$$

$$0 \sim b_2^{(l,2)} + a_2^{(l,2)} - \bar{b}_2^{(l,2)} - \bar{a}_2^{(l,2)}. \tag{C.55}$$

On the third sheet,

$$0 \sim b_1^{(l,3)} + c^{(l,3)} - \bar{b}_{23}^{(l,3)} - f_2^{(l,3)} \tag{C.56}$$

$$0 \sim \bar{b}_1^{(l,3)} + f_1^{(l,3)} - b_{23}^{(l,3)} + c^{(l,3)}. \tag{C.57}$$

Proof. The lemma follows by inspection of Fig. 25. Each of the listed sum of 1-chains is the boundary of an oriented disk. \square

In particular, it follows from the lemma that

$$\begin{aligned} \bar{a}_{123}^{(l)} &\sim a_{123}^{(l)} - e_1^{(l)} - e_2^{(l)} \\ \bar{b}_{123}^{(l)} &\sim b_{123}^{(l)} - f_1^{(l)} - f_2^{(l)}. \end{aligned}$$

Hence,

$$\begin{aligned} L(n\gamma_c) &\sim \alpha_n \sum_{l=1}^m \left\{ (m-l) \left(a_{123}^{(l)} + b_{123}^{(l)} \right) + l \left(a_{123}^{(l)} + b_{123}^{(l)} \right) \right\} + \alpha_n R_1 + \alpha_n R_2 \\ &\sim m\alpha_n \sum_{l=1}^m \left(a_{123}^{(l)} + b_{123}^{(l)} \right) + \alpha_n R_1 + \alpha_n R_2 \end{aligned} \tag{C.58}$$

where

$$R_1 = - \sum_{l=1}^m l \left\{ \mathbf{e}_1^{(l)} + \mathbf{e}_2^{(l)} + \mathbf{f}_1^{(l)} + \mathbf{f}_2^{(l)} \right\}$$

$$R_2 = \sum_{l=1}^m \left\{ \mathbf{a}_1^{(l)} + \mathbf{b}_1^{(l)} + \mathbf{c}^{(l)} - \overline{\mathbf{a}_{23}}^{(l)} - \overline{\mathbf{b}_{23}}^{(l)} \right\}.$$

Using (C.48), the first of these sums can be simplified,

$$\begin{aligned} R_1 &= - \sum_{l=1}^m l \left(\mathbf{e}_1^{(l)} + \mathbf{f}_2^{(l)} \right) - \sum_{l=1}^m l \left(\mathbf{e}_2^{(l)} + \mathbf{f}_1^{(l)} \right) \\ &= - \sum_{l=1}^m l \left(\mathbf{e}_1^{(l)} + \mathbf{f}_2^{(l)} \right) + \sum_{l=1}^{m-1} l \left(\mathbf{e}_1^{(l+1)} + \mathbf{f}_2^{(l+1)} \right) - m \left(\mathbf{e}_2^{(m)} + \mathbf{f}_1^{(m)} \right) \\ &= - \sum_{l=1}^m l \left(\mathbf{e}_1^{(l)} + \mathbf{f}_2^{(l)} \right) + \sum_{l=2}^m (l-1) \left(\mathbf{e}_1^{(l)} + \mathbf{f}_2^{(l)} \right) - m \left(\mathbf{e}_2^{(m)} + \mathbf{f}_1^{(m)} \right) \\ &= - \left(\mathbf{e}_1^{(1)} + \mathbf{f}_2^{(1)} \right) - m \left(\mathbf{e}_2^{(m)} + \mathbf{f}_1^{(m)} \right) - \sum_{l=2}^m \left(\mathbf{e}_1^{(l)} + \mathbf{f}_2^{(l)} \right) \\ &= -m \left(\mathbf{e}_2^{(m)} + \mathbf{f}_1^{(m)} \right) - \sum_{l=1}^m \left(\mathbf{e}_1^{(l)} + \mathbf{f}_2^{(l)} \right). \end{aligned} \tag{C.59}$$

To reduce R_2 , we use the following lemma.

Lemma C.6.

$$\mathbf{a}_1^{(l)} + \mathbf{b}_1^{(l)} + \mathbf{c}^{(l)} - \overline{\mathbf{a}_{23}}^{(l)} - \overline{\mathbf{b}_{23}}^{(l)} \sim \mathbf{e}_1^{(l)} + \mathbf{f}_2^{(l)}.$$

Proof. On sheet 1,

$$\mathbf{a}_1^{(l,1)} + \mathbf{b}_1^{(l,1)} + \mathbf{c}^{(l,1)} - \overline{\mathbf{a}_{23}}^{(l,1)} - \overline{\mathbf{b}_{23}}^{(l,1)} = \mathbf{a}_1^{(l,1)} + \mathbf{c}^{(l,1)} - \overline{\mathbf{a}_{23}}^{(l,1)}.$$

Using (C.49),

$$\begin{aligned} &\sim \mathbf{a}_1^{(l,1)} + \mathbf{c}^{(l,1)} + \left(\mathbf{e}_1^{(l,1)} - \mathbf{a}_1^{(l,1)} - \mathbf{c}^{(l,1)} \right) \\ &\sim \mathbf{e}_1^{(l,1)}. \end{aligned}$$

Similarly, on sheet 3, using (C.56) appropriately,

$$\begin{aligned} \mathbf{a}_1^{(l,3)} + \mathbf{b}_1^{(l,3)} + \mathbf{c}^{(l,3)} - \overline{\mathbf{a}_{23}}^{(l,3)} - \overline{\mathbf{b}_{23}}^{(l,3)} &= \mathbf{b}_1^{(l,3)} + \mathbf{c}^{(l,3)} - \overline{\mathbf{b}_{23}}^{(l,3)} \\ &\sim \mathbf{b}_1^{(l,3)} + \mathbf{c}^{(l,3)} + \left(\mathbf{f}_2^{(l,3)} - \mathbf{b}_1^{(l,3)} - \mathbf{c}^{(l,3)} \right) \\ &\sim \mathbf{f}_2^{(l,3)}. \end{aligned}$$

On sheet 2

$$\mathbf{a}_1^{(l,2)} + \mathbf{b}_1^{(l,2)} + \mathbf{c}^{(l,2)} - \bar{\mathbf{a}}_{23}^{(l,2)} - \bar{\mathbf{b}}_{23}^{(l,2)} = \mathbf{a}_1^{(l,2)} + \mathbf{b}_1^{(l,2)} - \bar{\mathbf{a}}_{23}^{(l,2)} - \bar{\mathbf{b}}_{23}^{(l,2)}.$$

Now, via (C.53) and (C.54)

$$\begin{aligned}\mathbf{a}_1^{(l,2)} &\sim \bar{\mathbf{a}}_3^{(l,2)} + \mathbf{b}_2^{(l,2)} + \mathbf{e}_1^{(l,2)} \\ \mathbf{b}_1^{(l,2)} &\sim \mathbf{a}_2^{(l,2)} + \bar{\mathbf{b}}_3^{(l,2)} + \mathbf{f}_2^{(l,2)}.\end{aligned}$$

Hence,

$$\begin{aligned}\mathbf{a}_1^{(l,2)} + \mathbf{b}_1^{(l,2)} + \mathbf{c}^{(l,2)} - \bar{\mathbf{a}}_{23}^{(l,2)} - \bar{\mathbf{b}}_{23}^{(l,2)} &\sim \left(\bar{\mathbf{a}}_3^{(l,2)} + \mathbf{b}_2^{(l,2)} + \mathbf{e}_1^{(l,2)} \right) \\ &\quad + \left(\mathbf{a}_2^{(l,2)} + \bar{\mathbf{b}}_3^{(l,2)} + \mathbf{f}_2^{(l,2)} \right) - \bar{\mathbf{a}}_{23}^{(l,2)} - \bar{\mathbf{b}}_{23}^{(l,2)} \\ &\sim \mathbf{b}_2^{(l,2)} + \mathbf{a}_2^{(l,2)} - \bar{\mathbf{b}}_2^{(l,2)} - \bar{\mathbf{a}}_2^{(l,2)} + \mathbf{e}_1^{(l,2)} + \mathbf{f}_2^{(l,2)} \\ &\sim \mathbf{e}_1^{(l,2)} + \mathbf{f}_2^{(l,2)},\end{aligned}$$

where the last reduction is due to (C.55). □

Thus,

$$R_2 \sim \sum_{l=1}^m \left(\mathbf{e}_1^{(l)} + \mathbf{f}_2^{(l)} \right);$$

so, with (C.59), we have

$$R_1 + R_2 = -m \left(\mathbf{e}_2^{(m)} + \mathbf{f}_1^{(m)} \right).$$

Substituting this result into (C.58),

$$L(n\gamma) \sim m\alpha_n \sum_{l=1}^{m-1} \left(\mathbf{a}_{123}^{(l)} + \mathbf{b}_{123}^{(l)} \right) + m\alpha_n \left[\left(\mathbf{a}_{123}^{(m)} + \mathbf{b}_{123}^{(m)} \right) - \left(\mathbf{e}_2^{(m)} + \mathbf{f}_1^{(m)} \right) \right].$$

After inspecting Fig. 25, by deforming slightly on the m th horse we can convince ourselves this is precisely a 1-chain representing γ_c .

To make this claim precise, let \mathbf{q} be a 1-chain on Σ such that $\partial\mathbf{q} \subset \pi^{-1}(z)$ for some $z \in C'$, and define $[\mathbf{q}]_R$ as the corresponding equivalence class in $\bigcup_{z \in C'} \Gamma(z, z)$. Then, for any $k = 1, \dots, m$

$$\begin{aligned}R_{\tau}(1, k)a_* &= \left[\sum_{l=1}^k \mathbf{a}_{123} \right]_R \\ R_{\tau}(1, k)b_* &= \left[\sum_{l=1}^k \mathbf{b}_{123} \right]_R.\end{aligned}$$

Furthermore, by parallel transporting the endpoints of \bar{a} and \bar{b} along an appropriate path contained in the m th horse⁶²

$$\begin{aligned}\bar{a}_* &= \left[\left(\mathbf{a}_{123}^{(m)} - \mathbf{e}_2^{(m)} \right) \right]_R \\ \bar{b}_* &= \left[\left(\mathbf{b}_{123}^{(m)} - \mathbf{f}_1^{(m)} \right) \right]_R.\end{aligned}$$

Thus,

$$[L(n\gamma_c)]_R = m\alpha_n \left[R_{\mathbf{r}}^{(1,k)} a_* + R_{\mathbf{r}}^{(1,k)} b_* + \bar{a}_* + \bar{b}_* \right]_R.$$

Applying the closure map to both sides, by (C.47) the proposition holds:

$$[L(n\gamma_c)] = m\alpha_n \gamma_c \in H_1(\Sigma; \mathbb{Z}).$$

C.9 Table of m -herd BPS indices $\Omega(n\gamma_c)$, for low values of n and m

Table 1. Values of $\Omega(n\gamma_c)$ for low n and m

	n						
	1	2	3	4	5	6	7
$m = 1$	1	0	0	0	0	0	0
$m = 2$	-2	0	0	0	0	0	0
$m = 3$	3	-6	18	-84	465	-2808	18123
$m = 4$	-4	-16	-144	-1632	-21720	-318816	-5018328
$m = 5$	5	-40	600	-12400	300500	-8047440	231045220
$m = 6$	-6	-72	-1800	-58800	-2251500	-95312880	-4325917260
$m = 7$	7	-126	4410	-208740	11579925	-710338104	46716068007

D Proof of Proposition 3.4

Define the sequence

$$b_l := \binom{(m-1)^2 l}{l};$$

we will show

$$\lim_{n \rightarrow \infty} \frac{\Omega(n\gamma_c)}{(-1)^{mn+1} \binom{m}{(m-1)^2 n^2} b_n} = 1. \quad (\text{D.1})$$

⁶²As per our notation motivated in Section C.4, we do not write this parallel transport map explicitly.

Indeed, from (3.21),

$$\frac{\Omega(n\gamma_c)}{(-1)^{mn+1} \left(\frac{m}{(m-1)^2 n^2}\right) b_n} = 1 + \overbrace{\sum_{\substack{d|n \\ d < n}} (-1)^{m(n+d)} \mu\left(\frac{n}{d}\right) \left(\frac{b_d}{b_n}\right)}^{R(n)},$$

but

$$|R(n)| \leq \sum_{\substack{d|n \\ d < n}} \frac{b_d}{b_n}.$$

Now, from the bounds

$$\sqrt{2\pi} n^{n+\frac{1}{2}} e^{-n} < n! \leq n^{n+\frac{1}{2}} e^{1-n}$$

it follows that

$$\frac{b_d}{b_n} < \left(\frac{e}{\sqrt{2\pi}}\right)^3 \left(\frac{n}{d}\right)^{1/2} e^{c_m(d-n)},$$

where c_m is the constant defined in (3.23). Hence,

$$|R(n)| < \left(\frac{e}{\sqrt{2\pi}}\right)^3 \left(n^{1/2} e^{-c_m n}\right) \sum_{\substack{d|n \\ d < n}} d^{-1/2} e^{c_m d}.$$

Now, the next largest divisor of n , other than n itself, is $\leq n/2$. Using this fact, the observation that $d^{-1/2} e^{c_m d}$ is a monotonically increasing function of d , and the crude bound that number of divisors of n is $\leq n$, we have

$$\sum_{\substack{d|n \\ d < n}} d^{-1/2} e^{c_m d} \leq n \left(\left(\frac{n}{2}\right)^{-1/2} e^{c_m n/2}\right) = \sqrt{2n} e^{c_m n/2};$$

so

$$|R(n)| < \sqrt{2} \left(\frac{e}{\sqrt{2\pi}}\right)^3 n e^{-c_m n/2},$$

which vanishes as $n \rightarrow \infty$, verifying (D.1). In other words, the $n \rightarrow \infty$ asymptotics of $\Omega(n\gamma_c)$ are given by the asymptotics of the largest term b_n of (3.21) inside the sum over divisors:

$$\Omega(n\gamma_c) \sim (-1)^{mn+1} \left(\frac{m}{(m-1)^2}\right) n^{-2} b_n.$$

Equation (3.22) follows by using Stirling's asymptotics on the binomial coefficient b_n : as $n \rightarrow \infty$,

$$b_n \sim \frac{1}{\sqrt{2\pi}} \left(\frac{m-1}{\sqrt{m(m-2)}}\right) n^{-1/2} e^{c_m n}.$$

E A sign rule

In this appendix we discuss a subtle point about signs which was not treated correctly in the first version of [33].

The issue concerns the proper way of extracting 4D BPS degeneracy information from the generating functions $Q(p)$ defined in (2.2.2). What we want to do is factorize $Q(p)$ as we wrote in (2.15), but to do so, we need a way of choosing the lifts $\tilde{\gamma} \in \tilde{\Gamma}$ of classes $\gamma \in \Gamma$.

We propose the following rule. First, represent γ as a sum of k smooth closed curves β_m on Σ . Each such curve has a canonical lift $\hat{\beta}_m$ to $\tilde{\Sigma}$ just given by the tangent framing. Then we define

$$\tilde{\gamma} = \sum_{m=1}^k (\hat{\beta}_m + H) + \sum_{m \leq n} \#(\beta_m \cap \beta_n) H. \quad (\text{E.1})$$

We need to check that $\tilde{\gamma}$ so defined is independent of the choice of how we represent γ as a union of β_m . First we check that $\tilde{\gamma}$ is stable under creation/deletion of a null-homologous loop. If β denotes such a loop then $\hat{\beta} = H$ modulo $2H$ (indeed, suppose β bounds a subsurface S ; S admits a vector field extending $\hat{\beta}$, with $\chi(S)$ signed zeroes in the interior; this vector field gives a 2-chain on $\tilde{\Sigma}$ which shows $\hat{\beta}$ is homologous on $\tilde{\Sigma}$ to $\chi(S)H$; but $\chi(S)$ is odd since S has a single boundary component.) Thus the extra term $\hat{\beta} + H$ added to $\tilde{\gamma}$ is zero modulo $2H$. Next we check $\tilde{\gamma}$ is stable under resolution of an intersection: indeed this changes $\sum_{m \leq n} \#(\beta_m \cap \beta_n)$ by -1 , and changes k by ± 1 , while not changing $\sum \hat{\beta}_m$; it thus changes $\tilde{\gamma}$ by either 0 or $-2H$, which is in either case trivial mod $2H$. Finally we note that any representation of γ as a union of smooth closed curves can be related to any other by repeated application of these two operations and their inverses. It follows that $\tilde{\gamma}$ is indeed well defined.

Moreover, this rule has the following property:

$$\tilde{\gamma} + \tilde{\gamma}' = \widetilde{\gamma + \gamma'} + \langle \gamma, \gamma' \rangle H. \quad (\text{E.2})$$

It follows that the corresponding formal variables

$$Y_\gamma = X_{\tilde{\gamma}} \quad (\text{E.3})$$

obey the twisted product rule

$$Y_\gamma Y_{\gamma'} = (-1)^{\langle \gamma, \gamma' \rangle} Y_{\gamma + \gamma'}. \quad (\text{E.4})$$

In turn it follows (using the arguments of [23, 33]) that, if we use this particular lifting rule to extract the 4D BPS degeneracies, all the wall-crossing relations (and in particular the KSWCF for the pure 4D degeneracies) will come out as they should.

F Spectral networks and algebraic equations

It has been noted by Kontsevich that the generating functions of Donaldson-Thomas invariants are often solutions of algebraic equations. The equation (1.2) is one example. This

equation determines the BPS degeneracies $\Omega(n\gamma_c)$ corresponding to an m -cohort. As we have seen in this paper, this equation can be derived from a close analysis of the spectral network corresponding to an m -herd.

While finding the precise equation (1.2) involved some hard work, the bare fact that the BPS generating function obeys *some* algebraic equation is not so mysterious. Indeed, this seems to be a general phenomenon, which we expect to occur for *any* theory of class S . Let us briefly explain why.

The junction equations (B.1) involve variables ν and τ attached to each street of the network. These variables lie *a priori* in the noncommutative algebra \mathcal{A}_S . However, one can replace them by variables lying in the commutative algebra \mathcal{A}_C simply by choosing local trivializations of the torsors $\tilde{\Gamma}(\tilde{z}, -\tilde{z})$; indeed such a trivialization gives an embedding of \mathcal{A}_S into the algebra of $K \times K$ matrices over \mathcal{A}_C ; taking the individual matrix components then gives equations where all of the variables lie in \mathcal{A}_C . These equations alone do not quite determine ν and τ — there are not quite enough of them. However, once one supplements them with the “branch point” equations from [33] (which are also algebraic), one then has one equation for each variable.

In principle the spectral network may involve infinitely many streets and joints, so at this stage we may have an infinite set of algebraic equations in an infinite number of variables. However, in all examples we have considered, only finitely many of these equations are relevant for determining any particular BPS generating function. Indeed, in these examples the set of “two-way streets” is always supported in some compact set K obtained by deleting small discs around punctures on C ; the intersection $\mathcal{W} \cap K$ only involves finitely many streets; and there are no streets which enter K from outside. It seems likely that these properties hold for *all* spectral networks, although we have not proven it. In any case, taking these properties for granted, it follows that the finitely many variables ν and τ attached to the finitely many streets in $\mathcal{W} \cap K$ are indeed determined by a finite set of algebraic equations.

The functions $Q(p)$ in turn are algebraic combinations of the ν and τ , as are the BPS generating functions $\prod_p Q(p)^{\langle \bar{a}, p \Sigma \rangle}$. Thus we expect that the BPS generating functions in any theory of class S always satisfy algebraic equations, which gives a natural explanation of Kontsevich’s observation, at least in those theories.

References

- [1] J. Wess, J. Bagger, “Supersymmetry and Supergravity,” Princeton University Press, 1992
- [2] N. Seiberg, E. Witten, “Monopole Condensation, and Confinement in $\mathcal{N} = 2$ Supersymmetric Yang-Mills Theory,” Nucl.Phys.B426:19-52, 1994, [arXiv:hep-th/9407087](#)
- [3] N. Seiberg, E. Witten, “Monopoles, Duality and Chiral Symmetry Breaking in $\mathcal{N} = 2$ Supersymmetric QCD,” Nucl.Phys.B431:484-550, 1994, [arXiv:hep-th/9408099](#)
- [4] A. Bilal, F. Ferrari, “The Strong-coupling Spectrum of the Seiberg-Witten Theory,” Nucl.Phys.B469:387-402, 1996, [arXiv:hep-th/9602082](#)
- [5] C. L. de Souza Batista, D. Li, “Analytic Calculations of Trial Wave Functions of the Fractional Quantum Hall Effect on the Sphere,” Phys.Rev.B55:1582, 1997, [arXiv:cond-mat/9607170](#)
- [6] F. Denef, “Quantum Quivers and Hall/Hole Halos,” JHEP 0210:023, 2002, [arXiv:hep-th/0206072](#)
- [7] M. Reineke, “The Harder-Narasimhan System in Quantum Groups and Cohomology of Quiver Moduli,” Invent. Math. 152, no. 2, 349, 2003, [arXiv:math/0204059](#)
- [8] M. Reineke, “The Use of Geometric and Quantum Group Techniques for Wild Quivers,” [arXiv:math/0304193](#)
- [9] V.V. Fock, A.B. Goncharov, “Moduli Spaces of Local Systems and Higher Teichmuller Theory,” [arXiv:math/0311149](#)
- [10] H. Ooguri, A. Strominger, C. Vafa, “Black Hole Attractors and the Topological String”, Phys.Rev.D70:106007, 2004, [arXiv:hep-th/0405146](#)
- [11] B. Fiol, “The BPS Spectrum of $\mathcal{N} = 2$ $SU(N)$ SYM,” JHEP 0602:065, 2006, [arXiv:hep-th/0012079](#)
- [12] J. de Boer, M.C.N. Cheng, R. Dijkgraaf, J. Manschot, E. Verlinde, “A Farey Tail for Attractor Black Holes”, JHEP 0611:24, 2006, [arXiv:hep-th/0608059](#)
- [13] M. Reineke, “Moduli of Representations of Quivers,” [arxiv:0802.2147](#)
- [14] J. de Boer, S. El-Showk, I. Messamah, D. Van den Bleeken, “Quantizing $\mathcal{N} = 2$ Multicenter Solutions,” [arXiv:0807.4556](#)
- [15] D. Gaiotto, G.W. Moore, A. Neitzke, “Four-dimensional Wall-crossing via Three-dimensional Field Theory,” [arXiv:0807.4723](#)
- [16] M. Kontsevich, Y. Soibelman, “Stability Structures, Motivic Donaldson-Thomas Invariants and Cluster Transformations,” [arXiv:0811.2435](#)
- [17] M. Reineke, “Cohomology of Quiver Moduli, Functional Equations, and Integrality of Donaldson-Thomas Type Invariants,” [arXiv:0903.0261](#)
- [18] T. Weist, “Localization in Quiver Moduli Spaces,” [arXiv:0903.5442](#)
- [19] D. Gaiotto, G.W. Moore, A. Neitzke, “Wall-crossing, Hitchin Systems, and the WKB Approximation,” [arXiv:0907.3987](#)
- [20] M. Gross, R. Pandharipande, “Quivers, Curves, and the Tropical Vertex,” [arXiv:0909.5153](#)
- [21] M. Kontsevich, Y. Soibelman, “Motivic Donaldson-Thomas Invariants: Summary of Results,”

[arXiv:0910.4315](#)

- [22] T. Dimofte, S. Gukov, “Refined, Motivic, and Quantum,” *Lett.Math.Phys.*91:1, 2010, [arXiv:0904.1420](#)
- [23] D. Gaiotto, G.W. Moore, A. Neitzke, “Framed BPS States,” [arXiv:1006.0146](#)
- [24] M. Kontsevich, Y. Soibelman, “Cohomological Hall Algebra, Exponential Hodge Structures and Motivic Donaldson-Thomas Invariants,” [arXiv:1006.2706](#)
- [25] G.W. Moore, PiTP Lectures on Wall-Crossing, PiTP School at the Institute for Advanced Study, July 27-29, 2010, <http://www.physics.rutgers.edu/~gmoore>
- [26] J. Manschot, B. Pioline, A. Sen, “Wall-Crossing from Boltzmann Black Hole Halos,” *JHEP* 1107:059, 2011, [arXiv:1011.1258](#)
- [27] J. Manschot, B. Pioline and A. Sen, “A Fixed Point Formula for the Index of Multi-centered N=2 Black Holes,” *JHEP* 1105: 057, 2011, [arXiv:1103.1887](#)
- [28] D. Gaiotto, G.W. Moore, A. Neitzke, “Wall-Crossing in Coupled 2d-4d Systems,” [arXiv:1103.2598](#)
- [29] F. Denef, G.W. Moore, “Split States, Entropy Enigmas, Holes and Halos,” *JHEP* 1111:129, 2011, [arXiv:hep-th/0702146](#)
- [30] M. Alim, S. Cecotti, C. Cordova, S. Espahbodi, A. Rastogi, C. Vafa, “ $\mathcal{N} = 2$ Quantum Field Theories and Their BPS Quivers,” [arXiv:1112.3984](#)
- [31] T. Weist, “On the Euler Characteristic of Kronecker Moduli Spaces,” [arxiv:1203.2740](#)
- [32] E. Andriyash, F. Denef, D.L. Jafferis and G.W. Moore, “Bound State Transformation Walls,” *JHEP* 1203:007, 2012, [arXiv:1008.3555](#)
- [33] D. Gaiotto, G.W. Moore, A. Neitzke, “Spectral Networks,” [arXiv:1204.4824](#)
- [34] D. Gaiotto, G.W. Moore, A. Neitzke, “Spectral Networks and Snakes,” [arXiv:1209.0866](#)
- [35] G.W. Moore, Felix Klein Lectures: “Applications of the Six-dimensional (2,0) Theory to Physical Mathematics,” October 1 - 11, 2012 at the Hausdorff Insitute for Mathematics, Bonn. <http://www.physics.rutgers.edu/~gmoore>
- [36] G.W. Moore, “Four-dimensional $\mathcal{N} = 2$ Field Theory and Physical Mathematics,” [arXiv:1211.2331](#)
- [37] S. Cecotti, “The Quiver Approach to the BPS Spectrum of a 4d $\mathcal{N} = 2$ Gauge Theory,” [arXiv:1212.3431](#)
- [38] D.-E. Diaconescu, G.W. Moore, “Crossing the Wall: Branes vs. Bundles”, *Adv. Theor. Math. Phys.* Volume 14, Number 6 (2010), 1621-1650, [arXiv:0706.3193](#)
- [39] W.-Y. Chuang, D.-E. Diaconescu, J. Manschot, G.W. Moore, Y. Soibelman, “Geometric Engineering of (Framed) BPS States.”, [arXiv:1301.3065](#)
- [40] D. Gaiotto, “N=2 dualities” , *JHEP* **1208**, 034 (2012) [[arXiv:0904.2715](#) [hep-th]].
- [41] M. Kontsevich, Private communication.
- [42] <http://www.physics.rutgers.edu/het/www/charge-disposition-movie.flv>
- [43] <http://www.physics.rutgers.edu/het/www/strong-coupling-full-range.flv>

- [44] <http://www.physics.rutgers.edu/het/wwc/focus-before-wall.flv>
- [45] <http://www.physics.rutgers.edu/het/wwc/spectrum-charges.flv>